8-1979

Rubidium-Strontium And Related Studies Of The Salado Formation, Southeastern New Mexico

Joseph K. Register Jr.

Joseph K. Register, Jr.
Candidate

Geology
Department

This thesis is approved, and it is acceptable in quality and form for publication on microfilm:

Approved by the Thesis Committee:

Douglas G. Brookins, Chairperson

Roger H. Anderson

Gary P. Landis

Accepted:

David T. Benedetti
Dean, Graduate School

July 10, 1979
Date

Rubidium-Strontium and Related Studies of the Salado Formation, Southeastern New Mexico

by

Joseph K. Register, Jr.

B.S., University of North Carolina, Chapel Hill, 1975

THESIS

Submitted in Partial Fulfillment of the
Requirements for the Degree of

Master of Science in Geology

The University of New Mexico
Albuquerque, New Mexico

August, 1979

Rubidium-Strontium and Related Studies of the Salado Formation, Southeastern New Mexico

by

Joseph K. Register, Jr.

B.S., University of North Carolina, Chapel Hill, 1975

ABSTRACT OF THESIS

Submitted in Partial Fulfillment of the
Requirements for the Degree of

Master of Science in Geology

The University of New Mexico
Albuquerque, New Mexico

August, 1979

TABLE OF CONTENTS

Page

ABSTRACT

The Salado Formation, a member of the Ochoa Series, is a bedded salt deposit which is found in the Delaware Basin of southeastern New Mexico and west Texas. It is comprised primarily of halite and sylvite with minor amounts of sulfate minerals. Rubidium-strontium age determinations of the evaporite minerals in the Salado indicate an age of final equilibration of 214 ± 15 m.y. This age is fairly consistent with the geologic age of the formation, precluding substantial alkali-alkaline earth migration since deposition. Polyhalite and anhydrite samples from the Salado give $^{87}Sr/^{86}Sr$ values of about .7078, which are consistent with reported values for Permian seawater. The REE and trace element concentrations of the polyhalite and anhydrite samples are very low, reflecting the composition of seawater.

Rubidium-strontium age determinations of the clay minerals extracted from the salt suggest a minimum age of 390 ± 77 m.y. This age probably represents the minimum age of the provenance of the clay minerals. The REE and trace element concentrations as well as the mineralogy of the clay minerals indicate a detrital origin for the clay minerals with some clay-brine interaction. Clay minerals seem generally depleted in the light REE (relative to NAS) which most likely were replaced by Ca^{2+} and Na^{+} from the evaporitic brines.

ACKNOWLEDGMENTS

The author wishes to express his sincere gratitude to D. G. Brookins, without whose direction and advice this study could not have been undertaken or completed. Appreciation is also due R. Y. Anderson and G. P. Landis for their criticisms and suggestions in improving the thesis.

Appreciation is extended to R. S. Della Valle, who performed the INAA analyses and provided helpful discussions about this study in general. Thanks go to John Husler, who provided some of the major element data contained herein.

Gratitude is also due R. T. Hicks, R. S. Miller and D. Olivas for their help in the geochronology laboratory. Appreciation is expressed to B. Swenson for drafting most of the figures and to S. Hamilton for typing the thesis.

Thanks go to S. J. Lambert for his help in obtaining samples and coordinating efforts with Sandia Laboratories, Albuquerque. Appreciation is also extended to the personnel of the Duval and Mississippi Chemical Company potash mines for their help in obtaining samples from underground.

This study was supported by research contracts 05-4105 and 13-2065 obtained from Sandia Laboratories, Albuquerque.

Finally, this study would have been impossible without the patience and encouragement of the author's wife, Marcia.

List of Figures

List of Tables

List of Appendices

INTRODUCTION

Purpose of Study

The bedded salt deposits located in southwestern New Mexico, which comprise nearly all the Salado Formation, are currently under investigation by Sandia Laboratories, Albuquerque, as a possible site for radioactive waste disposal. Bedded salt deposits have many characteristics which make them attractive as tentative waste disposal sites. These characteristics include their anhydrous nature, ability to flow rather than fracture when faulting occurs and flowage due to possible heat from radioactive waste.

However, it is not at all documented that all alkali, alkaline earth and rare earth elements present in these bedded salts have remained in place since deposition occurred during Permian time. In addition, if movement of these elements has taken place, it is imperative to determine whether such migration is attributable to dissolution with subsequent reprecipitation, diffusion or desorption. This study was conducted in order to evaluate more completely the bedded salt deposits of the Salado Formation as a possible containment of radioactive wastes.

Location

The Salado Formation which is part of the evaporite sequence of the Delaware Basin, is located in southeastern Eddy and southern Lea Counties, New Mexico, and in northern and Eastern Culberson, Reeves, Loving, western Ward, western Winkler, and northwestern Pecos Counties,

Texas (Fig. 1). The basin area is generally elliptical in outline with the major axis running northwest-southeast about 160 miles from northwest of Carlsbad, New Mexico, toward Pecos and Fort Stockton, Texas.

Geologic Setting

The Delaware Basin, which contains the Salado Formation is a tectonic and lithologic province of the Permian Basin, an area within the mid-continental United States containing Permian sediments, which extends from Kansas in the north to the Texas-Mexico boundary in the south. The southern end of the Permian Basin has been subdivided into geological provinces based upon tectonic and lithologic differences. The Delaware, Midland, Val Verde, Marfa and Tatum basins are areas which contain relatively thick sections of Paleozoic strata compared to the shelf, uplift and platform areas (Fig. 2).

The Delaware Basin is outlined to the south by the limestone-dolomite rocks of Upper Permian age in the Glass, Davis and Apache Mountains and to the west by the limestone-dolomite rocks of Upper Permian age in the Guadalupe Mountains and Sierra Diablo. The subsurface basin margin to the north and east consists of limestone-dolomite rocks of the Carlsbad shelf and the Central Basin platform (Fig. 2). The limestone-dolomite rocks which constitute the basin margin are collectively known as the Capitan Reef.

The Salado Formation, a bedded salt deposit, is a member of the Ochoa Series, in the Upper Permian section of the Delaware Basin.

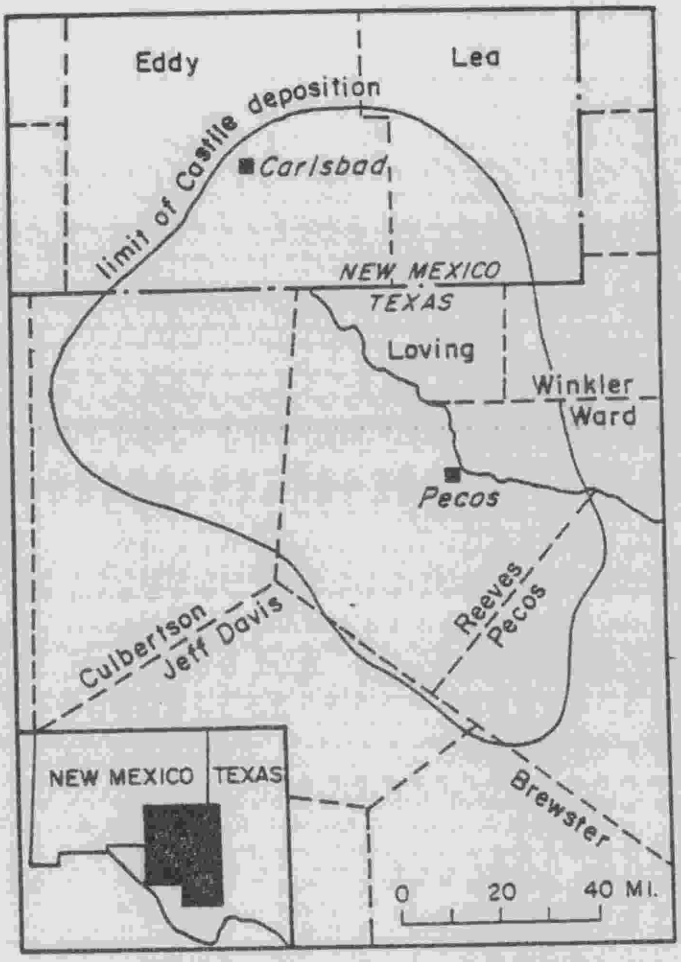

Figure 1. Index map showing the location of the Delaware Basin.

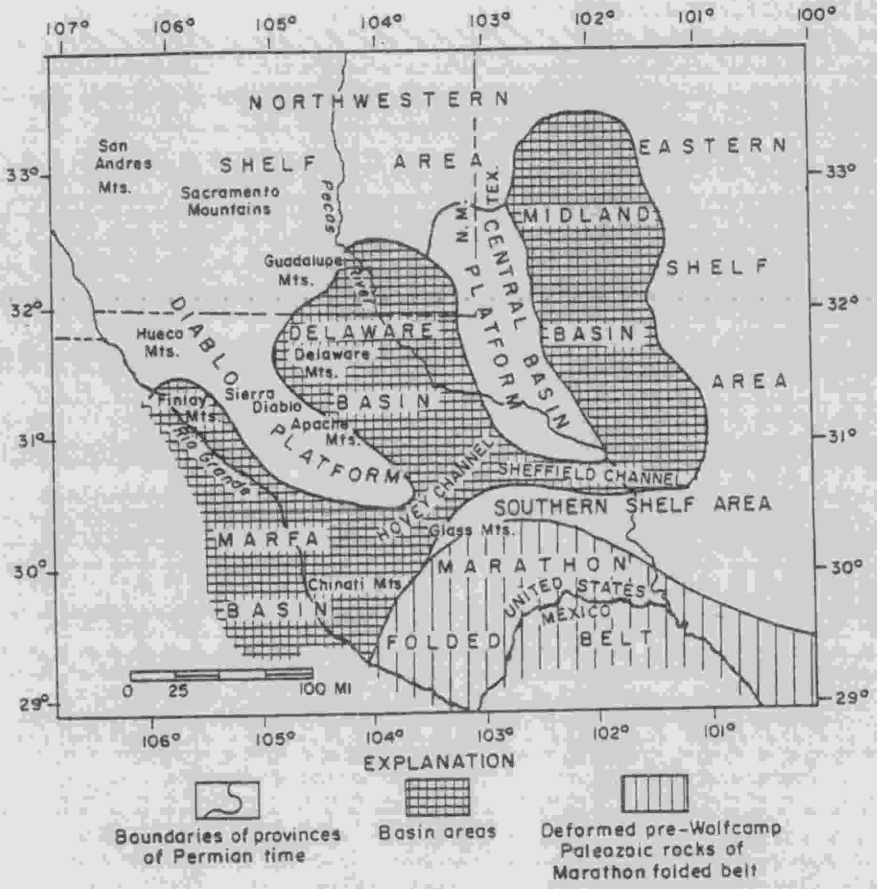

Figure 2. Map showing the regional geologic features near the Delaware Basin.

The detailed geology of the basin and the Salado Formation will be described later.

Previous Work

The mineralogy and stratigraphy of the Delaware Basin as well as the Salado Formation have been studied in some detail by many workers. General descriptions of the basin and its stratigraphy have been given by Udden (1924), Baker (1929), Bybee (1931), and Lang (1935). Extensive lithologic logs were compiled and interpreted by Schaller and Henderson in 1932. A very complete description of the Delaware Basin and surrounding areas can be found in King (1942). A condensed version of this description with some detailed work on the Castile Formation was published by King (1947). More recently, studies by Hills (1972), Anderson and others (1972), Anderson and Kirkland (1966) and Dean and Anderson (1973) have added information pertaining to the genesis and evolution of the basin.

Studies more specifically concerning the Salado Formation have been conducted by Kroenlein (1939) and Lang (1939, 1942). The geochemistry of the Salado Formation has been studied by some workers. Holser (1966) examined the Br content of the salts of the formation for the purpose of determining whether the salts were primary or recycled. Due to the low concentration of Br in the salts, he judged them to be second or third cycle evaporites (c.f., Braitsch, 1962). Adams (1967) also studied the Br concentration in halite from the Salado to ascertain the salinity of the water from which the salt precipitated.

The one study conducted on the Rb-Sr systematics of the Salado Formation (Tremba, 1973) is very limited in its scope. In all cases, the number of samples used on which conclusions were drawn was too small for meaningful statistics to be applied, due to the large variance present in the data. Rb-Sr isochron ages from 120 to 320 m.y. were obtained for five sets of samples.

Methods of Investigation

Portions of evaporite cores were obtained from core holes AEC-8, ERDA-9 and ERDA-6 from Sandia Laboratories and additional samples were collected from the walls of the Duval and Mississippi Chemical Company potash mines and analyzed for Rb and Sr concentration as well as Sr isotopic ratio. Initially, samples were analyzed as whole rocks; whole rocks are samples taken in which the smallest dimension of the sample is at least 10 times the size of the largest mineral grain. However, it was found to be more informative to consider each sample as two distinct entities, a water soluble (i.e., evaporite mineral) fraction and a clay mineral fraction (from the non-evaporite sample material). It was hoped that the Rb-Sr analyses would delineate an isochron. Also, Rb-Sr analyses of the clay minerals present in the rock were used to determine if the clay had acted as a sink for possible Rb or Sr migration and to address problems of provenance and diagenetic effects of clay minerals.

Some of the samples analyzed for Rb and Sr were also analyzed for other trace elements such as Cs, Ba and eight rare earth elements (REE).

These analyses were performed at Los Alamos Scientific Laboratories by instrumental neutron activation methods. Data from these analyses were also used to investigate possible elemental migration through the salt.

X-ray diffraction was used to determine the mineralogy of the samples. In some cases, the resultant mineralogical data were verified through major element analysis of the sample. When deemed essential, thin sections were prepared in order to examine the textural and crystallographic characteristics of the samples more fully.

Sample Locations

Core samples were taken from three drilling sites, AEC-8, ERDA-9, and ERDA-6; the spatial relationship of these core holes is shown in Fig. 3. The core footages noted in the text are the distances in feet from the surface to the depth from which the sample was taken. All DV prefixed samples were obtained from the tenth ore zone of the Duval potash mine; MC prefixed samples were collected from the seventh and tenth ore zones of the Mississippi Chemical potash mine. The locations of both mines with their spatial relationship to the drill holes are also indicated in Fig. 3. The seventh and tenth ore zones were intercepted by the ERDA-9 core at 1555 feet and 1475 feet, respectively.

The relationship of the known marker beds in the Salado Formation to the ERDA-9 core footages is shown in Fig. 4.

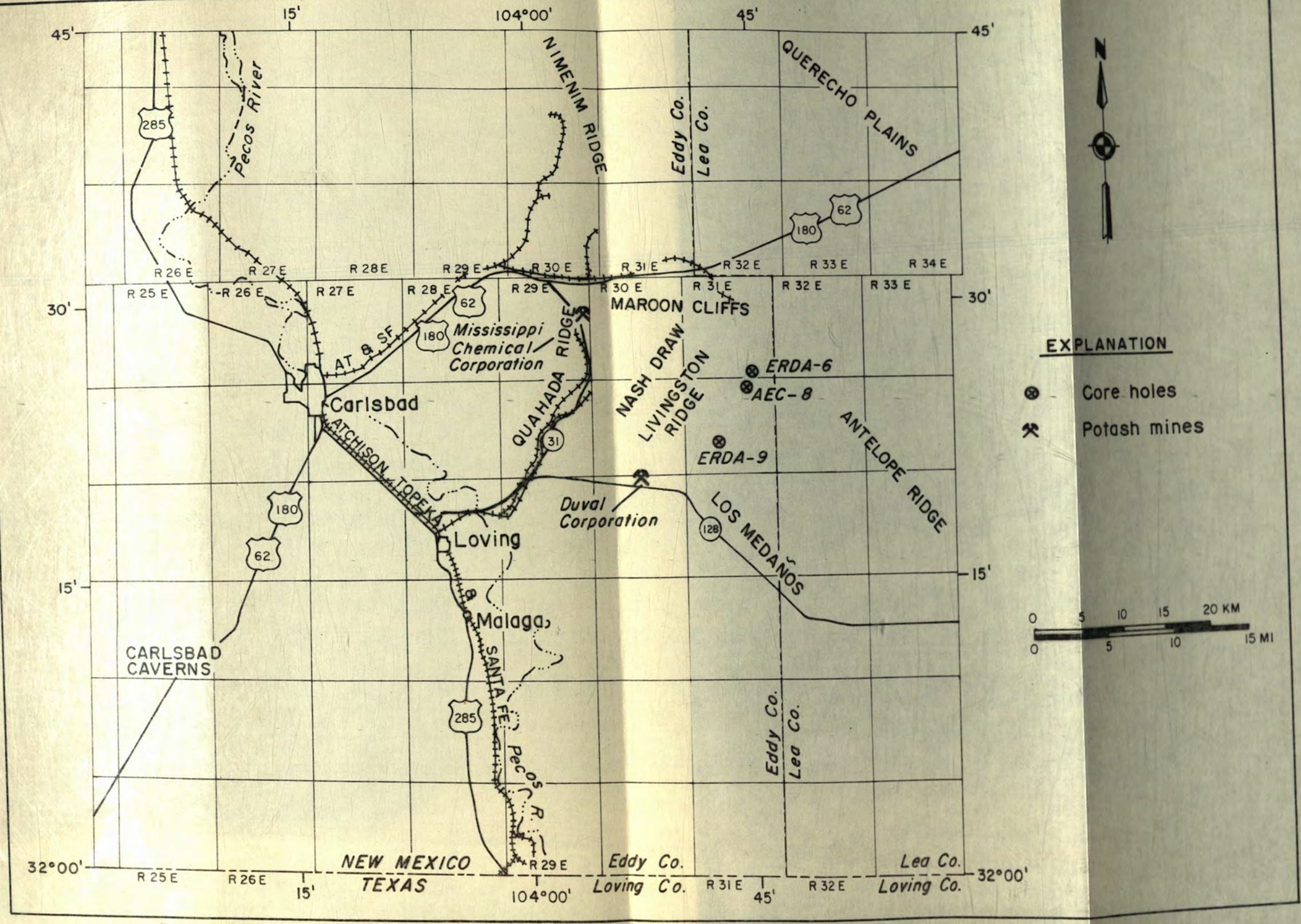

Figure 3. Map showing the locations of the mines and coreholes from which samples were obtained. (Modified from Griswold, 1977.)

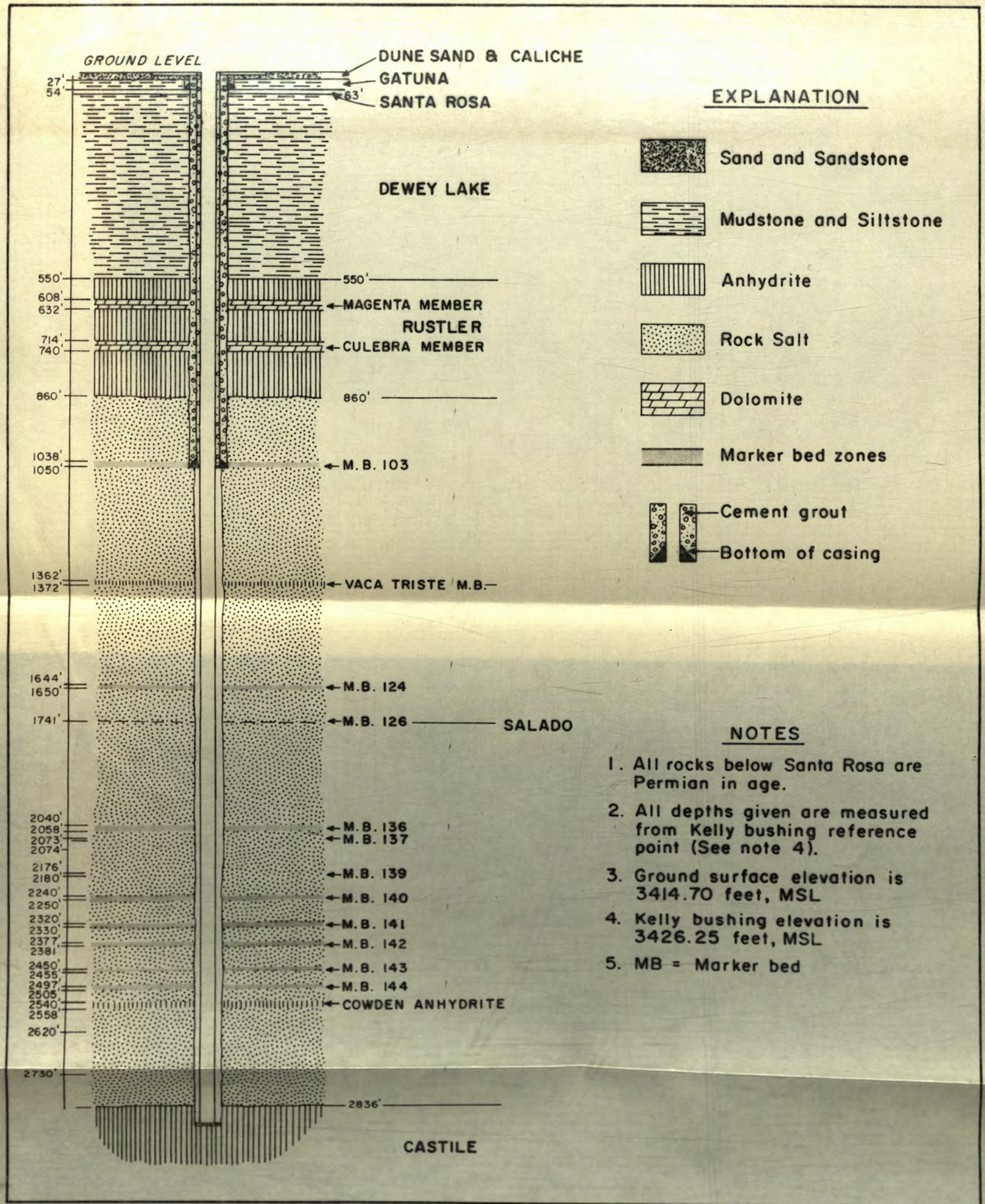

Figure 4. Diagram correlating the ERDA-9 core footages with known marker beds in the Salado Formation (after Griswold, 1977).

GEOLOGY OF THE DELAWARE BASIN

General Description

The Delaware Basin is an irregular, pear-shaped structural depression 160 miles long by 95 miles wide covering an area of about 10,000 square miles (Fig. 1 and 2). The basin has long been a major province for petroleum exploration and production and most knowledge of the geology of the basin has resulted from this activity.

Stratigraphy

Paleozoic rocks in the Delaware Basin have a total thickness of at least 33,000 feet, with every system in the Paleozoic probably represented (Table 1). Rocks of the Permian System have a maximum thickness of about 19,500 feet, or about 60 percent of the total Paleozoic section thickness.

The Permian rocks in the Delaware Basin have been divided into four series, which are (in ascending order) the Wolfcamp, Leonard, Guadalupe and Ochoa Series (Adams and others, 1939). The Wolfcamp Series, considered to be part of the Lower Permian, is represented here as a black, slightly shaly, thinly-bedded limestone which grades into the massive Hueco Limestone of the reef facies surrounding the basin margin. The thickness of the Wolfcamp Series in this area ranges from about 1000 feet in the deepest part of the basin to approximately 450 feet along its margins (King, 1942).

The Leonard Series, also part of the Lower Permian, conformably overlies the limestones of the Wolfcamp. The Bone Spring Limestone,

Table 1. Stratigraphic table of Paleozoic rocks of the Delaware Basin, west Texas and southeast New Mexico (modified from Vertrees and others, 1959).

System	Series		Stratigraphic units	Thickness (in feet)
Quaternary to Triassic				
Permian	Upper[a]	Ochoa	Dewey Lake Redbeds	0-600±
			Rustler Formation	0-550±
			Salado Formation	0-2000±
			Castile Formation	0-2000±
		Guadalupe	Delaware Mountain Group	
			Bell Canyon Fm.	700-1200±
			Cherry Canyon Fm.	1000±
			Brushy Canyon Fm.	0-1000±
	Lower[a]	Leonard	Bone Spring Limestone	800-3600±
		Wolfcamp		1000-7500±
Pennsylvanian			Black shale	0-200±
		Strawn		0-1100±
		Atoka		0-1100±
		Morrow		0-1200±
Mississippian		Chester Kinderhook		0-3100±
Devonian-Silurian			Cherty limestone (Miss.?)	0-500±
			Hunton Group	0-1800±
Ordovician		Upper	Montoya Formation	0-500±
		Middle	Simpson Formation	100-2250±
		Lower	Ellenburger Formation	500-1600±
			? ?	
Ordovician-Cambrian			Bliss Formation	0-150±
Precambrian				
			Total maximum thickness	33,050

[a]From Cohee (1960).

Note: Single lines across column of stratigraphic units represent probable regional unconformities.

which comprises the Leonard in this area, consists primarily of bedded limestones, interbedded and interfingered with calcareous shales. The Bone Spring thickens to 3600 feet in the Delaware Basin, but thins to a thickness of 750 feet along the basin margin.

Overlying the rocks of the Leonard Series is the somewhat thicker, more complex strata of the Guadalupe Series. The rocks of the Guadalupe Series deposited in the Delaware Basin constitute the Delaware Mountain Group, composed primarily of sandstone, and having a thickness of about 3500 feet. Along the margin of the basin, the sandstone thins considerably, and the upper part is replaced by thick reef masses. The Delaware Mountain Group was subdivided by Beede (1924) into three formations, named, in ascending order, the Brushy Canyon, the Cherry Canyon and the Bell Canyon. This subdivision was based primarily on subtle lithologic changes in the sandstones.

The Ochoa Series overlies the Guadalupe Series in the Delaware Basin and consists largely of evaporites. The Upper Permian Ochoa Series includes, in ascending order, the Castile, Salado, Rustler and Dewey Lake Formations.

The Castile Formation consists primarily of anhydrite, marked throughout by thin, light and dark laminae. Irregularly interbedded throughout the anhydrite are thin limestones and thick salt beds. The Castile attains its maximum thickness of about 2000 feet in the east-central and northeastern part of the Delaware Basin and thins to an eroded edge in the western part.

The Salado Formation, which overlies the Castile, consists almost entirely of chloride (salt) rocks. Layers of anhydrite, dolomitic limestone and clastic rocks are interbedded with the massive salt strata. The thickness of the Salado ranges from an eroded western margin to about 1000 feet near the eastern basin margin to a maximum of nearly 2500 feet in the east-central part of the basin. The detailed geology and mineralogy of the Salado is discussed in a later section.

Overlying the Salado Formation, sometimes unconformably, is the Rustler Formation, the youngest unit in the evaporite sequence. The Rustler consists primarily of sandstone and conglomerates at its base and anhydrite, dolomite and halite in the upper part of the section. The thickness of the Rustler Formation ranges from 250 feet to about 600 feet in the northern, central and eastern parts of the Delaware Basin.

The youngest formation of the Ochoa Series is the Dewey Lake. The Dewey Lake is a redbed formation in sharp contrast to the evaporites of the other members of the Ochoa Series. Gypsum present in the predominantly orange sands occurs only as cement and secondary crystals. The Dewey Lake does attain a maximum thickness of nearly 350 feet in some areas; however, it has been stripped entirely from the underlying Rustler Formation in places, apparently by pre-Triassic erosion (Adams, 1944).

Structure

The Delaware Basin evolved by downwarp of Precambrian basement terrane of the Texas foreland, a granitic craton (Adams, 1965).

Subsidence of the basin was accomplished mainly by downwarping without major marginal faulting and without subsequent folding or compressive tectonic deformation. However, buried normal faults of large displacement are present along the eastern edge of the basin (Adams, 1965).

The major structural features present in the pre-evaporite strata consist of minor faults and secondary warping. Most of the faults tend to trend north-northeast and are typically upthrown to the east. Small dome-like features and complimentary saddles (resulting from secondary warping) with amplitudes of several hundred feet occur at widely spaced intervals (Brokaw and others, 1972).

The only persistent structural feature present in the evaporite section is a general, uniform homoclinal dip of 1 to 3 degrees to the southeast. A rather complex system of salt flowage features is superimposed on this homocline, which vary in development from location to location (Jones, 1973). The Capitan Reef front seems to have played a major role in the development of large deformational features in the salt. Just basinward of the eastern buried reef mass is a southeast plunging structural trough paralleling the base of the reef. The most intense deformation of the evaporite sequence occurs near this trough. This deformation is characterized by buckling and downwarping in the evaporites as well as gentle arching of the basin strata (Jones, 1973).

Large and small scale flow features are also prevalent elsewhere in the evaporite strata, resulting from high shear stress combined with sufficient confining pressure. These flow features have caused

differential thickening of some evaporite units and (on a smaller scale) boudinage-appearing structures in some locations (Anderson, 1978).

Anderson (1978) also describes numerous, sharply defined localized depressions some of which may be attributed to "deep dissolution" processes taking place near the base of the Castile Formation. Anderson (1978) proposes that some of these dissolution features may have propogated upward forming cylinders of collapsed and partially dissolved debris known in much of the area.

Geologic History

The Delaware Basin is generally construed to be a Permian feature, but the tectonic history of the area indicates that the general outline of the basin was probably established as early as Late Pennsylvanian time, as a result of the orogenic movements coincident with the creation of the Marathon fold belt (New Mexico Geological Society, 1954). The Marathon Orogen probably marks convergence and final collision between Africa-South America and North America (Graham and others, 1975).

During the Permian the area was divided into a number of irregularly shaped provinces which received different types of deposits. These provinces were basin areas, like the Delaware Basin, shelf areas and narrow platforms, similar to the shelf areas, lying between the basins. These provinces are believed to be of tectonic origin, the basins being areas of greater subsidence, the platforms and shelves of less subsidence (King, 1942).

In early Permian time, seas spread over all of western Texas and eastern New Mexico, but from middle Permian time onward they became progressively more restricted. Finally, at the end of the Middle Permian, the seas appear to have been nearly restricted to the Delaware Basin. It was during this time that the first evaporites and marine sediments of the Ochoa Series were deposited (King, 1947). During this period of evaporite deposition, the Delaware Basin probably remained connected to the sea by a channel to the southwest which continually provided fresh seawater to take the place of that lost through evaporation. The basin continued to downwarp throughout the Permian and a thick accumulation of evaporite minerals was deposited. At the close of the Permian, a thick clastic blanket was deposited in the shallowing sea.

No lower Triassic strata occur in the Delaware Basin, nor are they known in the region. However, during this time, the region underwent epirogenic uplift and erosion; a slight angular unconformity is present between Late Permian and overlying strata. Bachman (1974) notes the possibility of some dissolution of Permian soluble rocks during this time, but cites no direct evidence. In the Late Triassic, inland basin streams laid down floodplain deposits, which represent the first record of non-marine deposition in the area. In the Early Cretaceous, a shallow sea transgressed across the basin, stripping off some of the Triassic strata and producing some dissolution of Permian salt and gypsum (Bachman, 1976).

During the Late Cretaceous, the sea withdrew, leaving the area blanketed with an unknown thickness of marine strata. Since no early or middle Tertiary deposits are known in this area, geologic events near the basin over the 60 million years after the end of the Cretaceous are not well known. Hayes (1964) indicates that the entire region was probably elevated and tilted slightly to the northeast by broad epirogenic uplift coincident with the Laramide Orogeny. This erosion again subjected Permian salt to further dissolution (Bachman, 1974). This last epirogenic uplift probably marks the conclusion of significant tectonic activity in the Delaware Basin area.

GEOLOGY OF THE SALADO FORMATION

General Description

The Salado Formation of the Permian Ochoa Series is one of the principal halite deposits of the North American continent and contains the Carlsbad potash district, which supplies much of the United States potash (Brokaw and others, 1972). The thickness of the Salado in the area studied ranges from about 1700 feet to a maximum of 2000 feet. Unlike the Castile, the Salado extends over and beyond the Capitan Reef masses to the north and east, overfilling the ancient reef-formed basin.

Mineralogy

The Salado Formation is composed primarily of halite, anhydrite and potassium salts with varying amounts of other evaporites and fine-grained clastic rocks. Eighty-five to ninety percent of the formation is comprised of halite; the next most abundant rock present is anhydrite. Polyhalite and other potassium-magnesium minerals with minor amounts of sandstone and claystone make up the remainder of the Salado.

There are two types of halite found in the Salado; they differ primarily in the amount of detritus they contain. One type is quite clayey and contains varying amounts of quartz; the other contains only minor amounts of clay material. Potassium-rich zones, occurring throughout the halite, are recognized by the presence of abundant sylvite and lesser amounts of carnallite, kieserite and other evaporite minerals.

Though these minerals are present in minor amounts in all of the Salado, their greatest abundance is noted near the middle of the section between salt beds.

Anhydrite and polyhalite nearly always occur in seams intercalated with thick halite sections. Brokaw and others (1972) indicate that the majority of the polyhalite found in the seams is probably due to replacement of anhydrite but suggest no time constraints of the replacement process.

Most of the detritus found in the evaporite minerals consists of clay minerals and quartz sand. Iron is also present, maybe some of it in the form of hematite or an equivalent hydrated form, although much of it is present in the clay minerals. Layer silicate mineral assemblages consisting of smectites, chlorite, illite, talc and serpentine are quite common in the insoluble portion of the halite.

ANALYTICAL PROCEDURE

General Statement

Due to the rather unique elemental composition of the samples examined in this study (compared to the majority of samples studied using standard geochemical techniques), a brief outline of analytical procedure is included. A more detailed explanation of these procedures is given in the Appendix.

Preparation of Samples

Cleaning and crushing

Samples of evaporites obtained from drill cores were first cut by an air-cooled saw to eliminate those portions which may have come in contact with drilling solutions. After cutting, a large portion of the remaining prism was crushed to about one to five mm. After crushing, the sample was quartered, and one of the quarters crushed to minus 100 mesh in a hardened steel crushing vial. Samples collected from potash mine walls were cleaned simply by removing the outer portion which had been exposed in the mine adit. After cleaning, the mine wall samples were crushed in the same manner as the samples obtained from core.

Separation of water soluble from water insoluble material

After crushing to minus 100 mesh, about 75 grams of each sample were carefully weighed into a 250 ml glass centrifuge tube. About 175 ml of distilled and deionized water was then added and the tube vigorously shaken for about three minutes. The sample was then

centrifuged for fifteen minutes and the solution decanted through S and S #576 filter paper into a 600 ml beaker. This process was repeated three times, thus assuring that all the water soluble material was separated from the water insoluble fraction.

The solution contained in the 600 ml beaker was then evaporated at 100° C on a hotplate until no more liquid remained. The water soluble salt was then quantitatively removed from the beaker, weighed and stored for analysis. A comparison of the whole rock weight to the weight of the water soluble salt easily yielded the concentration of water insoluble material in the evaporitic salt.

Separation of the minus 2 micron fraction

The minus 2 micron fraction was separated from the insoluble residue remaining from the above procedure. The insoluble material was washed and centrifuged repeatedly until the clay-sized material was deflocculated. The washed slurry was then transferred to 1000 ml graduated cylinders for gravity settling. The necessary time for settling was determined from the equation by Folk (1968). After settling for the proper length of time, the minus 2 micron fraction was siphoned off and the settling procedure repeated until a sufficient quantity of minus 2 micron material for analysis was obtained. A portion of the minus 2 micron fraction was retained as a slurry; the remainder was dried and ground to minus 100 mesh for geochemical analysis.

X-Ray Diffraction Identification

Whole Rocks

Whole rock samples were analyzed by loading a small amount of randomly oriented rock powder into a Norelco powder holder. This powder was then scanned from 5 to 80 degrees two theta and the resulting diffractogram compared to values compiled in the Joint Committee on Powder Diffraction Standards file to determine bulk mineralogic composition. Approximate mineralogic abundances were estimated by comparison of relative peak intensities of X-rayed samples with known major elemental composition to the diffractogram peak intensities of samples with unknown mineralogic abundance. Examples of typical evaporite diffractograms are given in Appendix 1.

Minus 2 micron fraction

Identification of clay minerals was based primarily on X-ray diffractograms because sufficient material for major element analysis was rarely present and access to a scanning electron microscope was severely limited. Untreated oriented powders were scanned from 2 to 60 degrees two theta. The untreated slide was glycolated by vapor-soaking on a rack in a container partially filled with ethylene glycol. An additional oriented powder was heated to 450° C. The glycolated and heated samples were scanned from 2 to 30 degrees two theta. These procedures are described in more detail in Appendix 2.

All samples X-rayed (clay minerals and whole rocks) were scanned by a Norelco X-ray diffractometer using Cu K_{α} Ni-filtered radiation.

A time constant of two seconds was used with a scintillation counter detector and pulse height analyzer. The goniometer slit system was comprised of a divergent and anti-scatter slit of 1 degree and a 0.003 inch receiving slit.

Chemical Preparation of Samples for Rb-Sr Analysis

Whole rock, clay mineral and water soluble samples were weighed to the nearest 0.00001 g and placed in 100 ml teflon evaporating dishes; the amount of sample to be dissolved was adjusted to ensure at least 10 micrograms of Sr and Rb in solution. The samples were then spiked with ^{84}Sr- and ^{87}Rb-enriched solutions. Whole rock and clay mineral samples were dissolved with 30 ml of reagent grade HF and 3 ml of vycor distilled $HClO_4$ at 100° C on a hotplate. Water soluble samples were dissolved with 50 ml of distilled and deionized H_2O and 10 ml vycor distilled 6N HCl. Samples containing large amounts of sulfate minerals were first treated with aqua regia and then dissolved with HF and $HClO_4$.

After complete dissolution of the sample and evaporation of all HF and $HClO_4$, the resulting residue was digested with 30 ml of vycor distilled 2N HCl. The HCl was allowed to evaporate completely and the sample was redigested with 30 ml of HCl. The mixture was reduced to about 3 ml by slow evaporation and allowed to cool overnight. The solution was then filtered through S and S #576 filter paper and loaded onto the top of a chromatography column charged with chromatographic grade sulfonated polystyrene. The column was washed with 2.25N HCl and Rb and Sr fractions collected as prescribed by column calibration (see Appendix 3).

The Rb and Sr fractions were subsequently dried, redissolved and placed into clean quartz microvials. The samples in the microvials were fused, cooled and stored for mass spectrometric analysis.

Mass Spectrometry

Samples were analyzed for Rb and Sr concentration as well as Sr isotopic ratio using a Nuclide Corporation 12 inch, 90 degree sector solid source mass spectrometer. Samples were evaporated onto Ta ribbon filaments, which were first "preconditioned" at a low temperature under high vacuum and then loaded into the mass spectrometer source for analysis. Sr and Rb were analyzed in the same manner. After a steady ion beam was obtained, the appropriate spectrum was scanned using a peak preselector to step from mass to mass. An integrating ratiometer served primarily as a single channel counter to count and record the intensity of each peak in the spectrum. Forty-eight scans of the spectrum of each sample were deemed to produce sufficiently accurate and precise data. Data were then reduced primarily by hand calculation.

Rb and Sr concentrations were calculated by standard isotope dilution techniques (Appendix 4). All $^{87}Sr/^{86}Sr$ ratios were normalized to $^{86}Sr/^{88}Sr = 0.1194$; the $^{85}Rb/^{87}Rb$ ratio was taken to be 2.593. Blank analyses averaged 0.03 micrograms Sr and 0.02 micrograms Rb; these values were insignificant as possible contaminants for all analyses. Multiple analyses of Eimer and Amend standard $SrCO_3$ gave an average $(^{87}Sr/^{86}Sr)_N$ of 0.7080 (Appendix 5). One standard deviation experimental errors are realistically estimated to be 1.0 percent for $^{87}Rb/^{86}Sr$ and 0.03 percent for $^{87}Sr/^{86}Sr$.

Instrumental Neutron Activation Analysis

Samples were analyzed for 24 elements by instrumental neutron activation analysis (INAA) at the Los Alamos Scientific Laboratory. Irradiation of the samples was performed at the Omega West Reactor, a thermal, heterogeneous, tank type reactor, which at the 8 megawatt level provides neutron fluxes up to 8×10^{13} neutrons/cm^2-sec.

Samples, ground to minus 200 mesh, were accurately weighed into polyethylene scintillation vials and introduced to a high thermal neutron flux using a He-charged pneumatic transfer system. A small length of nichrome wire was analyzed concurrently with each sample to monitor possible deviations in the neutron flux.

After irradiation, the resulting gamma emission spectrum from the sample was analyzed and counted by a Ge(Li) detector used in conjunction with a 4096 channel analyzer. Estimated percent error and the lower limit of detection for each element analyzed are given in Appendix

Silicate samples (clay minerals in this instance) and low Na rocks (such as polyhalite and anhydrite) are easily analyzed by INAA. However, rocks containing more than about 5 percent Na (rock salt) cannot be analyzed simply, due to the creation of ^{24}Na (by neutron bombardment of ^{23}Na) which emits a very intense gamma spectrum after irradiation. This strong gamma spectrum acts to "blind" the detector and makes analysis of the sample impossible.

In order to analyze high Na samples, such as rock salt, the Na must be separated from the remainder of the sample or the elements to be analyzed must be isolated from the Na and other elements of the

sample. First, it was attempted to remove Na from the sample by passing the dissolved sample through a chromatography column charged with hydrated antimony pentoxide (HAP) as suggested by Gills and others (1970). This rather time consuming procedure did in fact remove the Na, however enough Sb was added to the sample to produce nearly the same effect (to a lesser extent) as that produced by a high Na concentration.

Next, standard ion exchange chromatography was used to separate the elements to be analyzed from the remainder of the sample. This procedure was dismissed due to its lenghthiness and the uncertainty of element yield from the chromatography column.

At the time of this writing, a new procedure is being developed which will probably allow high Na samples to be irradiated and analyzed with the accuracy and rapidity of silicate sample analyses. Samples will be loaded into pure Mn metal rabbits which should block those specific energy level neutrons that create ^{24}Na from ^{23}Na. Theoretically, the procedure should be successful, but no actual sample analysis has yet been attempted.

ANALYTICAL DATA AND RESULTS

Whole Rocks

Mineralogy

Whole rock samples were analyzed by X-ray diffraction techniques to determine their major mineralogic composition. Evaporite mineral compositions of the samples were obtained from this procedure (Table 5). Though detailed evaporite mineral composition of the analyzed samples is discussed in the next section, it should be noted that most whole rocks consist primarily of halite or sylvite with minor amounts of sulfate minerals.

Samples with detectable insoluble material were separated into two fractions, a water soluble and a water insoluble portion. The percentage of water insoluble material in some of the samples was determined by this procedure (Table 2). Insoluble residue in most samples ranged from one to eighteen percent; however, some samples had insoluble residue concentrations as low as 0.1 percent and as high as 32 percent. The insoluble material was comprised primarily of quartz sand and clay minerals.

Major Element Data

Ten whole rock samples were analyzed for major element composition primarily to verify the X-ray identification of the mineralogies determined (Table 3). Many of the cationic species are reported simply as metals (instead of oxides) as the oxygen abundance of these samples is an unknown. The Na concentration in most of the samples is in excess

Table 2. Percentage of water insoluble residue in some samples from the Salado Formation.

Corehole	Footage	Percent Insoluble Residue
ERDA-9,	1404.8-1405.8	7.20
	1648.5-1649.0	2.1
	1759.1-1759.8	0.7
	1621.9-1622.2	0.8
	1709.0-1709.5	1.1
	1633.6-1634.1	0.4
	1652.8-1653.1	0.3
	1772.0-1772.4	12.6
	1713.6-1714.0	18.2
ERDA-6,	1421.0-1421.7	1.2
AEC-8,	1607.0-1608.0	9.0
	1610.8-1611.3	9.0
	1622.4-1622.9	2.0
	1636.6-1637.1	3.7
	1645.0-1645.3	0.8
	1715.4-1715.7	1.1
	1671.2-1671.8	11.3
	1782.2-1782.4	12.5
DV-4B		15.7
4C		12.3
4D		32.3
5A		10.3
4E		~0.0
5C		17.0
3B		17.2
2C		17.3

Table 3. Major element data for some whole rock samples from the Salado Formation.

Oxide or Element	AEC-8, 1607.0-1608.0	AEC-8, 1622.4-1622.9	AEC-8, 1671.2-1671.8	AEC-8, 1715.4-1715.7	AEC-8, 1782.2-1782.4
SiO_2	2.83	0.10	4.64	0.16	0.16
Al_2O_3	0.616	<0.01	0.750	0.080	0.01
Fe_2O_3	0.190	0.005	0.190	0.043	0.020
P_2O_5	0.028	<0.01	<0.01	<0.01	<0.01
Mg	1.34	0.155	1.33	0.026	9.83
Ca	0.330	0.457	0.277	0.358	0.031
Na	27.67	31.08	29.15	35.61	13.43
K	4.48	1.78	0.498	0.365	0.199
H_2O^-	0.84	0.02	0.84	0.06	9.60
Cl	52.66	55.18	48.70	57.78	3.48
SO_3	0.58	1.41	0.46	0.67	45.05

All concentrations expressed as weight percent.

Table 3. (continued).

Oxide or Element	ERDA-6 1421.0-1421.7	DV-2C	DV-3A	DV-5A	DV-5C
SiO_2	0.10	5.13	0.56	4.28	8.08
Al_2O_3	<0.01	1.12	0.118	0.922	0.185
Fe_2O_3	0.015	0.213	0.040	0.148	0.280
P_2O_5	<0.01	<0.01	<0.01	<0.01	<0.01
Mg	0.259	6.33	8.93	1.63	4.64
Ca	0.786	0.013	0.014	0.026	0.016
Na	36.13	17.43	10.83	33.90	24.11
K	0.797	7.47	13.53	1.02	2.66
H_2O^-	0.02	0.79	0.19	0.64	1.93
Cl	56.44	24.67	15.86	48.18	38.34
SO_3	3.00	22.90	41.88	1.43	5.34

All concentrations are expressed as weight percent.

of 20 percent, reflecting the large abundance of halite present. Any K found can generally be attributed partly to the occurrence of sylvite, and in the case of samples containing appreciable Mg, Ca and SO_3, to minerals such as polyhalite or langbeinite. All the SiO_2 and Al_2O_3 detected is attributed to the varying amounts of detrital silicate minerals found in the whole rock sample. Most of the Fe_2O_3 present is probably associated with non-evaporite material in the rocks, most likely the clay mineral fraction or as oxide-hydroxide coatings on other minerals.

Rubidium-Strontium Data

Eighteen whole rock samples were analyzed for Rb and Sr concentration as well as Sr isotopic ratio (Table 4). Rubidium concentration in these samples ranges from 0.27 ppm (AEC-8, 1782.2-1782.4) to 262.5 ppm (AEC-8, 1636.6-1637.1); most have Rb concentrations less than 10 ppm. The Sr concentration of these samples is quite a bit higher than the Rb and ranges from 5.04 ppm (ERDA-9, 1404.8-1405.8) to 156.9 ppm (ERDA-6, 1421.0-1421.7) with most samples in the range of 15 ppm to 50 ppm Sr. $^{87}Sr/^{86}Sr$ ratios vary from 0.7958 (ERDA-9, 1404.8-1405.8) to 0.7068 (AEC-8, 1622.4-1622.9). The majority of the whole rock samples have $^{87}Sr/^{86}Sr$ ratios under 0.7100, reflecting the low Rb/Sr ratio and young age of the rocks.

A plot of the $^{87}Sr/^{86}Sr$ ratio against the $^{87}Rb/^{86}Sr$ ratio for each whole rock sample yields an apparent isochron age of 171 ± 36 m.y. (Fig. 5) by the least squares cubic regression method of York (1969). The date of 172 m.y. must be considered very approximate as all but three

Table 4. Rb-Sr data for Salado Formation whole rock samples.

Sample Number		Rb (ppm)	Sr (ppm)	$\frac{^{87}Sr}{^{86}Sr}$	$\frac{Rb}{Sr}$	$\frac{^{87}Rb}{^{86}Sr}$
AEC-8,	1607.0-1608.0	25.53	54.78	.7274	0.466	1.352
	1610.8-1611.3	14.17	63.22	.7095	0.224	0.649
	1622.4-1622.9	5.00	111.73	.7068	0.045	0.130
	1636.6-1637.1	262.50	12.35	.7279	21.255	61.655
	1645.0-1645.3	0.36	50.04	.7152	0.007	0.021
	1671.2-1671.8	5.55	40.43	.7099	0.139	0.401
	1715.4-1715.7	0.70	91.65	.7089	0.008	0.022
	1762.0-1762.3	1.29	38.65	.7100	0.033	0.097
	1782.2-1782.4	0.27	5.81	.7147	0.046	0.135
ERDA-9,	1404.8-1405.8	66.98	5.04	.7958	13.290	38.813
	1621.9-1622.2	0.72	61.36	.7082	0.012	0.034
	1633.6-1634.1	6.57	80.42	.7096	0.082	0.237
	1648.5-1649.0	0.47	44.86	.7080	0.010	0.030
	1652.8-1653.1	0.41	23.44	.7074	0.017	0.051
	1709.0-1709.5	0.68	9.65	.7091	0.070	0.024
	1759.1-1759.8	0.32	52.10	.7081	0.006	0.018
ERDA-6,	1421.0-1421.7	0.59	156.94	.7097	0.004	0.011
DV-5A		10.57	5.94	.7243	1.779	5.160

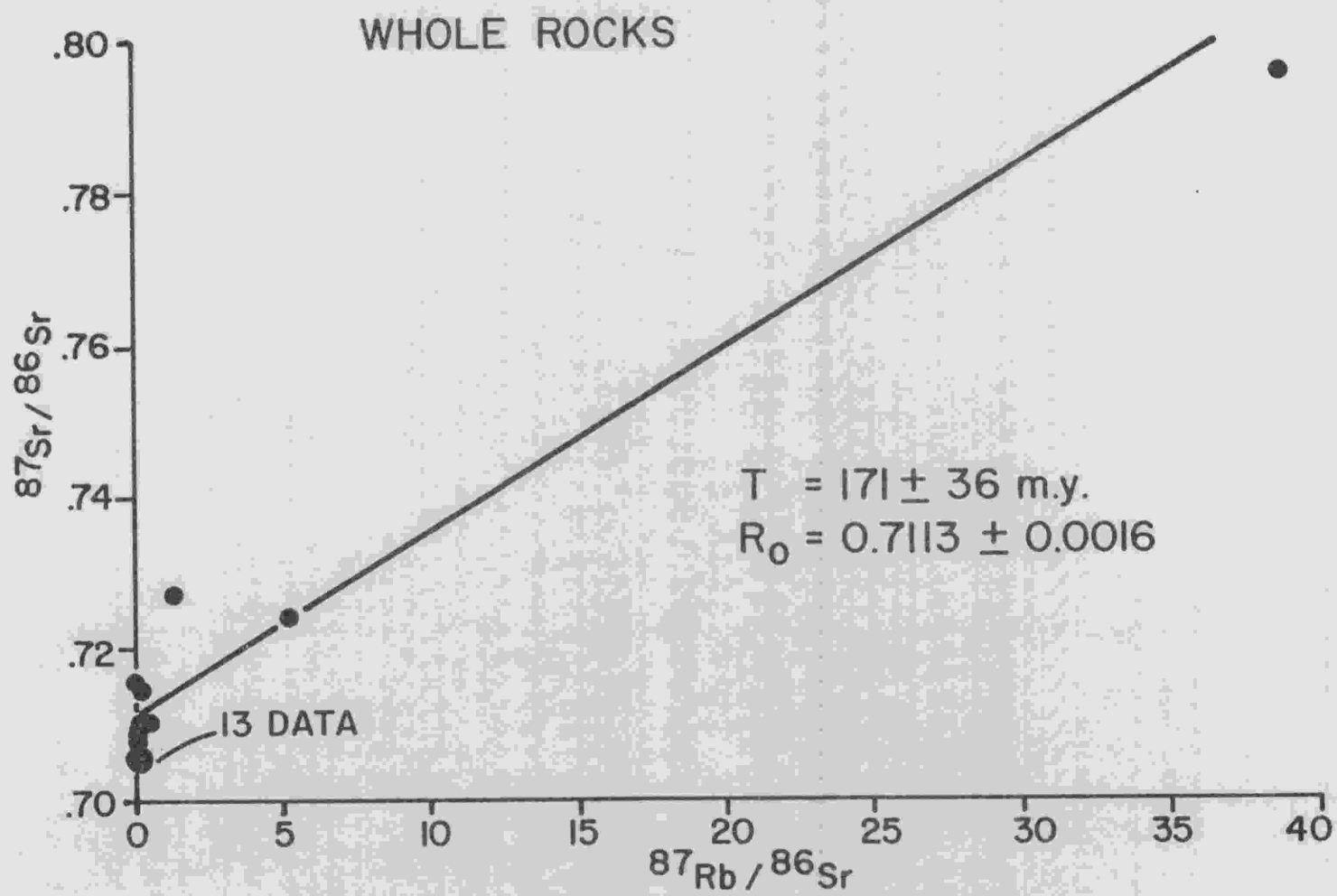

Figure 5. Rb-Sr isochron plot of whole rock samples from the Salado Formation.

samples plot essentially on the ordinate. Of the fifteen remaining samples, ten are used to produce a reasonable estimate of the initial $^{87}Sr/^{86}Sr$ ratio of 0.7085 ± 0.0010.

Evaporite Minerals

Mineralogy

Thirty-one samples were analyzed for mineralogic composition by X-ray diffraction techniques; the results are noted in Table 5. Nearly all the samples consist primarily of halite (80 to 90 percent in most cases); some samples (AEC-8, 1636.6-1637.1, for example) contain as much as 50 percent sylvite. Sulfate minerals are present in many samples. Polyhalite is probably the most common sulfate mineral and makes up as much as 90 percent of at least one sample (DV-1A). Langbeinite was found in only six samples but makes up as much as 70 to 80 percent of some of them (DV-4E, for example). The only carbonate mineral detected is magnesite, which is present in five samples with abundances of 5 to 30 percent. Loeweite is tentatively identified in two samples, but its identification was rather difficult due to large number of peaks present of the two diffractograms. Typical evaporite diffractograms are given in Appendix 1.

Most evaporite mineral samples were obtained by dissolving the whole rock samples in water and separating the water soluble material from the insoluble residue. In cases where very large amounts of partially soluble sulfate minerals were present, these minerals were physically separated from the remainder of the whole rock sample before dissolution.

Table 5. Evaporite mineral composition of some samples from the Salado Formation.

Sample Number	Loeweite	Halite	Sylvite	Anhydrite	Polyhalite	Magnesite	Langbeinite
ERDA-9, 1713.6-1714.0	-	90	10	-	-	-	-
1759.1-1759.8	-	85	5	-	10	-	-
1709.0-1709.5	-	85	10	-	5	-	-
1621.9-1622.2	-	65	5	-	-	30	-
1633.6-1634.1	-	90	5	-	-	5	-
1652.8-1653.1	-	85	5	-	-	10	-
1648.5-1649.0	-	95	5	-	-	-	-
1404.8-1405.8	-	40	5	5	-	-	50
ERDA-6, 1421.0-1421.7	-	90	10	-	-	-	-
AEC-8, 1782.2-1782.4	25	5	5	-	25	-	-
1762.0-1762.3	-	100	-	-	-	-	-
1671.2-1671.8	-	95	5	-	-	-	-
1715.4-1715-7	-	95	5	-	-	-	-
1636.6-1637.1	-	45	50	-	-	-	5
1645.0-1645.3	-	100	-	-	-	-	-
1622.4-1622.9	-	85	15	-	-	-	-
1610.8-1611.3	-	85	10	-	5	-	-
1607.0-1608.0	-	65	35	-	-	-	-

All units given are in percent abundance.

Table 5 (continued).

Sample	Loeweite	Halite	Sylvite	Anhydrite	Polyhalite	Magnesite	Langbeinite
DV-1A	-	5	5	-	90	-	-
1B	-	40	60	-	-	-	-
1C	-	50	-	-	50	-	-
1D	-	50	50	-	-	-	-
2A	5	45	50	-	-	-	-
2B	-	15	5	-	80	-	-
4A	-	5	5	-	-	15	75
4B	-	95	5	-	-	-	-
4C	-	95	5	-	-	-	-
4D	-	95	-	-	-	5	-
4E	-	15	-	-	-	-	85
5A	-	100	-	-	-	-	-
5B	-	75	20	-	-	-	5

All units given are in percent abundance.

Major Element Data

Major element analyses were obtained for eight evaporite mineral samples (Table 6) to aid in identification of mineralogies present and to determine which elements detected in the whole rock samples were attributable to silicate minerals (non-evaporite material). No SiO_2 or Al_2O_3 is found in these samples, reflecting the rather insoluble nature of these two elements. The remainder of the elemental abundances are quite similar to those reported for the whole rock samples. The only exception is the Fe_2O_3 content, which is appreciably lower in the evaporite minerals indicating its probable association with the non-evaporite portion of the sample.

Rubidium-Strontium Data

Forty-one evaporite mineral samples were analyzed for Rb and Sr concentration in addition to Sr isotopic ratio. Two anhydrite samples were analyzed for Sr isotopic composition only (Table 7). Rubidium concentration in the salt rich samples ranges from 0.22 ppm (AEC-8, 1782.2-1782.4) to 70.69 ppm (ERDA-9, 1404.8-1405.8). However, most samples have Rb concentrations of less than 10 ppm. Strontium concentration in the salt-rich samples is between 0.27 ppm (DV-2C) and 269.5 ppm (AEC-8, 1610.8-1611.3); most samples have from 30 to 70 ppm Sr. The four polyhalite samples analyzed have much higher Sr concentrations; from 767.6 ppm (ERDA-9, 1499.0-1500.0) to 1563 ppm (AEC-8, 1618.9-1619.4).

$^{87}Sr/^{86}Sr$ ratios for all samples range from 0.7071 (AEC-8, 1715.4-1715.7) to 1.6412 (DV-2C). Most samples possess $^{87}Sr/^{86}Sr$

Table 6. Major element analysis of evaporite mineral samples from the Salado Formation.

Oxide or Element	AEC-8, 1622.4-1622.9	AEC-8, 1782.2-1782.4	ERDA-9, 1404.8-1405.8	ERDA-9, 1709.0-1709.5
Fe_2O_3	<0.01	<0.01	<0.01	<0.01
P_2O_5	<0.01	<0.01	<0.01	<0.01
Mg	0.096	7.54	8.08	1.71
Ca	0.393	0.014	<0.01	0.043
Na	35.61	15.95	3.78	29.75
K	1.77	0.108	12.62	3.51
H_2O^-	0.04	0.21	<0.01	0.69
Cl	57.78	2.57	8.91	48.41
SO_3	1.58	53.16	40.94	10.70

All concentrations are expressed as weight percent.

Table 6 (continued).

Oxide or Element	DV-2C	DV-3A	DV-3B	DV-5A
Fe_2O_3	<0.01	<0.01	<0.01	<0.01
P_2O_5	<0.01	<0.01	<0.01	<0.01
Mg	2.71	1.71	7.84	0.573
Ca	<0.01	0.043	<0.01	<0.01
Na	21.66	29.75	9.87	36.05
K	7.72	3.51	12.04	0.789
H_2O^-	1.68	0.69	0.99	0.34
Cl	32.10	48.41	16.60	57.44
SO_3	23.44	10.70	40.26	1.49

All concentrations are expressed as weight percent.

Table 7. Rb-Sr data for evaporite mineral samples from the Salado Formation.

Sample Number	Rb (ppm)	Sr (ppm)	$\frac{^{87}Sr}{^{86}Sr}$	$\frac{Rb}{Sr}$	$\frac{^{87}Rb}{^{86}Sr}$
AEC-8, 1607.0-1608.0	26.65	45.61	.7175	0.584	1.693
1610.8-1611.3	14.78	269.53	.7126	0.055	0.159
1622.4-1622.9	1.23	111.80	.7076	0.011	0.032
1636.6-1637.1	39.54	9.54	.7223	4.145	12.016
1645.0-1645.3	0.28	44.29	.7107	0.006	0.018
1671.2-1671.8	0.78	42.16	.7083	0.019	0.054
1715.4-1715.7	1.11	83.88	.7071	0.013	0.038
1762.0-1762.3	1.07	37.59	.7081	0.028	0.082
1782.2-1782.4	0.22	4.95	.7156	0.044	0.129
ERDA-9, 1404.8-1405.8	70.69	2.36	.9625	29.953	88.857
1621.9-1622.2	0.94	142.84	.7086	0.007	0.019
1633.6-1634.1	0.31	144.93	.7207	0.002	0.006
1648.5-1649.0	0.29	43.30	.7081	0.007	0.019
1652.8-1653.1	0.25	64.06	.7100	0.004	0.011
1709.0-1709.5	0.99	8.44	.7100	0.117	0.340
1713.6-1714.0	2.02	34.20	.7075	0.059	0.171
1759.1-1759.8	1.83	52.84	.7085	0.035	0.100
1772.0-1772.4	1.49	57.81	.7073	0.026	0.075
ERDA-6, 1421.0-1421-7	1.42	182.64	.7086	0.008	0.023
DV-1C	60.17	4.25	.8623	14.158	41.601
1D	29.08	5.78	.7481	5.031	14.622

Table 7 (continued).

Sample Number	Rb (ppm)	Sr (ppm)	$\frac{^{87}Sr}{^{86}Sr}$	$\frac{Rb}{Sr}$	$\frac{^{87}Rb}{^{86}Sr}$
DV-2B	20.69	6.71	.7428	3.083	8.957
2C	29.04	0.27	1.6412	107.556	329.012
3A	6.90	5.63	.7616	1.226	3.567
3B	39.36	1.37	.9618	28.730	85.222
4B	4.42	45.28	.7112	0.098	0.283
4C	2.58	26.80	.7112	0.096	0.279
4D	13.11	2.09	.7203	6.273	18.182
4E	13.20	8.08	.7216	1.634	4.736
5A	4.14	4.01	.7076	1.032	2.989
5C	10.98	1.55	.7352	7.084	20.563
MC-1A	1.36	48.61	.7083	0.028	0.081
2A	2.19	65.84	.7099	0.033	0.096
2C2	3.98	93.44	.7074	0.043	0.123
2C3	1.62	60.40	.7121	0.027	0.078
2C4	2.85	76.61	.7076	0.037	0.108
3A	19.92	2.08	.7259	9.577	27.775
Polyhalite and Anhydrite					
Polyhalite					
ERDA-9, 1215.2-1215.3	4.35	1108.37	.7078	0.004	0.011
1499.0-1500.0	5.21	767.63	.7074	0.007	0.020
1784.2-1784.3	3.98	845.53	.7082	0.005	0.014

Table 7 (continued).

Sample Number	Rb (ppm)	Sr (ppm)	$\frac{^{87}Sr}{^{86}Sr}$	$\frac{Rb}{Sr}$	$\frac{^{87}Rb}{^{86}Sr}$
AEC-8, 1618.9-1619.4	5.68	1563.25	.7081	0.004	0.011
anhydrite					
ERDA-9, 1630.7-1631.0			.7071		
2836.0-2836.4			.7074		

ratios less than 0.7200. The extremely Sr-rich polyhalite and anhydrite samples analyzed have an average $^{87}Sr/^{86}Sr$ ratio of 0.7077 ± 0.0004 (1σ).

Plotting the $^{87}Sr/^{86}Sr$ ratio against the $^{87}Rb/^{86}Sr$ ratio for each sample yields an isochron age of 199 ± 20 m.y. and an initial $^{87}Sr/^{86}Sr$ ratio of 0.7076 ± 0.0014 (Fig. 6). The data that plot essentially on the ordinate give an average $^{87}Sr/^{86}Sr$ ratio of 0.7084 ± 0.0014. The same data were used to construct Fig. 7 but the scale was expanded to show the data scatter below the isochron in the lower left-hand corner of the plot. This scatter (samples AEC-8, 1636.6-1637.1, DV-4D, DV-5C, MC-3A) can probably be attributed to contamination of the small amount of evaporite mineral Sr in these samples by the lower $^{87}Sr/^{86}Sr$ ratio Sr present in seawater. The sample which lies distinctly above the isochron near the ordinate may have incorporated excess radiogenic ^{87}Sr from the detrital material contained within the whole rock. With the five samples deleted which fall well off the isochron, an isochron age of 214 ±15 m.y. is obtained with an initial $^{87}Sr/^{86}Sr$ ratio of 0.7093 ± 0.0007 (Fig. 8). This 214 ± 15 m.y. age most likely represents the most meaningful determination of the time of deposition or final equilibration of the evaporite minerals. Further, this date is within the stated limits of error given by Tremba (1973; see Discussion).

Trace Element Data

Four polyhalite and two anhydrite samples taken from the ERDA-9 and AEC-8 cores were analyzed for twelve trace elements as well as Na_2O

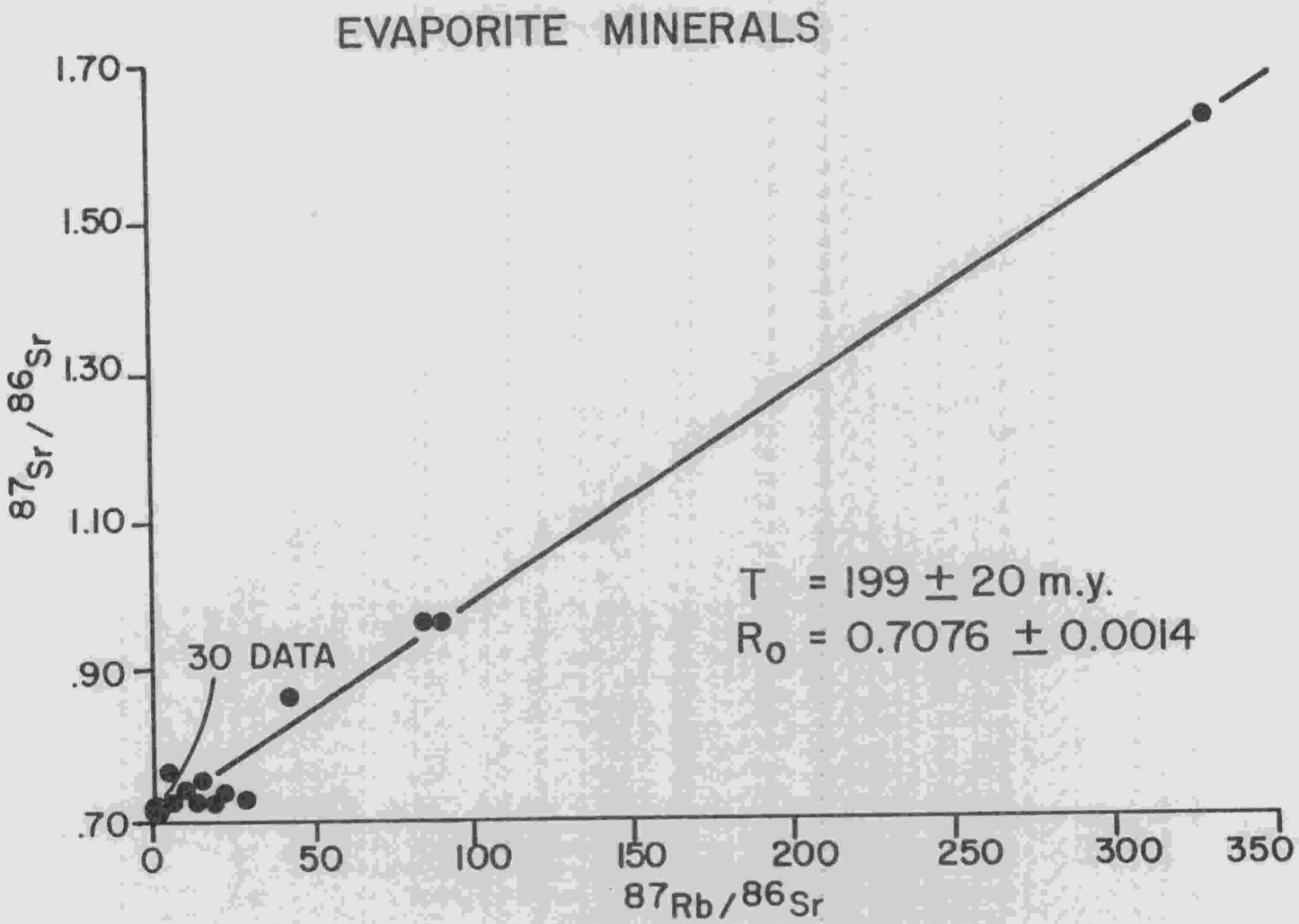

Figure 6. Rb-Sr isochron plot of evaporite mineral samples from the Salado Formation.

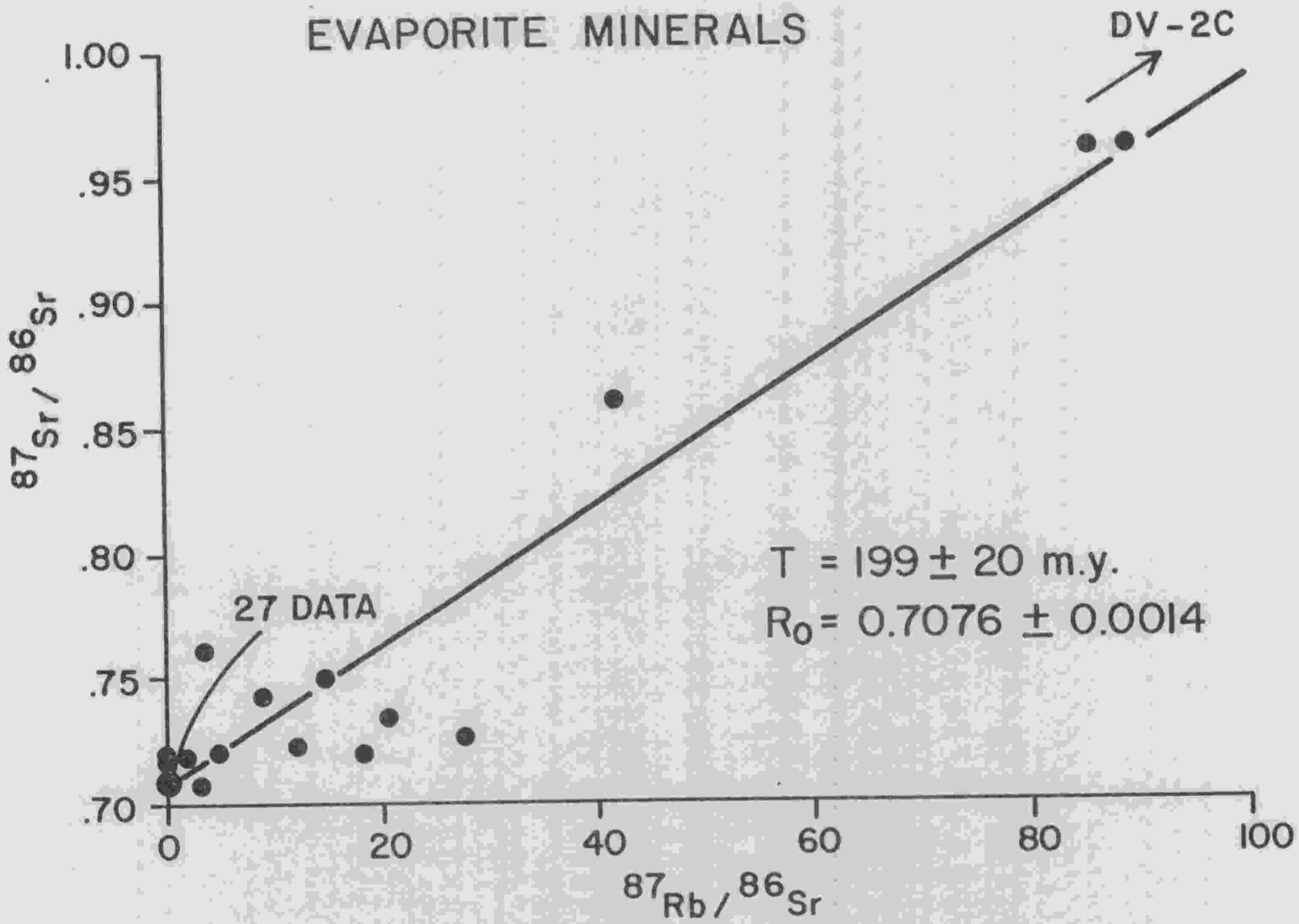

Figure 7. Rb-Sr isochron plot of evaporite mineral samples from the Salado Formation with the scale expanded.

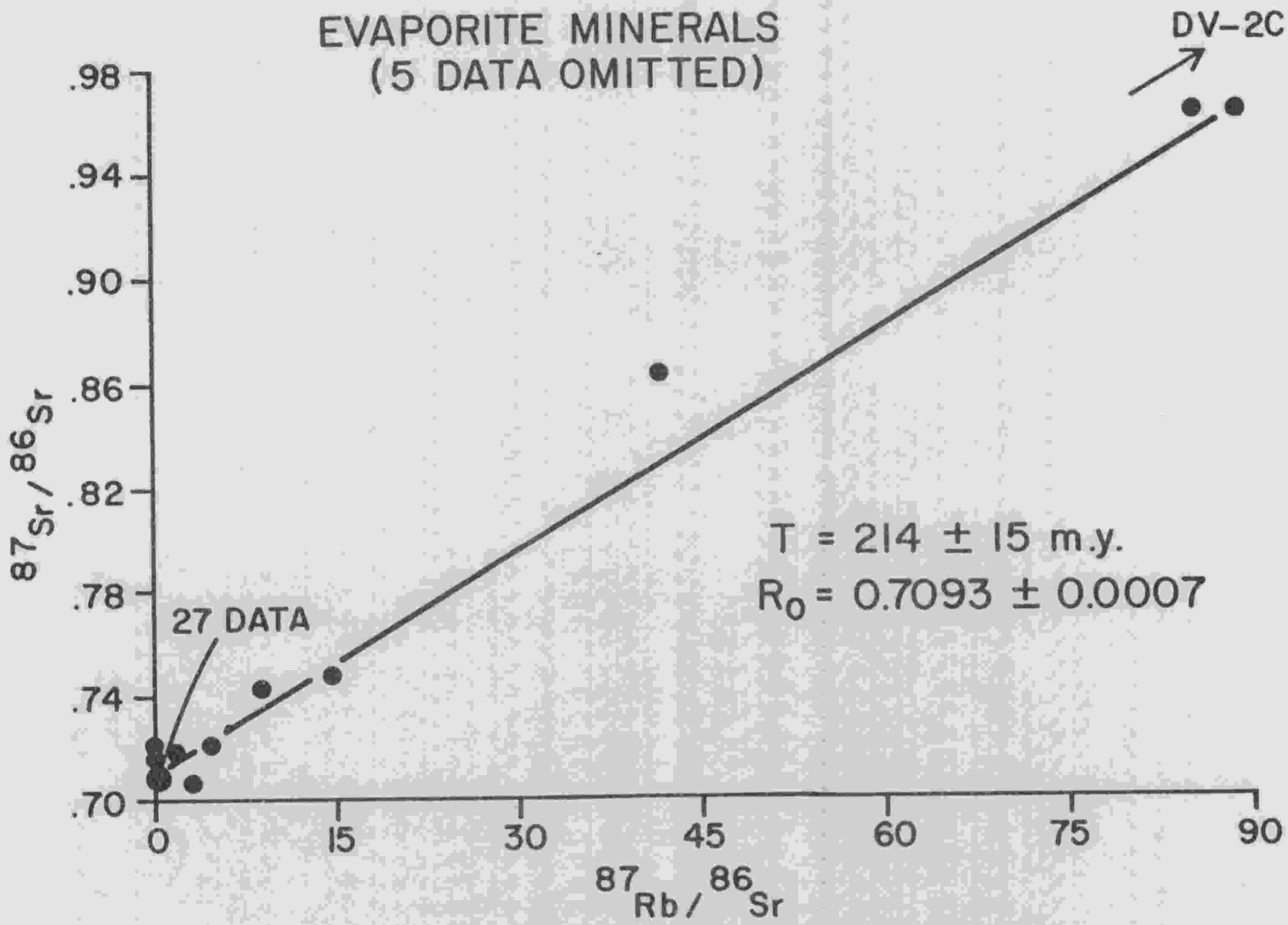

Figure 8. Rb-Sr isochron plot of evaporite mineral samples from the Salado Formation with five data deleted.

and Fe_2O_3 by INAA. The results for each sample are given in Appendix 7; the averages are given in Table 8. Samples were also analyzed for K_2O, but the K_2O content in the polyhalite samples is well above that found in the highest calibration standard, so the analysis is subject to question.

The polyhalite samples were analyzed to try to determine the general trace element chemistry present in the evaporitic brines. Also, it was thought that since many workers (c.f., Schaller and Henderson, 1932) construe the polyhalite in the Salado to be a secondary or replacement mineral, that it may have concentrated any trace elements present. Unfortunately, the trace element concentration in all four polyhalite samples is so low that most fall below the lower limits of detection of the method of analysis.

Of the elements detected, Na_2O and Fe_2O_3 are the most abundant in the polyhalites. The average Na_2O_3 concentration is about 6725 ppm, lower than one would expect for a mineral located within a few inches of massive halite. However, most of the polyhalite analyzed for this study is nearly stoichiometric. The average Fe_2O_3 content is about 3275 ppm which may reside in the polyhalite lattice (substituting for Mg) but which is probably present as Fe-oxides for Fe-hydroxides disseminated throughout the sample.

Zirconium and Ni also occur in the samples. Both Zr and Ni may be present in the polyhalite itself but more probably occur as oxides or hydroxides. Hafnium was detected in two samples, which is not surprising given the Zr concentration of the polyhalites. Scandium is

Table 8. Average trace and rare earth element concentration for four polyhalite and two anhydrite samples from the Salado Formation.

Element	Polyhalite Average (ppm)	Anhydrite Average (ppm)
Sm	ND	ND
Lu	ND	ND
Yb	ND	ND
Ba	ND	ND
Nd	2.37 in one sample	3.95 in one sample
La	0.55 in one sample	ND
Na_2O	6725.1	2584.7
K_2O	68975.7	385.1 in one sample
Ce	0.55 in one sample	ND
Th	0.15	0.10 in one sample
Cr	ND	ND
Rb	12.86	11.8
Tm	ND	0.12 in one sample
Hf	0.25 and 3.14 in two samples	ND
Zr	34.00	63.0
Ni	18.11	19.54 in one sample
Tb	0.11	0.09
Sc	0.07 and 0.14 in two samples	ND
Fe_2O_3	3274.0	1538.0
Ta	0.10	ND
Co	0.90	0.55 in one sample
Eu	0.07 in one sample	0.06 in one sample
Sb	0.21 and 0.07 in two samples	0.19 in one sample

ND = not detected

generally diadochic with Fe and was detected in two samples. Tantalum, Co, Th and Sb are present in most of the samples in low concentrations (less than 1 ppm).

Polyhalite is thought to be a replacement mineral or at least formed from very late stage brine solutions. Most of the trace elements present probably are simply distributed throughout the polyhalite rock as hydroxides or oxides, which were transported into the basin by run-off from the surrounding terrane.

The average trace element content of the two anhydrite samples analyzed is quite similar to that of the polyhalites. The primary difference noted is that the Fe_2O_3 and Na_2O contents of the anhydrite are only about half those in polyhalite. The other element concentrations are very similar, possibly suggesting a genetic relationship. If polyhalite is indeed a replacement or alteration product of anhydrite, it is quite conceivable that the trace elements noted in polyhalite simply reflect the trace element geochemistry of the original anhydrite. However, much more work needs to be conducted in this area before any firm, conclusive statements can be made.

Rare Earth Element Data

Nine rare earth elements (REE) were analyzed by INAA in four polyhalite and two anhydrite samples; the average values are given in Table 8, values for individual samples in Appendix 7. Unfortunately, the REE content of these samples was too low for meaningful conclusions to be drawn from the data. Many of the REE, Lu and Yb, for example, were below limits of detection (Appendix 7). The main point of interest

here is that the REE concentration in these samples is quite low, which is very similar to the REE concentration in seawater as reported by Hogdahl (1968).

Clay Minerals

Mineralogy

Twenty-two clay mineral samples obtained from evaporite whole rocks and clay seams within the salt were analyzed by X-ray diffraction techniques (Table 9); all abundances given are semi-quantitative at best. Interlayered chlorite-saponite and illite are the two most abundant clay minerals present and are both found in nearly every sample. The abundance of chlorite-saponite in the clay mineral fractions varies from about 95 percent (AEC-8, 1622.4-1622.9) to an undetectable level (AEC-8, 1671.2-1671.8, for one). Most samples average about 50 percent chlorite-saponite. Illite abundance ranges from 60 percent (AEC-8, 1610.8-1611.3) to less than five percent (ERDA-6, 1421.0-1421.7); the majority of the samples contain about 40 percent illite. Illite occurs primarily as the 2M polytype based on comparison of its diffraction spectra with those noted by Yoder and Eugster (1955).

Kaolinite is identified in most samples and comprises about 10 to 15 percent of the clay mineral fractions. Chlorite and saponite appear as separate species in a few samples but are much more common as interlayered species. Talc is found in about a third of the samples and constitutes as much as about 30 percent of one sample (AEC-8, 1782.2-1782.4).

Table 9. Mineralogic composition of minus 2 micron fraction samples from the Salado Formation.

Sample Number	Chlorite-Saponite	Illite	Kaolinite	Talc	Chlorite	Saponite
ERDA-9, 1404.8-1405.8	25	48	13	14	-	-
1648.5-1649.0	-	44	18	23	9	6
1713.6-1714.0	61	20	19	-	-	-
1772.0-1772.4	89	11	-	-	-	-
ERDA-6, 1421.0-1421.7	88	-	12	-	-	-
AEC-8, 1607.0-1608.0	69	20	11	-	-	-
1610.8-1611.3	25	60	15	-	-	-
1622.4-1622.9	95	5	-	-	-	-
1636.6-1637.1	33	53	14	-	-	-
1645.0-1645.3	18	40	12	5	25	-
1671.2-1671.8	-	17	-	-	-	83
1715.4-1715.7	5	54	18	-	23	-
1762.0-1762.3	21	40	11	28	-	-
1782.2-1782.4	13	44	11	32	-	-
DV-2C	71	19	10	-	-	-
3A	-	15	7	-	-	78
3B	55	34	11	-	-	-
4B	50	35	10	5	-	-
4C	58	34	8	-	-	-
4D	79	13	8	-	-	-
5A	72	16	6	6	-	-
5C	37	49	14	-	-	-

All concentrations are expressed as percent relative abundance.

It is readily apparent from the clay mineralogy described above that a large percentage of the clay minerals found represent allogenic material incorporated into the rocks during evaporite deposition. Though kaolinite often occurs authigenically in sedimentary rocks (Grim, 1968), it is generally formed in high-alumina environments. An evaporite-forming brine is certainly not such an environment. The lack of Al in the brine is also evidenced by the occurrence of saponite, a trioctahedral smectite containing little, if any, Al in the exchangeable octahedral sites. The chlorite-saponite interlayered clay may represent an incomplete alteration product formed from interaction of the Mg-rich brine solution with more commonly occurring dioctohedral montmorillonite. In any case, the clay mineralogy suggests that a significant amount of the clay minerals found in the evaporite rocks are detrital in origin and not authigenic.

Major Element Data

Two mineralogically representative clay mineral samples were analyzed to determine their major element chemistry (Table 10). Since anions other than oxygen, Cl and SO_3, are very low in abundance in these samples, element concentrations are expressed as oxides. SiO_2 and MgO comprise the bulk of these samples, making up some 60 percent of both. As expected, the Al_2O_3 concentration is rather low, attributable to the lack of Al in the octahedral sites of saponite, which makes up a large portion of both samples. Most of the MgO detected is probably resident in chlorite-saponite though some is probably present in illite replacing a portion of the K generally found in this mineral. The Fe_2O_3 content

Table 10. Major element composition of two representative minus 2 micron fraction samples from the Salado Formation.

Oxide or Element	ERDA-9, 1713.6-1714.0	ERDA-9, 1772.0-1772.4
SiO_2	33.33	31.99
TiO_2	0.438	0.312
Al_2O_3	12.10	11.00
Fe_2O_3	0.98	1.96
MnO	0.043	0.059
MgO	28.50	29.40
CaO	0.330	0.240
Na_2O	0.130	0.450
K_2O	1.13	0.560
P_2O_5	0.048	0.042
H_2O^+	4.41	4.75
H_2O^-	13.26	13.58
Cl	1.04	0.92
SO_3	<0.01	<0.01

of these samples is one to two percent giving these clays their characteristic red color. The rather high TiO_2 concentration found in these samples (approximately 0.5 percent) again argues for their detrital origin as Ti is quite insoluble in seawater and probably would not have been available during any possible *in situ* clay genesis.

Rubidium-Strontium Data

Rubidium and Sr concentration and Sr isotopic data were obtained for thirteen clay mineral samples (Table 11). The Rb concentration for these samples ranges from 29.37 ppm (ERDA-9, 1772.0-.772.4) to 84.39 ppm (ERDA-9, 1404.8-1405.8). The samples contain 14.75 ppm (DV-5A) to 82.42 ppm (AEC-8, 1607.0-1608.0) Sr. The $^{87}Sr/^{86}Sr$ ratio varies from 0.7185 (ERDA-9, 1772.0-1772.4) to 0.7632 (ERDA-9, 1404.8-1405.8).

An isochron plot of the clay mineral samples yields an age of 390 ± 77 m.y. and an initial $^{87}Sr/^{86}Sr$ ratio of 0.7112 ± 0.0049 (Fig. 9). Since much of the clay found in the evaporite rocks is probably detrital in origin, this older apparent age is not unexpected. Many workers (c.f., Hurley and others, 1962) have noted that detrital clay minerals will generally reflect the age of their provenance. In this case, it is felt that the clay minerals analyzed reacted with the brine solution containing them. This is confirmed by scanning electron microscopy (SEM) which shows corroded, rounded ditrital clay minerals and some second generation salts such as halite (D. G. Brookins, unpublished report, *in press*). Therefore, their apparent isochron age falls between the age of their provenence and the approximately 200 m.y. age obtained

Table 11. Rb-Sr data for minus 2 micron fraction samples from the Salado Formation.

Sample Number	Rb (ppm)	Sr (ppm)	$\frac{^{87}Sr}{^{86}Sr}$	$\frac{Rb}{Sr}$	$\frac{^{87}Rb}{^{86}Sr}$
AEC-8, 1607.0-1608.0	42.85	82.42	.7232	0.520	1.507
1671.2-1671.8	43.78	35.31	.7281	1.240	3.597
1636.6-1637.1	84.05	55.80	.7419	1.506	4.374
ERDA-9, 1404.8-1405.8	84.39	24.21	.7632	3.486	10.146
1713.6-1714.0	46.29	47.95	.7363	0.965	2.803
1772.0-1772.4	29.37	47.95	.7185	0.613	1.775
DV-2C	52.91	20.69	.7524	2.557	7.435
3A	31.86	19.04	.7551	1.673	4.867
4B	47.26	36.93	.7371	1.280	3.715
4C	36.65	26.70	.7234	1.373	3.980
4D	36.37	18.39	.7357	1.978	5.741
5A	36.93	14.75	.7432	2.504	7.273
5C	59.22	27.00	.7416	2.193	6.371

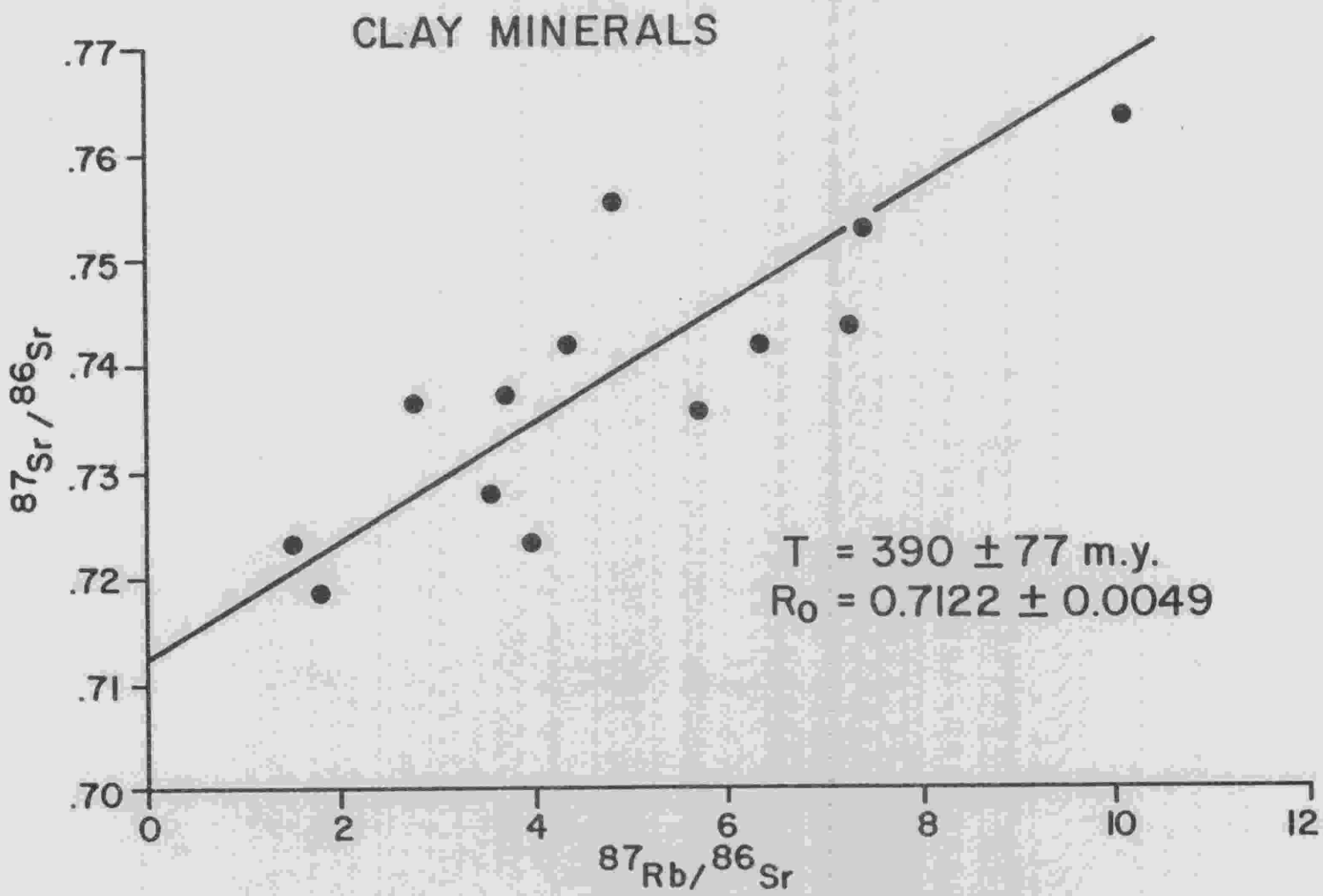

Figure 9. Rb-Sr isochron plot of clay mineral samples from the Salado Formation.

for the evaporite minerals. In actuality, detritus from rock ranging in age from Precambrian to late Paleozoic could have been transported either by normal, intermittent flooding or possibly by turbidity current transport into the evaporite basin.

Trace Element Data

Fourteen clay mineral samples obtained from the water insoluble fraction of salt samples and from clay seams within the massive salt strata were analyzed by neutron activation for twelve trace elements. Also included in the analyses were determinations of Na_2O, K_2O (for some samples) and Fe_2O_3. The results are given in Table 12.

These analyses were undertaken to help establish a data base for clay minerals which have been immersed in an evaporitic brine solution. Also, it was felt that an examination of the trace element and REE concentrations of these clays might help explain probable clay mineral-brine reactions. Furthermore, to understand the geochemical systematics of the evaporitic rocks of the Delaware Basin, it is certainly desirable to ascertain the role of the clay minerals as scavengers or ion exchangers.

Sodium concentration in these samples averages about 0.32 percent; most of the Na is probably present in the mixed layer chlorite-saponite, although some may be present in chloride minerals. The Na concentration is rather low for a clay which has been immersed in an evaporite brine solution, but much of it was probably replaced by Mg.

All samples analyzed contain at least one percent Fe_2O_3; many of them have Fe_2O_3 concentrations over two percent. Much of the Fe_2O_3 is

Table 12. Trace and rare earth element concentration for minus 2 micron fraction samples from the Salado Formation.

<2μ FRACTION

Neutron Activation Analysis & Delayed Neutron Activation Analysis

Sample Number	NAA																									DNAA
	% Na_2O	% K_2O	% Fe_2O_3	Cs	Ba	Sc	Zr	Hf	Ta	Cr	Rb	Co	Ni	Ag	Sb	Th	La	Ce	Nd	Sm	Eu	Tb	Tm	Yb	Lu	ΣRE.E.	K/Cs x 10^4
AEC-8, 1671.2 - 1671.8	0.159	NA	4.515	3.92	200.83	9.10	212.01	6.53	ND	102.58	119.65	7.00	ND		0.93	7.94	28.05	17.13	45.81	4.45	1.12	0.94	0.27	1.90	0.38	100.1	
1762.0 - 1762.3	0.365	NA	4.952	6.14	278.29	9.71	282.48	3.30	0.04	107.66	156.02	11.93	20.23		1.36	6.04	19.37	50.36	16.79	3.90	1.22	0.66	0.37	0.93	0.38	94.0	
ERDA-9, 1709.0 - 1709.5	0.247	NA	10.53	4.27	2529.9	11.17	3791.6	8.94	ND	572.59	297.19	35.08	ND		ND	14.86	75.83	61.80	242.0	14.69	ND	ND	0.83	56.80	2.55	454.5	
1713.6 - 1714.0	1.47	NA	2.47	2.73	237.60	9.42	186.16	1.19	ND	85.56	84.49	8.18	20.19		0.78	8.40	20.68	48.50	43.18	3.39	0.88	0.09	0.19	1.52	0.28	118.4	
1772.0 - 1772.4	0.128	NA	3.97	1.85	ND	8.90	222.69	1.79	0.12	2.65	31.53	7.95	25.15		1.56	7.33	19.56	17.18	17.00	3.38	1.01	0.39	0.25	2.26	0.21	61.24	
DV- 2B	0.110	NA	3.94	4.95	1294.8	9.68	1204.3	2.94	2.04	ND	109.95	6.59	38.76		10.84	6.36	20.17	78.77	81.81	4.77	2.96	1.25	0.70	2.80	0.86	194.1	
2C	0.143	1.17	3.09	2.00	171.52	9.59	ND	1.94	1.02	54.09	92.52	5.00	40.80		1.84	6.90	18.80	38.87	31.13	5.15	0.91	ND	0.24	1.22	0.30	96.6	0.49
3A	0.102	0.536	1.59	1.71	63.56	7.99	62.84	1.23	0.25	47.22	40.46	3.31	14.42		3.51	4.44	15.88	27.12	19.26	2.79	0.77	ND	ND	0.98	0.24	67.0	0.26
3B	0.114	NA	1.92	1.21	140.77	8.20	ND	0.61	0.53	42.40	20.39	4.74	ND		6.17	5.69	13.35	35.85	19.46	6.98	0.78	ND	0.20	6.37	0.71	83.7	1.01
4B	0.133	2.84	3.45	2.33	120.62	9.53	213.77	1.58	0.15	52.17	97.35	4.92	18.94		NA	6.14	27.42	45.48	33.42	6.02	0.54	0.22	ND	1.18	0.33	114.61	0.14
4C	0.230	0.534	1.41	3.07	2.49	7.20	157.67	0.73	0.14	45.79	ND	16.71	ND		ND	3.76	0.29	20.64	0.33	0.29	0.41	ND	0.12	0.08	0.35	22.51	NA
4D	NA	NA	2.63	1.83	NA	7.80	147.49	1.04	0.38	32.92	40.12	3.51	18.14		0.31	3.80	12.15	23.98	10.14	1.64	0.23	ND	0.12	0.39	0.14	48.8	0.18
4E	0.222	0.870	2.32	4.10	903.81	11.13	733.15	ND	1.74	84.90	169.93	15.40	33.96		35.27	6.50	17.89	70.77	42.08	5.17	0.71	ND	0.32	5.39	1.78	144.1	ND
5A	0.587	1.395	2.15	1.56	ND	7.85	ND	0.98	0.45	55.09	44.72	3.14	27.95		ND	5.16	29.49	11.59	21.07	1.18	0.19	0.03	0.22	1.14	0.15	65.06	0.74
														Average			22.78	39.15	44.53	4.56	0.84	0.26	0.27	5.93	0.62		

Concentrations in ppm except where noted
ND = Not detected
NA = Not analyzed

most likely contained in the chlorite-saponite mixed layer phase present in all samples.

The Cs concentration in these clay mineral samples ranges from 1.2 ppm to about 5.0 ppm; this concentration falls well within the reported range for Cs concentration in shales of 1.0 to 5.0 ppm (Gaines, 1972). Cs was probably incorporated into the clays during their formation and was not released into the brine solution during evaporite formation. This is supported by K/Cs ratios of 10,000 to 1400; most are between 1400 and 7000.

Barium concentration in the analyzed samples is highly variable, ranging from 2.5 ppm to 2530 ppm. Most of the Ba found is probably present as adsorbed ions on the clay particles, but samples with higher Ba concentrations may contain small amounts of $BaSO_4$, a highly insoluble compound known to precipitate from sea water (Pilkey, 1972).

The Sc concentration of these samples is only slightly variable and ranges from about 7.0 ppm to 11.0 ppm. This concentration of Sc is much higher than that observed in deep-sea carbonates (Curtis, 1972) indicating that the majority of Sc present in the clay minerals probably originated from their provenance and was not adsorbed from the evaporite brine solution.

Zirconium is abundantly present in these analyzed clay minerals; the concentration of Zr ranges from an undetectable level to as much as 3800 ppm. Most of Zr detected probably resides as adsorbed ions on the clay minerals, however, some may be present as very fine-grained zircon.

Hafnium and Zr are very closely related chemically and are generally found together in the geochemical environment; such is the case here. Hf concentration varies from an undetectable level to about 9.0 ppm; most samples have 1.0 to 2.0 ppm Hf. The Hf/Zr ratio is fairly constant in nature and averages about 0.02 (Fleischer, 1955). For these samples, the average Hf/Zr ratio is about 0.12, well within the limits of accepted variability for geologic samples.

Tantalum is known to be associated with hydrolysate sediments, such as clays (Rankama and Sahama, 1950) and is found in these samples in concentrations of below detectability to about 2.0 ppm. This concentration range is quite normal for clay minerals.

Since Cr readily substitutes for Fe, it is generally present in clays, such as those studied in this thesis, which contain appreciable amounts of Fe. The Cr concentration in these samples ranges from about 3.0 ppm to about 600 ppm; most samples contain approximately 50 ppm Cr.

Rubidium is present in these samples in concentrations of about 20 ppm to about 300 ppm. For the samples with available K analyses, the K/Rb ratio ranges from about 250 to 30. Most authigenic marine clays have an average K/Rb ratio of approximately 240, the mean crustal K/Rb ratio (Heier and Adams, 1964). However, it has been noted that Rb is adsorbed more strongly than K on most clay minerals, especially illites and smectites, during the weathering process (Reynolds, 1972). This preferential adsorption of Rb may lead to initial K/Rb ratios as low as 30. Also, clay minerals preferentially remove Rb over K from seawater, thus lowering the K/Rb ratio observed in many marine sediments.

Considering these possibilities, it is not surprising that some of these clay mineral samples have low K/Rb ratios. This is also consistent with the low K/Cs ratios mentioned earlier.

The Co concentration in the samples analyzed ranges from about 3.0 ppm to 35.0 ppm; most samples contain from 3.0 ppm to 10.0 ppm Co. Cobalt is generally considered to be quite mobile in the geologic environment (Young, 1957) and thus concentrated in marine deposits. In fact, some deep-sea sediments have been reported to contain as much as 70 ppm Co although the mean abundance for shales is reported as 19 ppm (Curtis, 1972). The clay samples analyzed for this study do not show any profound Co enrichment but fall in the generally accepted range for Co concentration in clay minerals.

The Ni concentration of the clay minerals analyzed ranges from approximately 14.0 ppm to about 40.0 ppm. This concentration of Ni is not unusual as Ni is siderophile and the samples analyzed contain abundant Fe. Since the Ni content of seawater is quite low, about 0.002 ppm (Mason, 1966), all the Ni present in clay minerals was probably derived from their provenance and not adsorbed during transport or deposition. The extremely low concentration of Ni in seawater also indicates that most of the Ni released by weathering and carried to the sea remains in the solid products of weathering in this case, clay minerals.

The crustal and seawater abundance of Sb is quite low (less than 1.0 ppm, Goldschmidt, 1954); some of the high Sb concentrations noted in the analyzed clays may be due to analytical error. Most of the samples analyzed have Sb concentrations of approximately 1.0 to 2.0 ppm. The

Sb found in these clay samples was probably adsorbed during their formation or scavenged from solutions during transport to the evaporite basin.

Thorium concentration in the samples analyzed ranges from about 4.0 ppm to 14.0 ppm. The average abundance of Th in shales is about 12.0 ppm (Adams and others, 1959) which is only slightly higher than the average abundance detected in these samples. Much of Th present in the samples probably was incorporated in the clay minerals during their formation through some may have been adsorbed during transport or after deposition into the Delaware Basin.

Rare Earth Element Data

Nine rare earth elements (REE) were analyzed in fourteen clay mineral samples; the results are given in Table 12. The average REE concentration (Table 12) of the fourteen samples relative to the composite of North American shales (NAS) is plotted in Fig. 10. Plots of the REE concentration of each sample relative to NAS are given in Appendix 8.

The total REE content of these samples is rather variable and ranges from 22.5 ppm to 455 ppm. The absolute concentration of each REE in the samples is also quite variable; however, the plots of REE concentration of each sample relative to NAS (Appendix 8) indicate that the normalized relative REE concentrations for each sample are quite similar. For this reason, only the average REE concentrations of the fourteen samples will be considered.

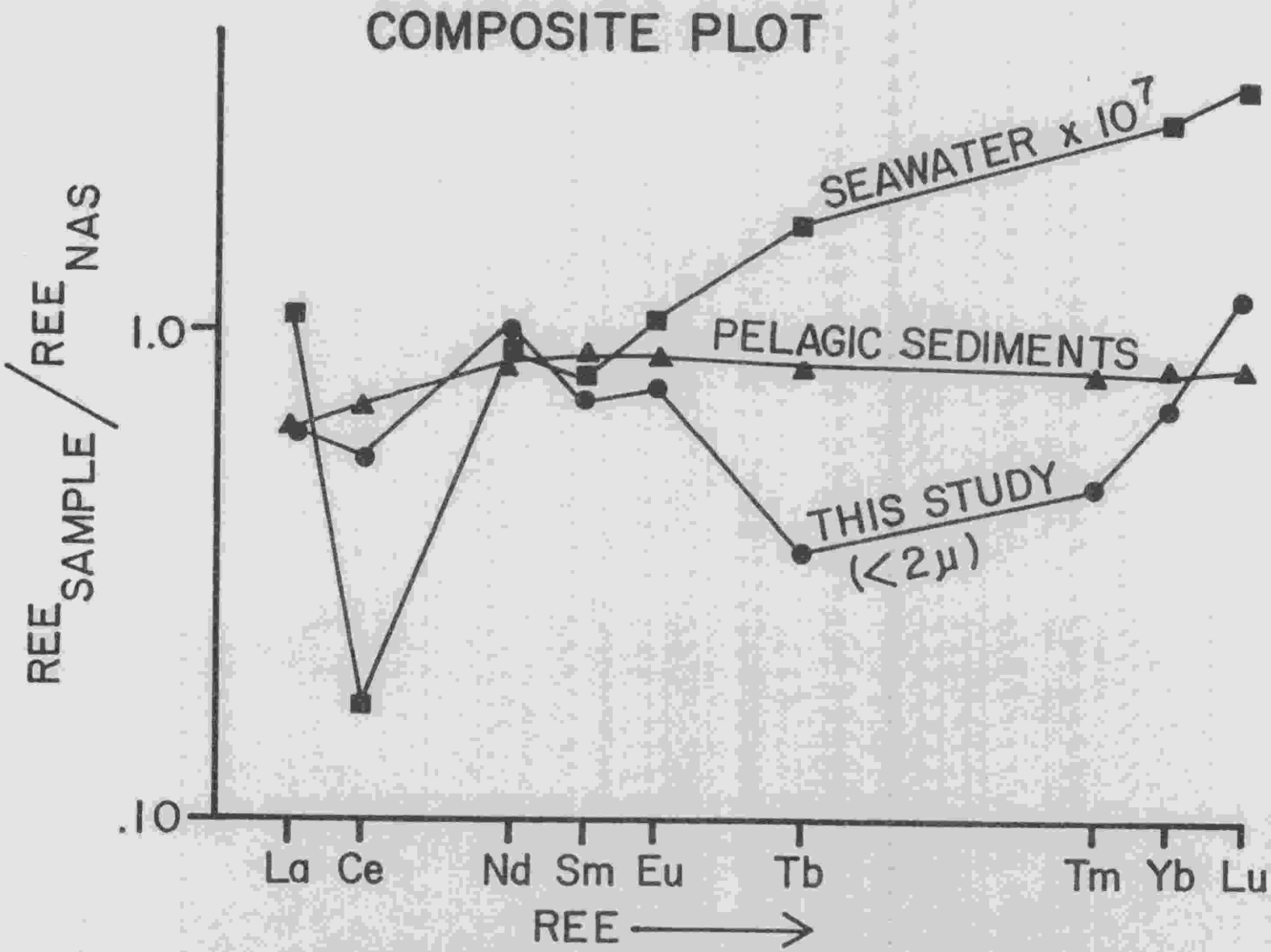

Figure 10. Plots of the average REE concentration relative to North American shales of the clay minerals from the Salado Formation (this study), seawater (Hogdahl, 1968) and pelagic sediments (Wildeman and Haskin, 1965).

If Tb and Tm are ignored (there are probably problems with Tb and Tm analyses), the average REE abundance for the samples relative to NAS is nearly unity for most elements. There are two anomalies noted in Fig. 10. First, there is a small negative Ce anomaly; second, it appears as though the heavier REE, such as Yb and Lu are generally enriched relative to the lighter REE. The negative Ce anomaly and the enrichment of the heavy REE is similar to the pattern observed in seawater (Hogdahl, 1968) but rather dissimilar to that seen in pelagic marine sediments (Wildeman and Haskin, 1965).

Seawater exhibits a negative Ce anomaly due to the loss of Ce from seawater, probably by creation of the relatively insoluble Ce^{4+} species and subsequent incorporation into ferromanganese nodules, which pave much of the ocean floor (Goldberg, 1961). The monotonic increase in the abundance of REE from Sm to Lu can most likely be attributed to the greater stability of complexes of heavy REE relative to those of lighter REE (Goldberg and others, 1963).

In the case of these clay samples, the Ce anomaly is not nearly as pronounced as that of seawater and may not be real if near maximum errors are assumed for both La and Ce. However, if Ce is anomalously low, it is quite conceivable that the clay minerals could have undergone ion exchange with the brine solutions, which most probably exhibited a strong negative Ce anomaly. The apparent increase in abundance of heavier REE relative to the lighter REE is probably also a product of clay mineral-brine solution interaction. This seems to be a plausible explanation for the REE abundances observed in these clay minerals as

this type of ion exchange has been previously noted by many workers (c.f., Carrol and Starkey, 1960; Russell, 1970). Depletion of the light REE in the clay fraction would be expected by substitution of Ca^{2+} or Na^{+} for the light REE whereas the ionic radii of the heavy REE would preclude such subsitution.

In order to explain more fully the interaction of the evaporite brine solution with the apparently detrital clay material, much more data must be collected and analyzed.

DISCUSSION

Many workers have studied the mineralogy, petrology and genesis of the Salado Formation so no effort will be made here to again describe the mineralogy. The Salado is made up primarily of halite and sylvite with minor sulfate mineralization. The Rb-Sr geochronology indicates that these minerals are probably all temporally cogenetic.

A discussion of the results of the dates obtained for the Salado Formation depends on knowledge of the age of the Permian-Triassic boundary. Webb and McDougall (1967) have recently estimated the age of this boundary to be 235 ± 5 m.y. This date was based on a K-Ar determination of a biotite from a tuff occurring in an Upper Permian sequence in the Bowen Basin of Australia. A supporting date of 220 m.y. was obtained for the Middle Triassic strata from southeastern Queensland, Australia and additional supporting dates by K-Ar mineral (217 ± 25 m.y.) and Rb-Sr whole rock isochron methods (218 m.y.) were noted. Other workers, such as Polevaya and others (1964) and Smith (1964) have determined the Permian-Triassic boundary to be about 235 ± 5 m.y.; this date is probably the best estimate of the boundary.

As noted previously, the Ochoa Series is generally considered to be Late Permian in age based on the occurrence of an invertebrate fauna occurring in the Rustler Formation in Culberson County, Texas (Walter, 1953). If the Salado Formation has remained a closed system with little internal elemental migration since deposition, the Rb-Sr geochronologic age should agree rather closely with the apparent geologic-geochronologic age of 235 m.y.

In this study, a Rb-Sr isochron age of 214 ± 15 m.y. has been determined for the evaporite minerals. This date is probably the best estimate of the age of final equilibration of the Salado Formation. Some data scatter is observed on the evaporite mineral isochrons but the scatter is not so severe as to create large uncertainties in the determined age. If substantial elemental migration had occurred recently, data scatter should be much more pronounced. It is quite unlikely that migration of Rb and Sr would have been regular enough not to create quite a bit of scatter on an isochron plot, as Rb and Sr have somewhat different chemical properties.

Even if the maximum error is assumed for the 214 m.y. date, an age of 229 m.y. is obtained, which is still about 6 m.y. less than the apparent geologic age of the Salado Formation. However, since there is very little Triassic strata present in this area, the time of final evaporite deposition of the Salado is difficult to ascertain. In final deposition occurred some 225 m.y. before the present, the age of the Salado Formation would correspond with the range of dates reported for the Permian-Triassic boundary. A 225 m.y. date is also within the limits of error of the 214 ± 15 m.y. date obtained in this study.

An initial $^{87}Sr/^{86}Sr$ ratio of 0.7093 ± 0.0007 is obtained from the evaporite mineral isochron. An average initial $^{87}Sr/^{86}Sr$ ratio is also obtained by consideration of the samples with low Rb/Sr ratios. This average initial $^{87}Sr/^{85}Sr$ ratio is 0.7084 ± 0.0014. Both methods of obtaining the initial $^{87}Sr/^{86}Sr$ ratio produce a value which is similar, but slightly higher, than the 0.7073 value reported by Peterman

and others (1970) for fossil shells of Late Permian age and the 0.7078 value reported by Brass (1973) for seawater-deposited limestones of the Late Permian. However, the 0.7093 ± 0.0007 and the 0.7084 ± 0.0014 values are within the limits obtained for the $^{87}Sr/^{86}Sr$ ratio of Permian seawater.

Four polyhalite samples were analyzed for Rb, Sr and Sr isotopic ratio; two anhydrite samples were analyzed for Sr isotopic ratio only. The Rb/Sr ratios of all four polyhalite samples are below 0.008. Therefore, the $^{87}Sr/^{86}Sr$ ratio is a reasonable approximation of the initial Sr isotopic ratio of the evaporitic brine solutions only if major re-equilibration of Sr has not occurred long after deposition. Since anhydrites generally contain very little Rb and copious quantities of Sr, their analyzed Sr isotopic content usually reflects their initial Sr isotopic concentration. The average $^{87}Sr/^{86}Sr$ ratio obtained from two anhydrite samples of 0.7073. The average $^{87}Sr/^{86}/Sr$ ratio obtained from the polyhalite samples is 0.7078. Both of these average values fall well within the range of Sr isotopic ratios reported for Permian seawater. Polyhalite is generally thought to be a replacement product of anhydrite and the Sr isotopic ratios measured for this study do not preclude this possibility; however, they do indicate that replacement probably occurred soon after deposition.

The evaporite mineral data seem to discount theories of substantial alkali-alkaline earth migration in the Salado Formation since its deposition. This hypothesis is in direct contrast to the discussion given by Tremba (1973). Tremba obtained Rb-Sr isochron dates of 129 ±

5 m.y. and 120 ± 28 m.y. for the Salado Formation. These ages were interpreted as an indication of isotopic re-equilibration during the Cretaceous. Unfortunately, Tremba based his hypothesis on very limited data which exhibited substantial scatter on the isochron plots. Also, in at least one case, one point (of a total of five data) which plotted well above the 129 m.y. isochron was discarded with no tangible reason given. If this point is included, the age calculated increases substantially. More important, Tremba's model age date, based on large, composite samples, yielded 230-240 m.y.

The apparent Rb-Sr isochron age of the clay minerals obtained from the massive salt rocks and clay seams within the Salado is 390 ± 77 m.y. The data scatter is reflected by the large uncertainty attached to the date. The data scatter can be attributed to ion exchange between the clay minerals and the brine solution. There are two major processes which would affect the measured Rb-Sr age; both would tend to make the clay minerals appear younger.

It is known that clays preferentially adsorb Rb over K from solutions containing both elements (Reynolds, 1972). As previously noted, the K/Rb ratio in many of these clay samples is significantly lower than the mean crustal K/Rb ratio. The lowering of this ratio probably represents replacement of K in the clays by Rb from the brine solution, a process which would incorporate excess Rb into the sample and thus lower its apparent Rb-Sr age.

Another process which would make the Rb-Sr age of clay minerals appear younger is the incorporation of low $^{87}Sr/^{86}Sr$ ratio Sr from the

brine solutions into the clay minerals. The addition of such Sr would lower the measured age of the clay minerals.

There is a third alternative which would tend to decrease the apparent age of clay minerals. It is possible to lose radiogenic ^{87}Sr while most of the normal Sr is retained. The ionic charge and radius of ^{87}Sr (+1 and 1.47Å) is quite different than that of ^{87}Sr (+2 and 1.12Å). The position once occupied by a ^{87}Rb atom is taken by the daughter ^{87}Sr atom after radioactive decay. This scheme can lead to loss of radiogenic ^{87}Sr while normal Sr remains in the mineral; this process would also cause a lowering of the measured Rb-Sr age. This process is not too likely for clay minerals, however, as clays such as saponites generally retain divalent cations at least as well as monovalent species.

Since most normal geochemical processes would generally make the clay minerals appear younger, the age of 390 m.y. must represent a minimum age for the clay minerals. This implies that the provenance for some of the detrital sediments must be Devonian or older strata. Precambrian to Devonian strata were probably exposed to the northwest as well as to the west of the Delaware Basin during the Late Permian (Eardley, 1949 and McKee, 1967). The clays present in the evaporite rocks of the Delaware Basin might very well have been derived from these areas. Unfortunately, the Rb-Sr systematics of the clay minerals affected by brine would also mask post-Devonian, pre-Salado detritus as well.

The REE and trace element content of the polyhalite and anhydrite samples are quite low; many elements are present in undetectable

concentrations. This is not surprising as the trace element and REE concentration of seawater is also very low. Most elements found, such as Fe, Zr, Hf and Co are probably present in the evaporites as oxides or hydroxides, forming very thin coats around mineral grains.

The REE and other trace element concentrations of the polyhalite samples is very similar to those found in the anhydrite samples. This may suggest a primary origin for polyhalite in the Salado or indicate that most of the trace elements present in the anhydrite were retained during its possible alteration to polyhalite.

The trace element concentrations of the clay minerals suggest a detrital origin for the clays. Most of the trace element concentrations noted are much too high for the clays to have formed in situ. The REE concentrations indicate that these detrital clays probably underwent some ion exchange with the evaporite brine solutions. This is evidenced by a depletion of the lighter REE, which were probably leached from the clays or replaced by Ca^{2+} and Na^{+} from the brine solutions.

CONCLUSIONS

The results of this study support the following conclusions:

1. The Salado Formation yields a Rb-Sr geochronologic age of 214 ± 15 m.y.
2. The $^{87}Sr/^{86}Sr$ ratio of the evaporite brines present in the Permian Delaware Basin was between 0.7073 and 0.7093.
3. There is no evidence of substantial alkali-alkaline earth migration within the Salado Formation since deposition.
4. The suggested minimum age of the clay minerals found in the Salado is 390 ± 77 m.y.
5. The mineralogy of the clay minerals as well as their REE and trace element contents indicate a detrital origin.
6. The clay minerals underwent ion exchange with brine solutions, which tended to deplete their light REE contents.
7. The REE content of evaporite minerals is very low, probably reflecting the low REE concentration of the evaporite brine solution.
8. Interpretation of the geochemical systematics of the Salado Formation does not support a mid-Cretaceous chemical "event" as proposed by Tremba (1973).
9. The combined Rb-Sr, REE and clay mineralogic studies argue for continued work on the WIPP site to more fully investigate alkali, alkaline earth, halide, REE and, by inference, actinide behavior during silicate-brine interactions.

APPENDIX 1

EVAPORITE MINERAL DIFFRACTOGRAM

Fig. A1 shows a diffractogram produced by X-raying a mixture of halite and sylvite; the peaks at 2.81 Å and 3.24 Å are indicative of halite, peaks at 3.13 Å and 2.22 Å are characteristic of sylvite. The general lack of different d-spacings reflects the high symmetry of these two minerals.

Fig. A2 is a diffractogram of a polyhalite rich sample. The diffraction maxima at 3.16 Å and 2.89 Å are characteristic of polyhalite. Also, the 5.91 Å diffraction peak is nearly always present on the diffractogram of polyhalite. All the other spacings noted on Fig. A2 are attributed to polyhalite, which is a triclinic mineral.

Fig. A3 is a typical diffractogram of langbeinite. The maxima at 3.11 Å and the less intense peaks occurring at 4.00 Å, 2.63 Å, and 2.96 Å are characteristic of all the langbeinite identified in this study.

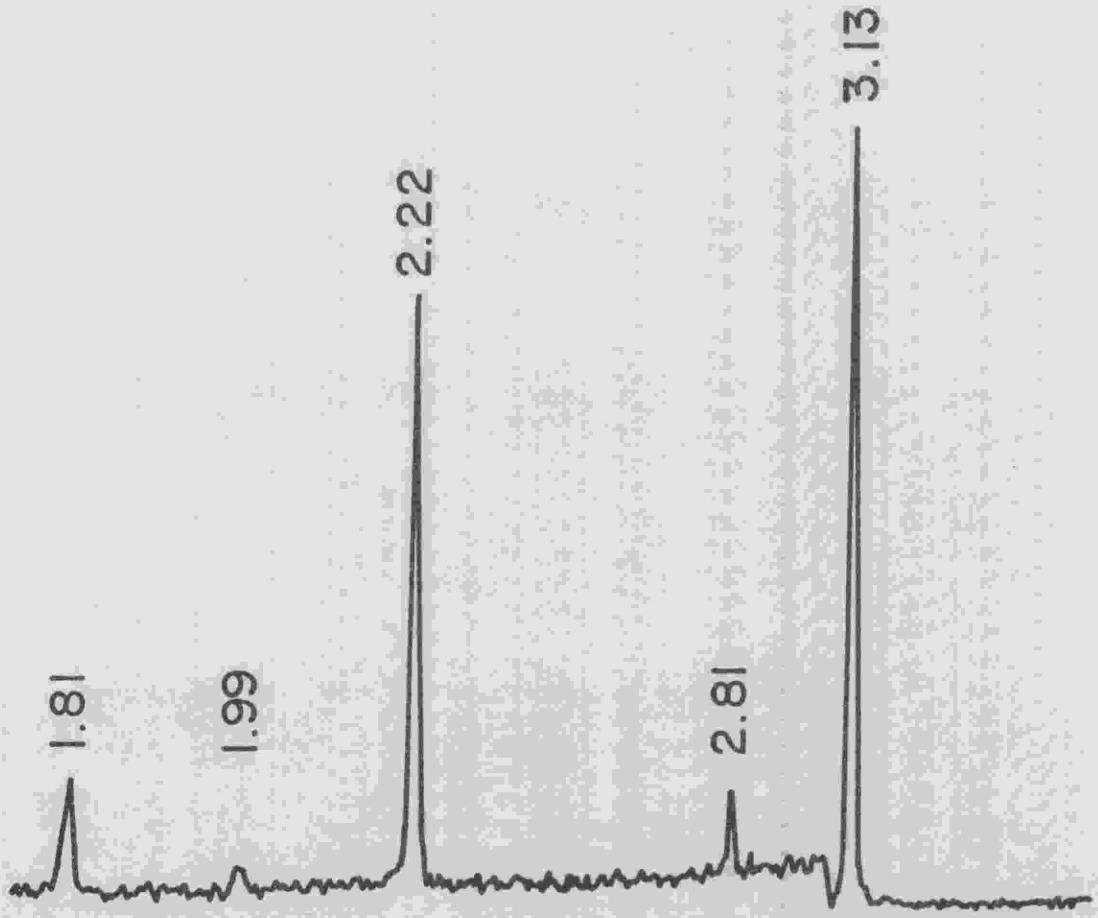

Figure A1. Diffractogram of a mixture of halite and sylvite. Units given are angstroms (Å).

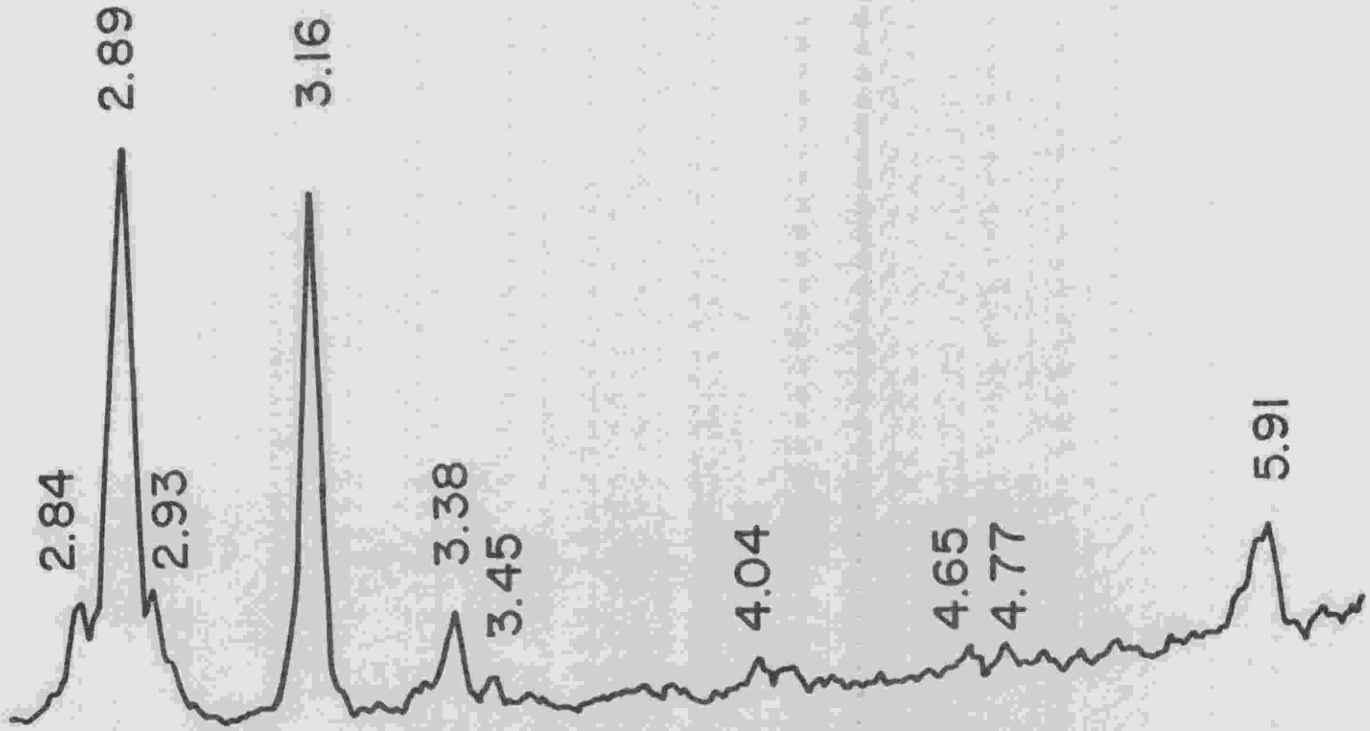

Figure A2. Diffractogram of polyhalite. Units given are angstroms (Å).

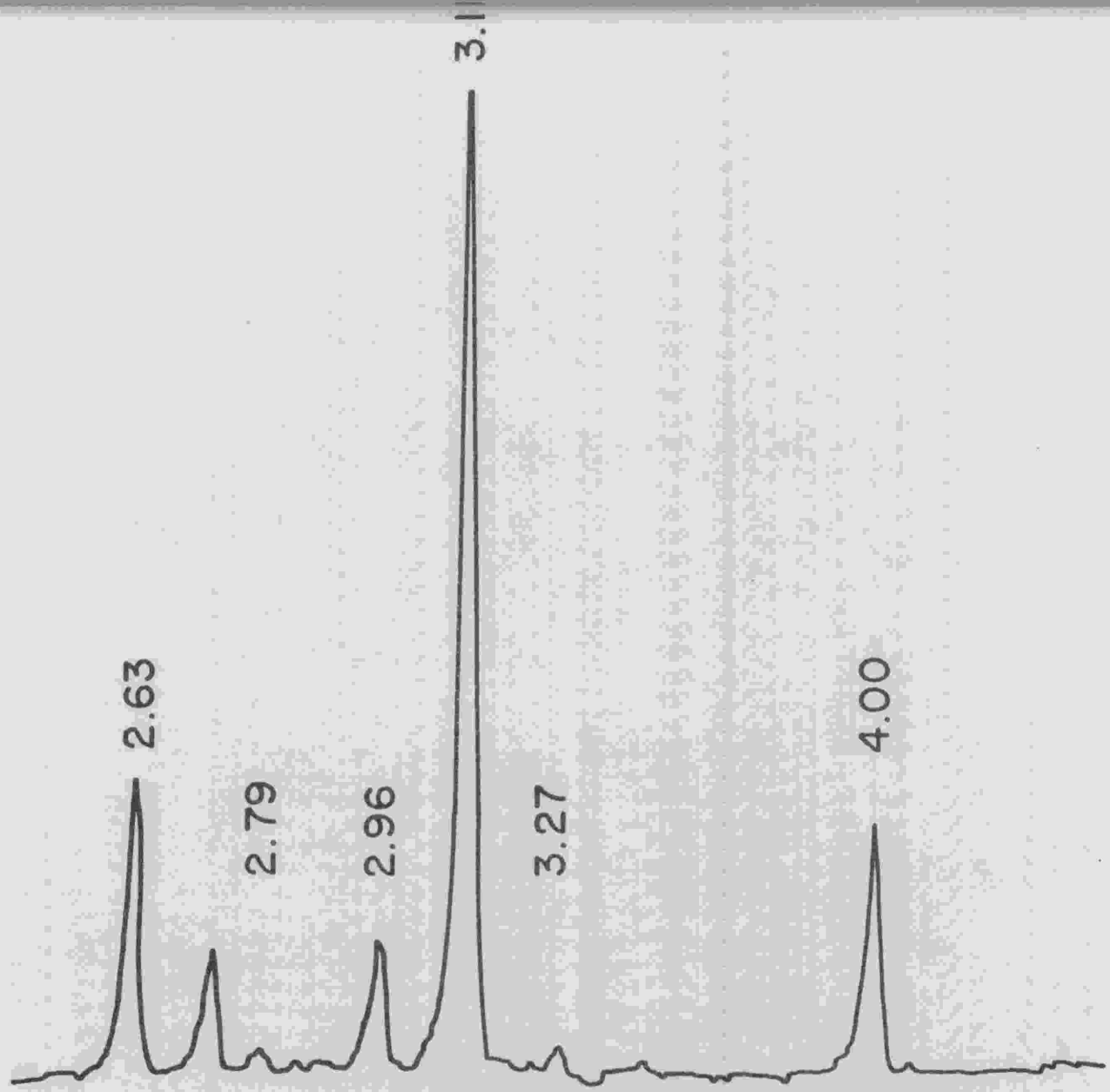

Figure A3. Diffractogram of langbeinite. Units given are angstroms (Å).

APPENDIX 2

PROCEDURE FOR CLAY MINERAL IDENTIFICATION

After the minus 2 micron fraction was separated from the water insoluble fraction of evaporite whole rock, it was settled onto a clean glass slide. By allowing the clay mineral grains to settle in this fashion, an oriented mount was obtained which placed the c-axis of each grain at right angles to the surface of the slide. Thus, the diffractogram obtained from such a sample indicated the basal d-spacings which characterize the various clay minerals. The samples were first run after air-drying only. A typical air-dried diffractogram is shown on Fig. A4. The same sample was then saturated with ethylene glycol by vapor soaking on a rack suspended over a considerable amount of the liquid in a closed container. Ethylene glycol causes an increase in the basal spacing of expandable clays such as montmorillonites. Fig. A5 is the diffractogram of the same sample after glycolation. Another slide of the same sample was then heated at 450° C for one hour and X-rayed; the resulting diffractogram is shown of Fig. A6.

Chlorite-saponite mixed layer clay exhibits a 13.8-14.2 Å basal spacing (Fig. A4) which expands to about 15.0 Å after glycolation (Fig. A5). The chlorite-saponite peak often broadens upon glycolation, probably due to slight irregularities in layering of non-expandable chlorite and expandable saponite. Heating removes a majority of the water from chlorite-saponite causing the saponite lattice to partially collapse. This collapse produces a basal spacing of about 12.5 Å.

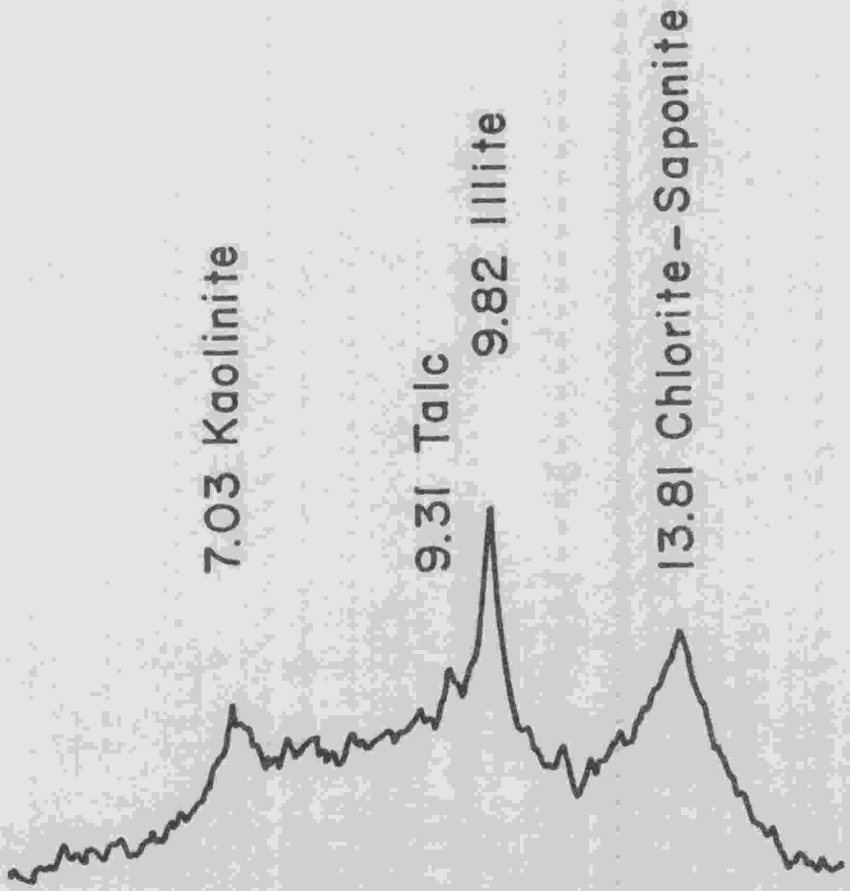

Figure A4. Diffractogram of a typical clay mineral assemblage from the Salado Formation. Air-dried. Units given are angstroms (Å).

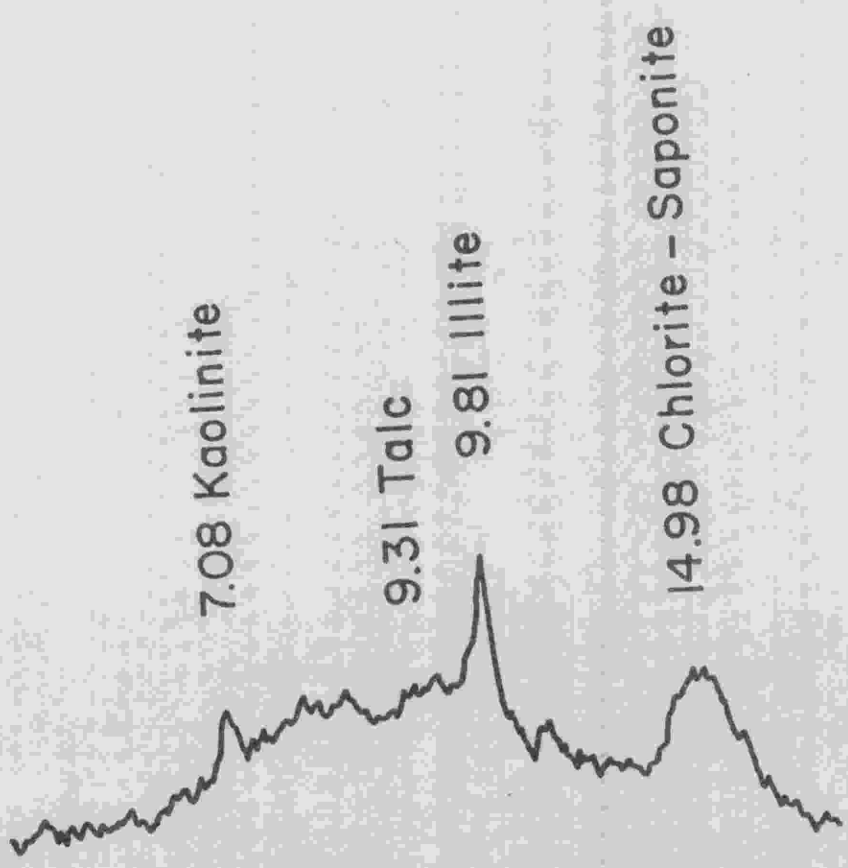

Figure A5. Diffractogram of a typical clay mineral assemblage from the Salado Formation. Glycolated. Units given are angstroms (Å).

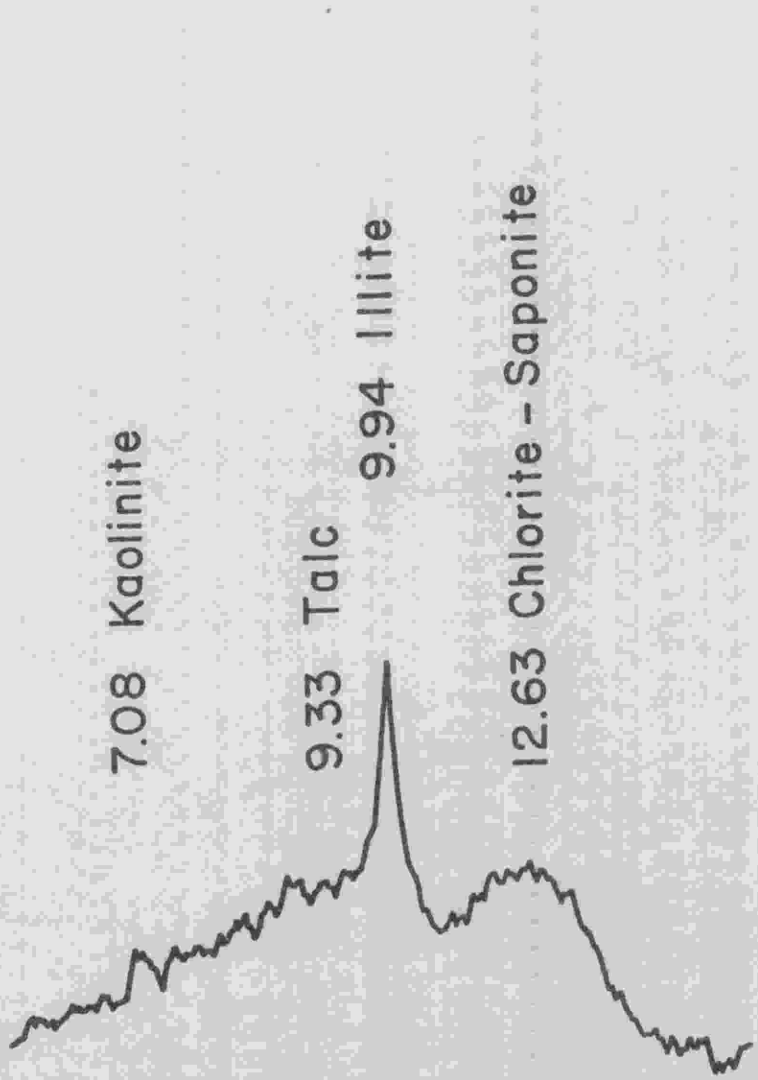

Figure A6. Diffractogram of a typical clay mineral assemblage from the Salado Formation. Heated to 450°C. Units given are angstroms (Å).

Illite is not expandable nor is it very much altered by heating at 450° C; its characteristic 9.5 to 10.0 Å basal spacing is observed on all three diffractograms. Kaolinite is recognized by the occurrence of a diffraction peak at about 7.1 Å on the air-dried and glycolated samples. Heating destroys kaolinite with time; the intensity of the peak at 7.1 Å has slightly decreased on the heated sample diffractogram.

Talc was recognized by its diffraction maxima at about 9.5 Å, which is unchanged by glycolation or heating. Chlorite as a distinct (non-interlayered) phase exhibits a basal spacing of about 14 Å, which is unaffected by glycolation or heating. Non-interlayered saponite, identified in some samples, also has a basal spacing of 14 Å, but expands to 16 Å or more upon glycolation and collapses to about 12 Å upon heating.

APPENDIX 3

COLUMN CALIBRATION

Previous studies conducted in this laboratory (c.f., Lee, 1976) used a flame-test method to determine the elemental composition of the effluent from the ion exchange columns utilized in preparing dissolved samples for mass spectrometric analysis. Due to the rather unique chemical composition of the majority of the samples analyzed for this work (compared to silicate rocks), a different procedure was derived to separate the Rb and Sr from the remainder of the dissolved rock.

In order to achieve good separation and isolation of Rb and Sr from dissolved rock, the columns were calibrated. Calibration was achieved by loading a solution of KCl, $CaCl_2$, and $SrCl_2$ onto the column followed by elution with 2.25N HCl. Six ml aliquots were collected after each 25 ml of column effluent. These aliquots were then analyzed by atomic absorption and the concentration of each element plotted against volume of column effluent. Such a plot is shown by Fig. A7. Though Rb is collected from the sample, not K, it was felt that loading a substantial amount of Rb onto the column could cause Rb contamination problems in the future. Therefore, K was used in place of Rb; the volume needed to elute Rb from the column was calculated from the volume used to elute K by the methods described in Samuelson (1963).

It can be noted from Fig. A7 that Rb should be collected between 50 and 75 mls and Sr collected between 170 and 240 mls. Sr collection is done carefully in order to avoid collection of large amounts of Ca with the Sr aliquot.

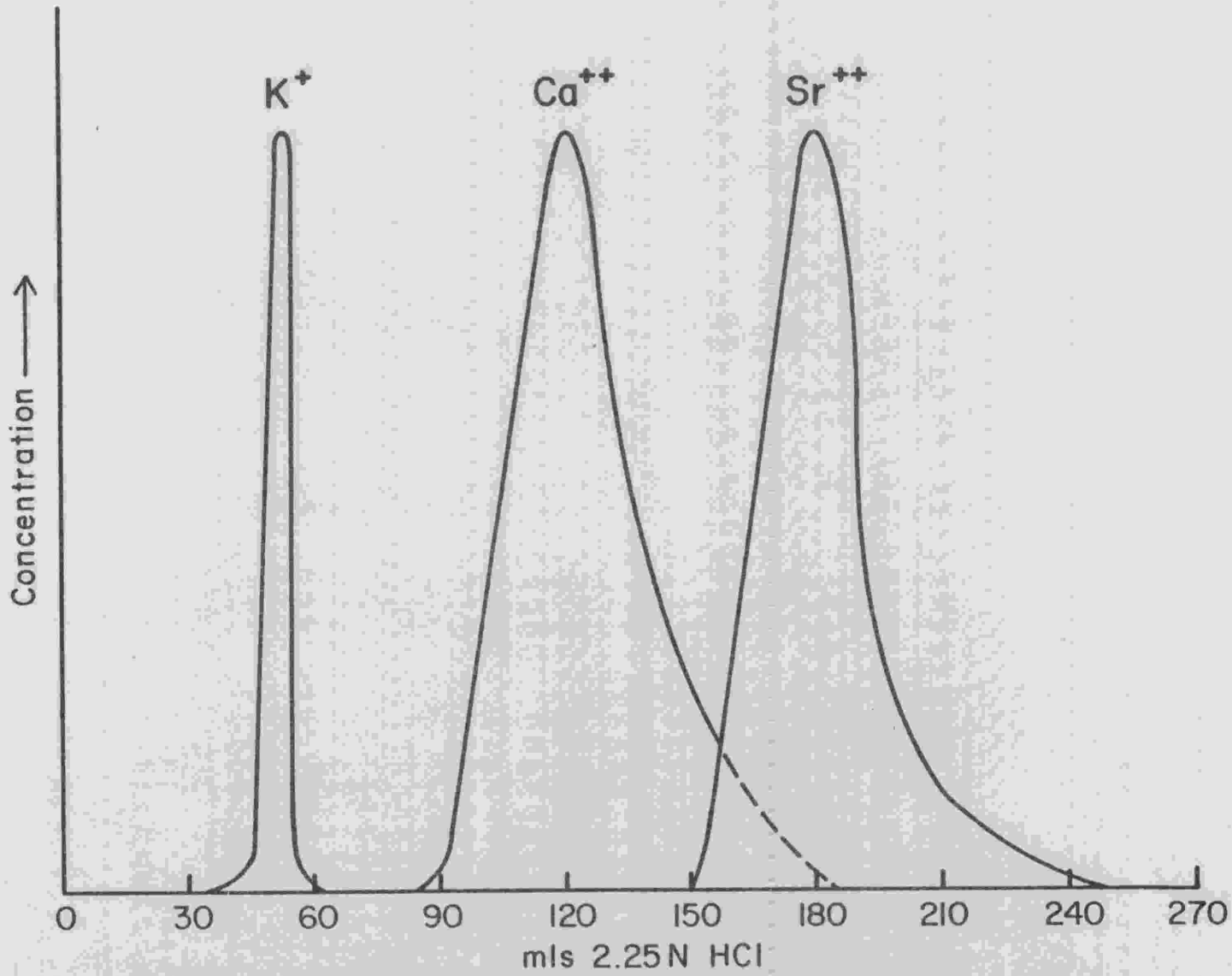

Figure A7. Elution curves for ion exchange columns used to separate Rb and Sr from samples for mass spectrometric analysis.

APPENDIX 4

ISOTOPE DILUTION

Isotope dilution analysis for many elements is considered to be the most accurate technique available, especially for elements present in low concentrations. Commonly, for mass spectrometric determination of the Rb and Sr concentration of geologic samples, solutions enriched in ^{87}Rb and ^{84}Sr are used as spikes.

After carefully weighing a sample to be analyzed into a suitable vessel, measured amounts of ^{87}Rb-enriched and ^{84}Sr-enriched solutions are added. The amount of each to be added is determined in such a way that the ratio of the enriched isotope to one of the naturally occurring isotopes of the element in the sample will be approximately 0.3 to 1.2.

For this study, a Sr spike highly enriched in ^{84}Sr and a Rb spike enriched in ^{87}Rb were used. The exact isotopic composition of each spike as determined during this study is given in Table A1.

For Sr spike, after the isotopic composition is known, its exact Sr concentration must be determined. This is done most simply and accurately by preparing a "shelf solution" of $SrCO_3$ with a known concentration and isotopic composition. A known volume of the $SrCO_3$ solution is then added to a known volume of spike solution, the resulting mixture evaporated to dryness and analyzed on the mass spectrometer. The following calculation can be used to determine the concentration of the Sr spike:

Table A1. Isotopic proportions of the Rb and Sr spikes used in this study.

Isotopic Proportion of the ^{84}Sr Spike

Strontium Isotope	Percent Abundance
84	99.77
86	0.10
87	0.02
88	0.11

Atomic weight = 83.9204

Isotopic Proportion of the ^{87}Rb Spike

Rubidium Isotope	Percent Abundance
85	1.996
87	98.004

Atomic weight = 86.9601

$$\frac{^{84}Sr}{^{86}Sr_m} = \frac{\dfrac{V_{sp} \times C_{sp} \times {}^{84}AP_{sp}}{GAW_{sp}} + \dfrac{V_{sh} \times C_{sh} \times {}^{84}AP_{sh}}{GAW_{sp}}}{\dfrac{V_{sp} \times C_{sp} \times {}^{86}AP_{sp}}{GAW_{sp}} + \dfrac{V_{sh} \times C_{sh} \times {}^{86}AP_{sh}}{GAW_{sh}}}$$

where GAW_{sp}, GAW_{sh} = gram atomic weight spike, shelf

V_{sp}, V_{sh} = volume of spike, shelf

C_{sp}, C_{sh} = total Sr concentration in spike, shelf

$^{84}AP_{sp}$, $^{84}Ap_{sh}$ = atomic proportion of ^{84}Sr in spike, shelf

$^{86}AP_{sp}$, $^{86}AP_{sh}$ = atomic proportion of ^{86}Sr in spike, shelf.

The $(^{84}Sr/^{86}Sr)_m$ is obtained by mass spectrometric measurement and since all other variables are known, the concentration of the spike (C_{sp}) can be determined. The concentration of ^{84}Sr spike used in this study is 1.506 µg/ml, based on multiple determinations.

Samples are analyzed for Sr concentration in an analogous fashion to that which is used to determine the concentration of the spike. In this case, however, the exact isotopic composition of the sample is unknown as the $^{87}Sr/^{86}Sr$ ratio varies in nature. Therefore, the proportion of each isotope of Sr in the sample must be determined before the Sr concentration can be determined. The Sr isotopic ratios calculated after mass spectrometric measurement are 84/86, 87/86, and 88/86. As the 84/86 isotopic ratio of Sr is a constant in nature, the concentration of ^{86}Sr in the sample can be calculated as given below:

$$^{86}Sr_{sl} = \frac{\frac{^{86}Sr}{^{84}Sr_m} - \frac{^{86}Sr}{^{84}Sr_{sp}}}{1 - \frac{^{86}Sr}{^{84}Sr_m}\,\frac{^{84}Sr}{^{86}Sr_{sl}}} \times {}^{84}Sr_{sp}$$

where, $^{86}Sr_{sl}$ = concentration ^{86}Sr in sample

$\frac{^{86}Sr}{^{84}Sr_m}$, $\frac{^{86}Sr}{^{84}Sr_{sp}}$, $\frac{^{86}Sr}{^{84}Sr_{sl}}$, = $\frac{^{86}Sr}{^{84}Sr}$ ratio measured, of spike, of sample

$^{84}Sr_{sp}$ = concentration of ^{84}Sr in spike.

In order to determine the total Sr concentration in the sample from the concentration of ^{86}Sr in the sample, the proportion of each isotope of Sr in the sample is determined from the measured isotopic ratios. When it is established what proportion of the Sr in the sample is ^{86}Sr, it is a simple matter to calculate total Sr concentration. A more complete discussion of this technique is given in Webster (1960).

For Rb isotope dilution analysis a similar procedure is used. First, the isotopic composition of the spike is determined (Table A1). Its concentration is then obtained by mixing a known volume of Rb spike with a known volume of a RbCl shelf solution of predetermined Rb concentration. The mixture is then analyzed on the mass spectrometer and the Rb concentration of the spike determined by the calculation given below:

$$\frac{^{85}Rb}{^{87}Rb_m} = \frac{\dfrac{V_{sp} \times C_{Sp} \times {}^{85}AP_{sp}}{GAW_{sp}} + \dfrac{V_{sh} \times C_{sh} \times {}^{85}AP_{sh}}{GAW_{sh}}}{\dfrac{V_{sp} \times C_{sp} \times {}^{87}AP_{sp}}{GAW_{sp}} + \dfrac{V_{sh} \times C_{sh} \times {}^{87}AP_{sh}}{GAW_{sh}}}$$

where GAW_{sp}, GAW_{sh}, = gram atomic weight spike, shelf

V_{sp}, V_{sh} = volume of spike, shelf

$^{85}AP_{sp}$, $^{85}AP_{sh}$, = atomic proportion of ^{85}Rb in spike, shelf

$^{87}AP_{sp}$, $^{87}AP_{sh}$ = atomic proportion of ^{87}Rb in spike, shelf.

The concentration of ^{87}Rb spike used in this study is 7.20 µg/ml.

The isotopic composition of Rb is considered to be constant in nature so the Rb concentration in any sample is more simply determined than the Sr concentration. After measuring the $^{85}Rb/^{87}Rb$ ratio of a sample-spike mixture the Rb concentration (C_{sl}) can be calculated as given below:

$$\frac{^{85}Rb}{^{87}Rb_m} = \frac{\dfrac{V_{sp} \times C_{sp} \times {}^{85}AP_{sp}}{GAW_{sp}} + \dfrac{W_{sl} \times C_{sl} \times {}^{85}AP_{sl}}{GAW_{sl}}}{\dfrac{V_{sp} \times C_{sp} \times {}^{87}AP_{sp}}{GAW_{sp}} + \dfrac{W_{sl} \times C_{sl} \times {}^{87}AP_{sl}}{GAW_{sl}}}$$

where GAW_{sp}, GAW_{sl} = gram atomic weight spike, sample

V_{sp} = volume of spike

W_{sl} = weight of sample

C_{sp}, C_{sl} = concentration of spike, sample

$^{85}AP_{sp}$, $^{85}AP_{sl}$ = atomic proportion of ^{85}Rb in spike, shelf

$^{87}AP_{sp}$, $^{87}AP_{sl}$ = atomic proportion of ^{87}Rb in spike, shelf

A more complete treatment of isotope dilution technique is given in Webster (1960).

APPENDIX 5

RESULTS FOR STANDARDS

The validity of the isotope dilution techniques employed in this study were confirmed by multiple analysis of two U.S.G.S. standards. The results as shown in Table A2 are in good agreement with the reported values.

Eimer and Amend $SrCO_3$ has been extensively utilized as a standard for the mass spectrometric measurement of the $^{87}Sr/^{86}Sr$ ratio. All $^{87}Sr/^{86}Sr$ ratios reported for this standard are generally normalized to correct for machine fractionation. The correction factor is designed to correct the $^{86}Sr/^{88}Sr$ ratio to 0.1194 and thus correct the measured $^{87}Sr/^{86}Sr$ ratio for machine fractionation. The correction factor used to normalize the $^{87}Sr/^{86}Sr$ ratio is

$$C.F. = \frac{2M}{M + 0.1194},$$

where $M = {}^{86}Sr/{}^{88}Sr$ measured.

Also, $(^{87}Sr/^{86}Sr)$ normalized = $(^{87}Sr/^{86}Sr)$ measured x C.F.

The normalized ratios obtained for the Eimer and Amend $SrCO_3$ are given in Table A3 are in very good agreement with accepted $^{87}Sr/^{86}Sr$ value of 0.7080.

Table A2. Comparison of the Rb-Sr values for two U.S.G.S. standards obtained during this study with the reported values.

Analytical Data of the U.S.G.S. Standards

(units are ppm)

Standard	Present Study		Flanagan (1973)		Fairbairn and Hurley (1971)	
	Rb	Sr	Rb	Sr	Rb	Sr
G-2	170	479	168	479	171	479
	173	473				
	171	482				
	166	481				
Avg.	170	477				
GSP-1	261	237	254	233	251	234
	283	234				
	264	234				
	272	235				
	260	237				
Avg.	268	235				

Table A3. $^{87}Sr/^{86}Sr$ data obtained for Eimer and Amend $SrCO_3$ during this study.

Date	$^{87}Sr/^{86}Sr$
1- 6-76	0.7079
2-11-76	0.7080
2-12-76	0.7080
11- 4-76	0.7082
2-13-77	0.7083
3- 3-77	0.7079
3- 4-77	0.7078
3-26-77	0.7080
4- 7-77	0.7078
6-28-77	0.7080
12-13-77	0.7079
2-16-78	0.7078
10-28-78	0.7082
12-22-78	0.7077
12-27-78	0.7081
Avg.	0.7080
Standard deviation	0.0002

APPENDIX 6

MASS SPECTROMETER MODIFICATION AND PROCEDURE

Studies conducted in this laboratory prior to this work (c.f., Lee, 1976) used a substantially different method of mass spectrometric data collection. For this reason, a brief description of the methods now employed is included.

Previously, Rb-Sr isotopic data was collected by scanning the Rb spectrum from mass 87 to mass 85 and the Sr spectrum from mass 88 to mass 84. The spectrum was recorded on a strip chart recorder. The peak heights were read from the strip chart, the baseline subtracted from these values and the numbers divided to produce the isotopic ratios used for interpretation. Each sample analysis generally consisted of 48 scans across the entire isotopic spectrum of the element being analyzed.

After installation of a more up-to-date magnet power supply, peak preselector and integrating ratiometer, data was collected in a different fashion. The peak preselector is adjusted to step to the top of each peak in the isotopic spectrum of the element analyzed and to the places between the peaks where baseline readings are desirable. After stepping, the peak or baseline magnitude is measured by the ratiometer. The ratiometer measures by counting the signal fed it over a ten second time interval and dividing each count by a ten volt signal. Due to the length of time each peak or baseline is read, small

irregularities in the ion beam being collected are averaged out and smaller signals can be used for precise measurement.

The addition of a triple filament thermionic source and a compatible source control allows a more stable ion beam to be produced with less machine fractionation. Since installation of this new equipment, the analysis failure rate has decreased substantially.

APPENDIX 7

Trace Element and REE Concentration in Polyhalite and Anhydrite

The following page (Table A4) gives the trace element and REE concentration of polyhalite and anhydrite samples from the Salado Formation.

Table A4. Trace and rare earth element concentration of polyhalite and anhydrite samples from the Salado Formation.

Neutron Activation Analysis & Delayed Neutron Activation Analysis

Sample Number	% Na_2O	% K_2O	% Fe_2O_3	Cs	Ba	Sc	Zr	Hf	Ta	Cr	Rb	Co	Ni	Ag	Sb	Th	La	Ce	Nd	Sm	Eu	Tb	Tm	Yb	Lu	ΣR.E.E.
											NAA															
Polyhalite																										
AEC-8 1618.9-1619.4	1.98	7.26	0.39	NA	ND	ND	ND	0.25	0.09	ND	29.72	1.51	29.31	NA	0.21	0.07	ND	ND	ND	ND	ND	0.05	ND	ND	ND	0.05
ERDA-9, 1215.2-1215.3	0.13	7.33	0.43	NA	ND	0.14	41.40	3.14	ND	ND	ND	0.89	10.23	NA	ND	0.37	ND	ND	ND	ND	0.07	0.20	ND	ND	ND	0.07
1499.0-1500.0	0.50	6.23	0.25	NA	ND	ND	53.11	ND	0.10	ND	13.06	0.77	16.82	NA	0.07	0.14	0.55	ND	2.37	ND	ND	0,08	ND	ND	ND	3.00
1784.2-1784.3	0.07	6.77	0.24	NA	ND	0.07	41.47	ND	0.20	ND	8.64	0.44	16.06	NA	ND	ND	ND	0.55	ND	ND	ND	0.09	ND	ND	ND	0.64
Anhydrite																										
ERDA-9 1630.7-1631.0	0.05	0.04	0.14	NA	ND	ND	21.92	ND	ND	ND	8.29	0.55	ND	NA	ND	ND	ND	ND	ND	ND	ND	0.07	0.12	ND	ND	0.19
2836.0-2836.4	0.46	ND	0.16	NA	ND	ND	103.7	ND	ND	ND	15.36	ND	19.54	NA	0.19	0.10	ND	ND	3.95	ND	0.06	0.11	ND	ND	ND	4.12

Concentrations in ppm except where noted
ND = Not detected
NA = Not analyzed

APPENDIX 8

REE Plots of Clay Mineral Samples

The following pages (Fig. A8 through A21) show NAS normalized plots of the REE concentrations of clay mineral samples from the Salado Formation.

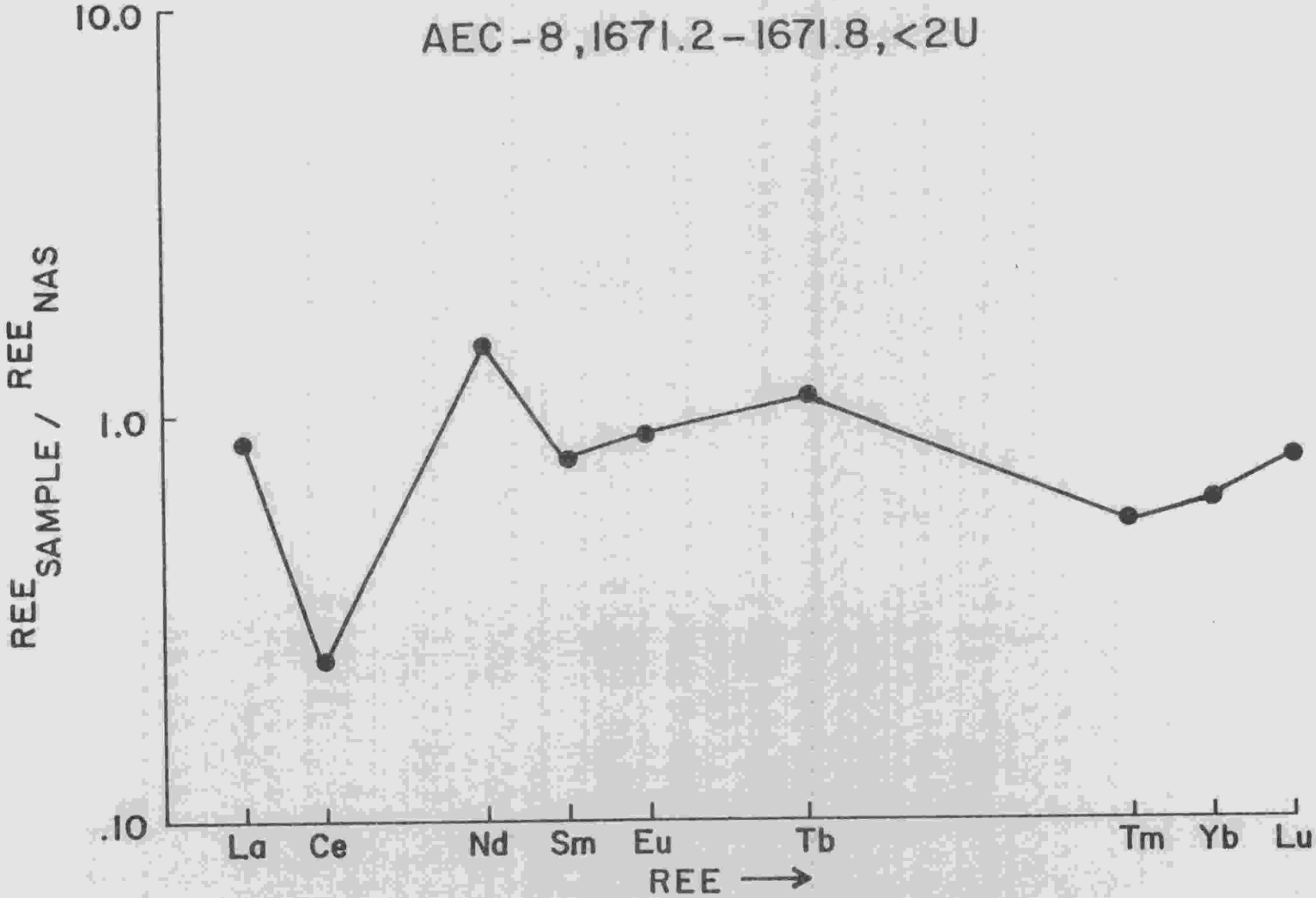

Figure A8. NAS normalized REE plot of clay mineral sample from the Salado Formation.

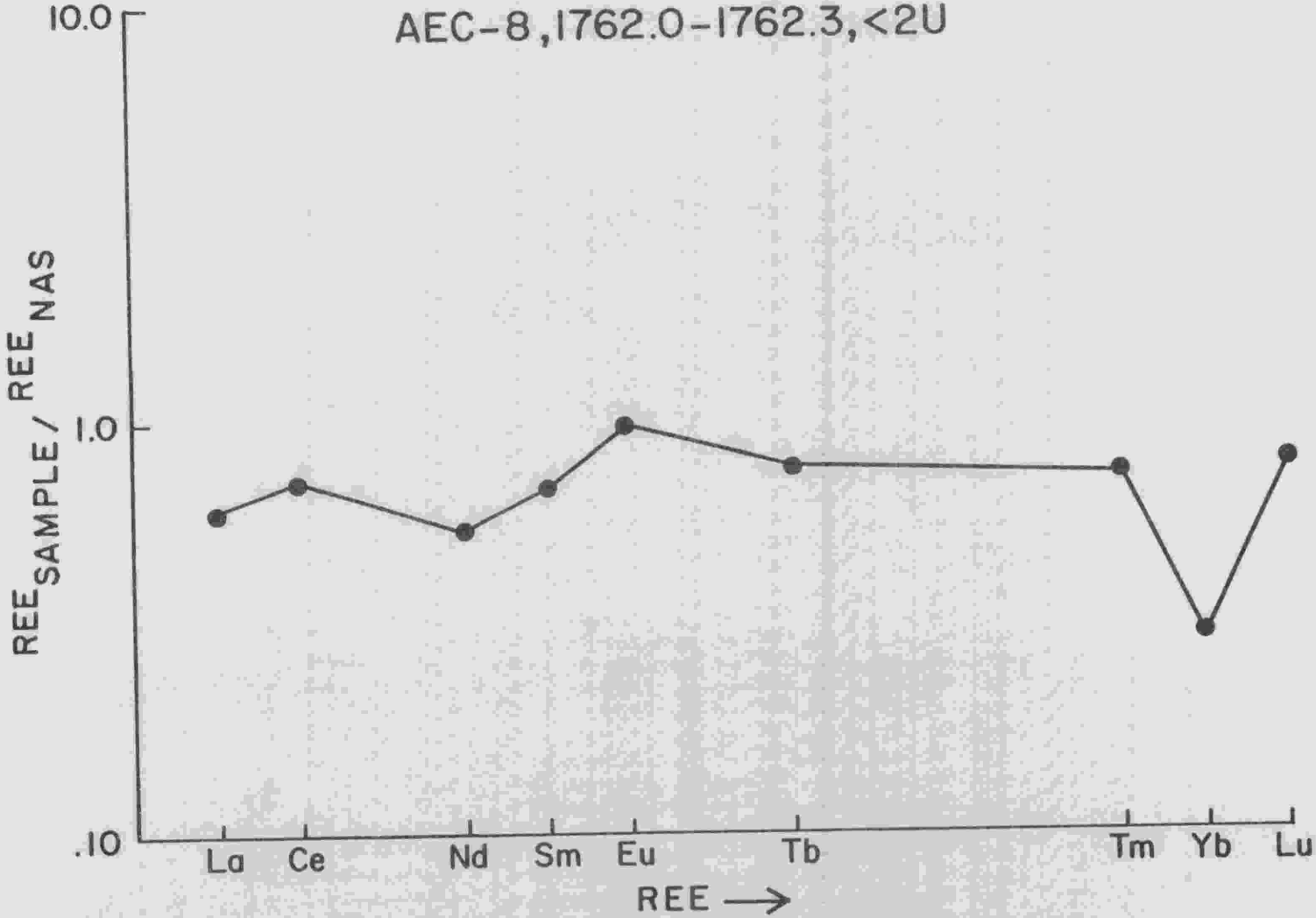

Figure A9. NAS normalized REE plot of clay mineral sample from the Salado Formation.

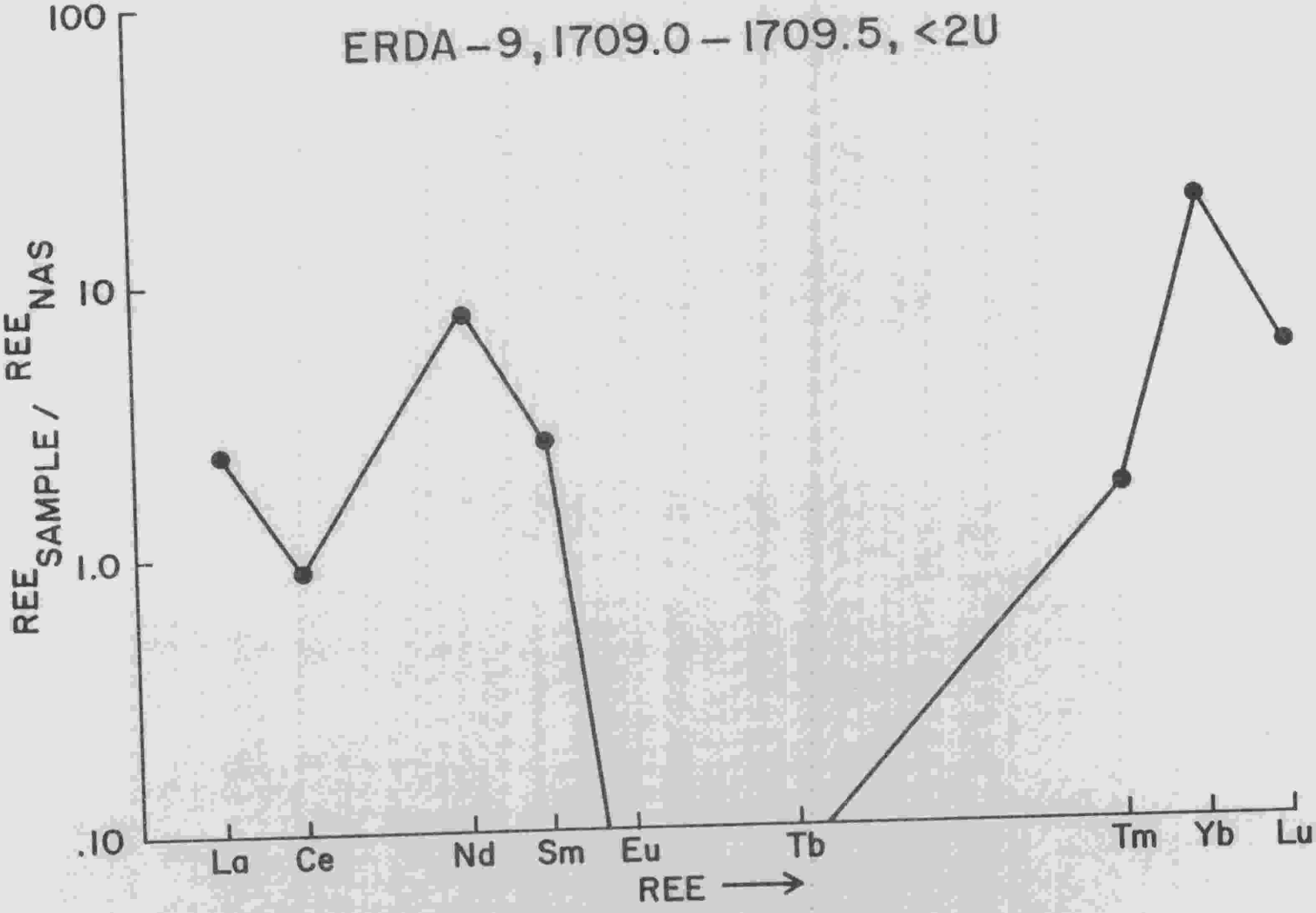

Figure A10. NAS normalized REE plot of clay mineral sample from the Salado Formation

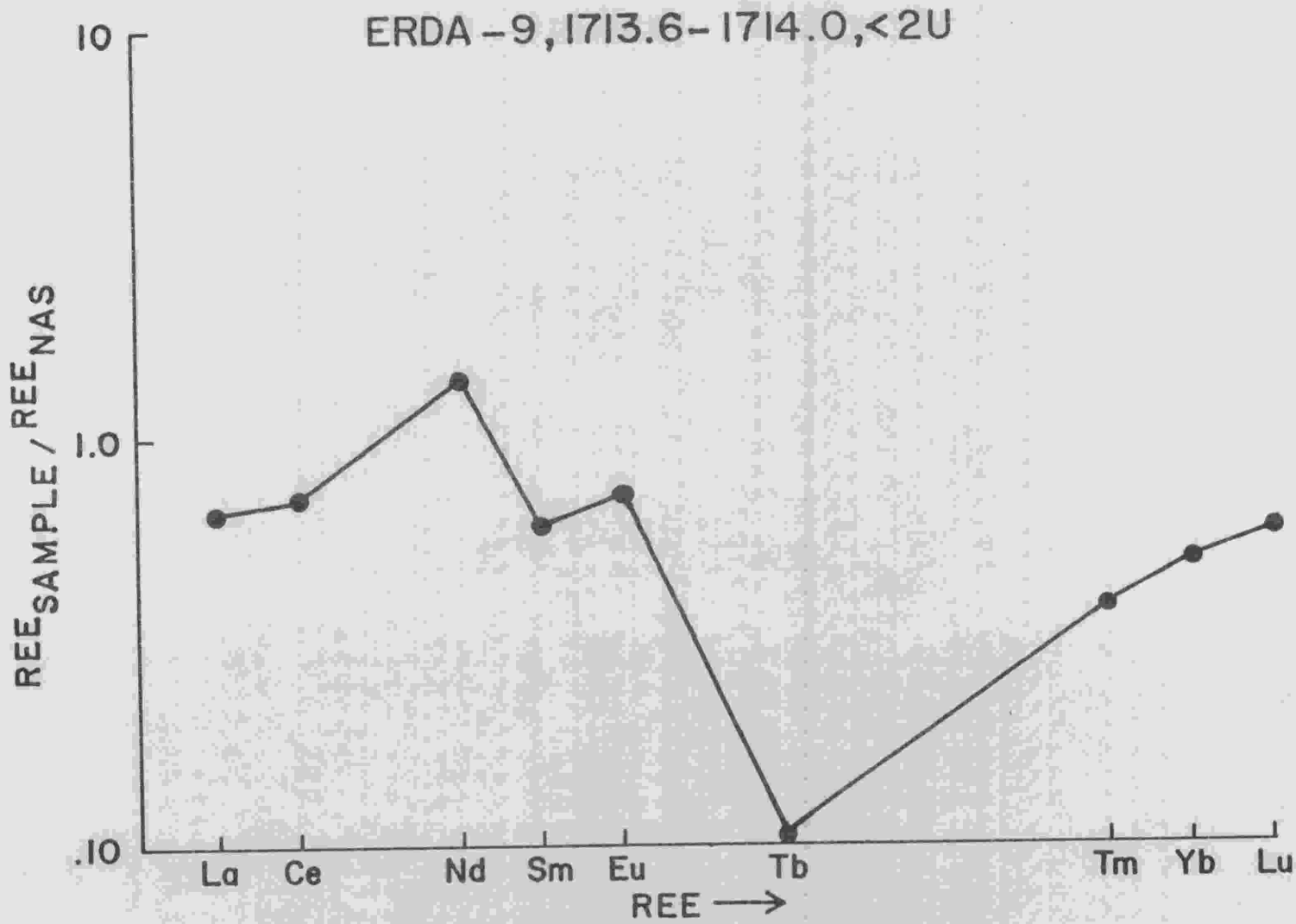

Figure All. NAS normalized REE plot of clay mineral sample from the Salado Formation.

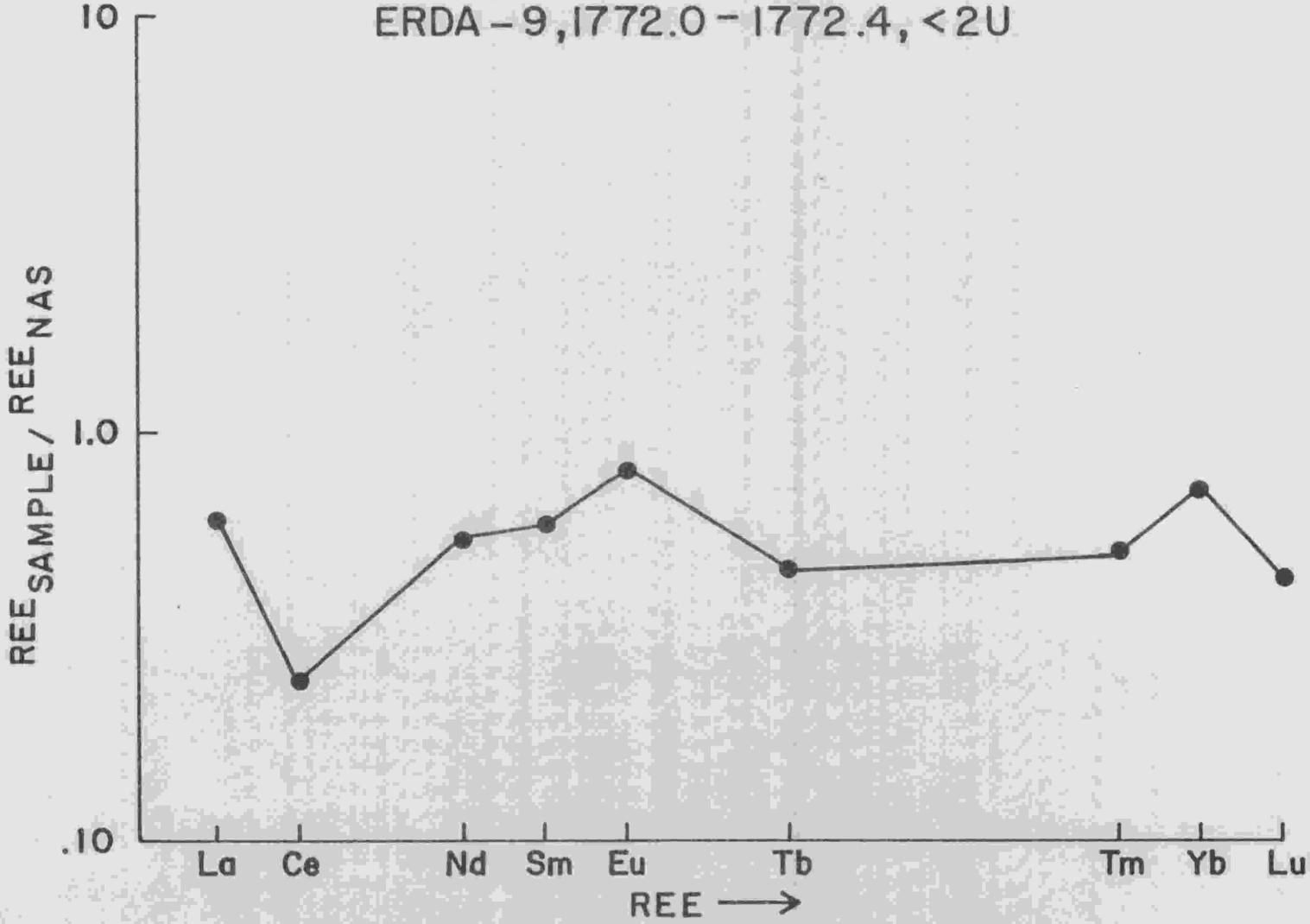

Figure A12. NAS normalized REE plot of clay mineral sample from the Salado Formation.

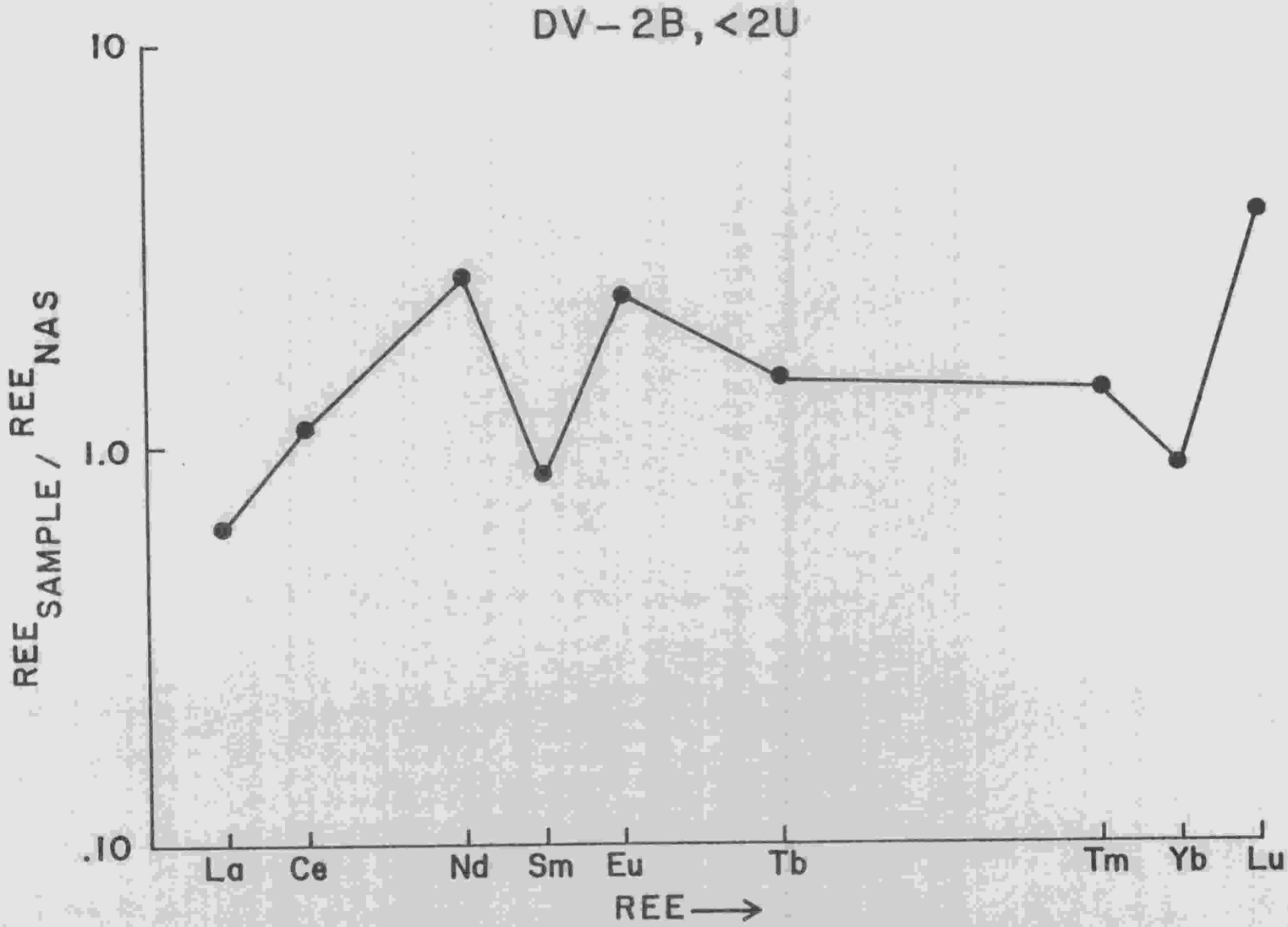

Figure A13. NAS normalized REE plot of clay mineral sample from the Salado Formation.

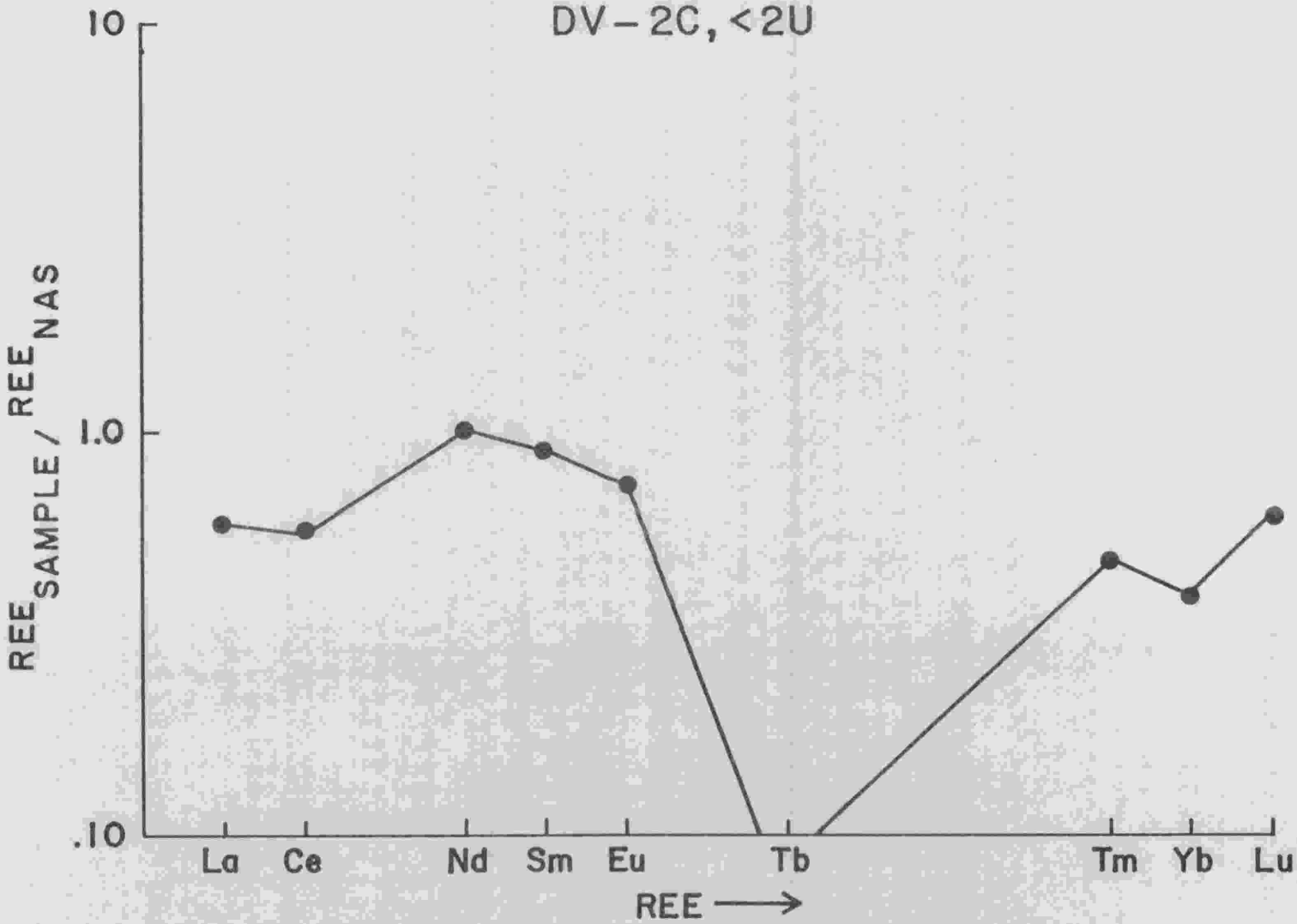

Figure A14. NAS normalized REE plot of clay mineral sample from the Salado Formation.

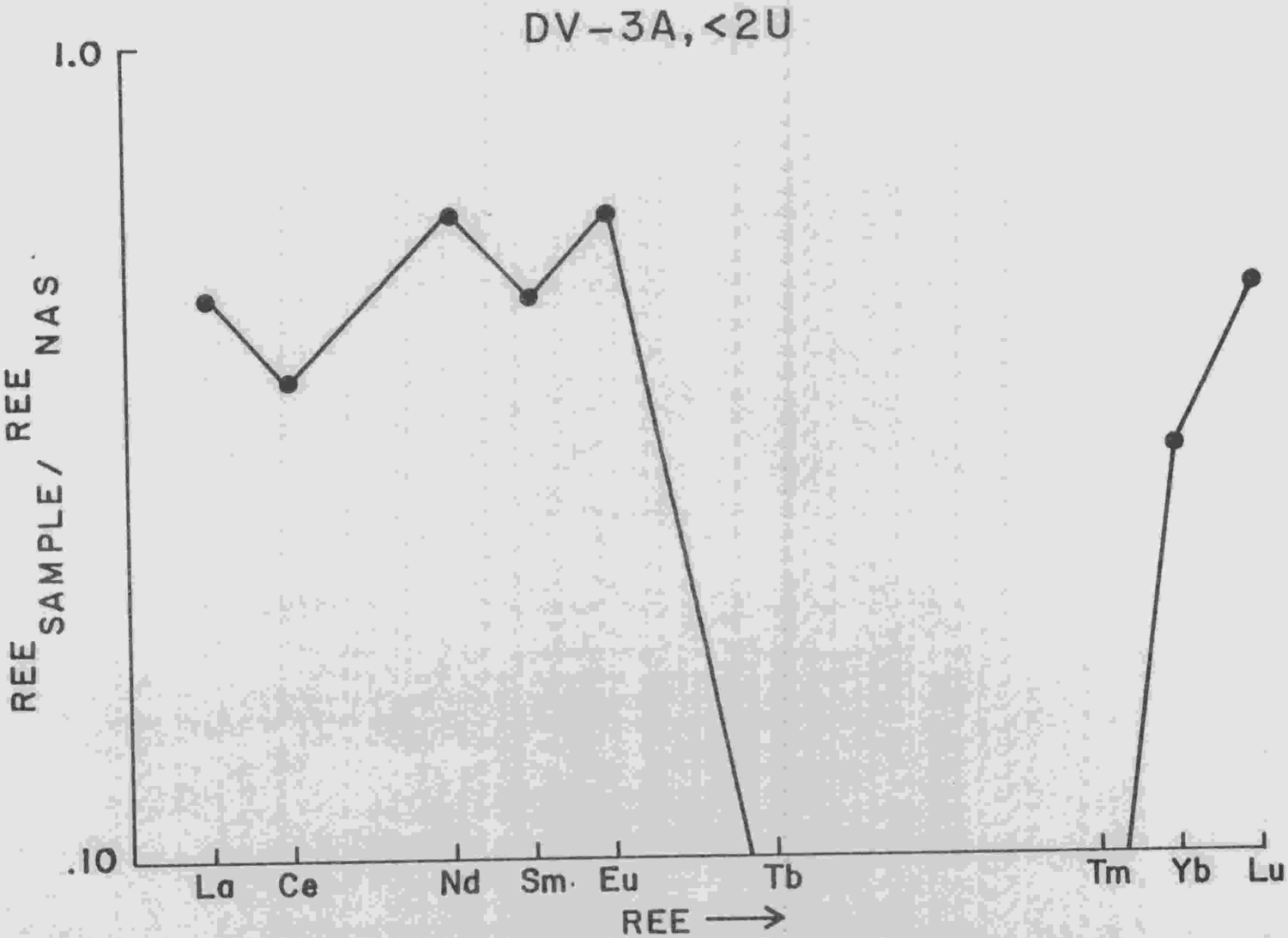

Figure A15. NAS normalized REE plot of clay mineral sample from the Salado Formation.

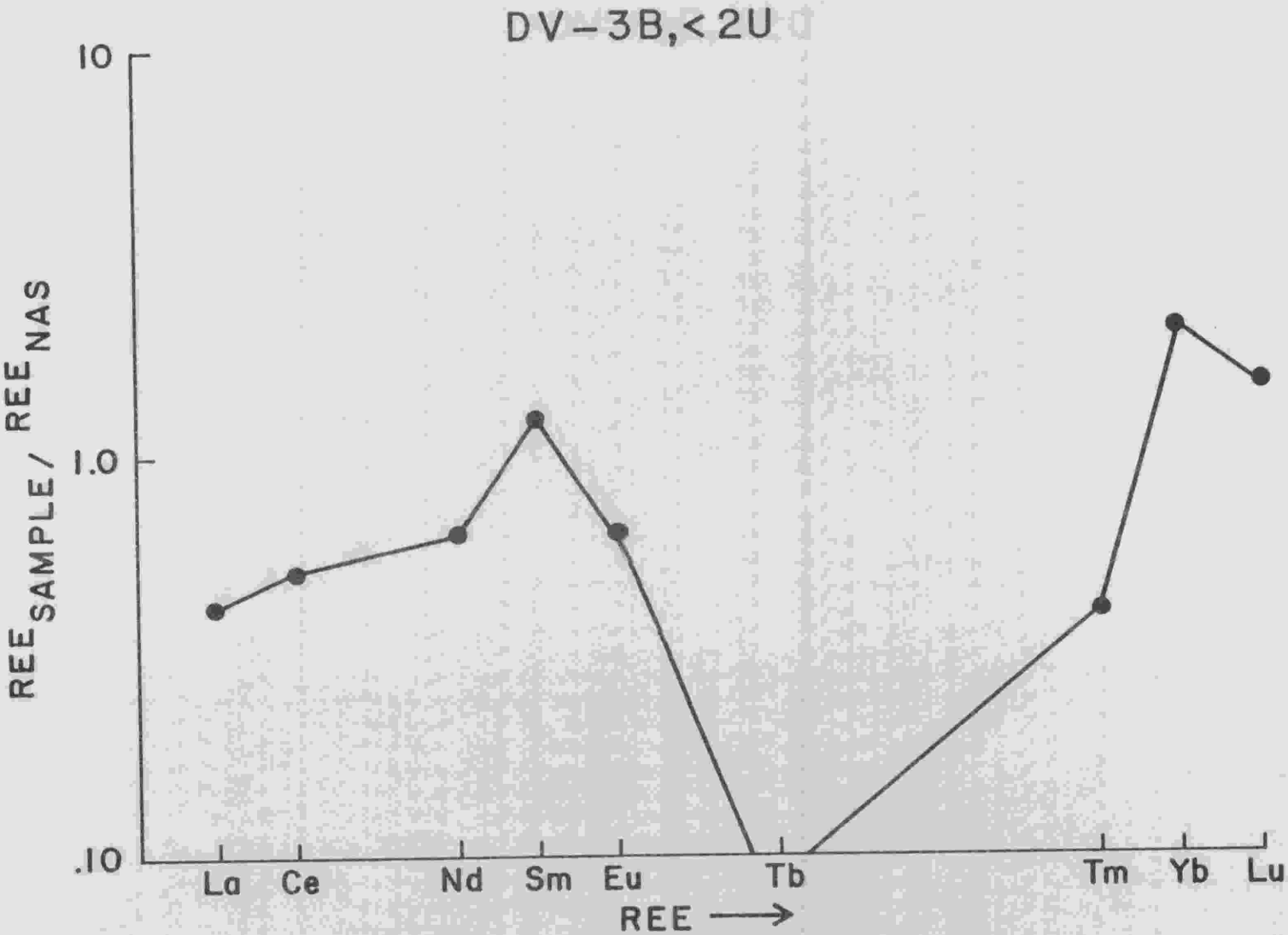

Figure A16. NAS normalized REE plot of clay mineral sample from the Salado Formation.

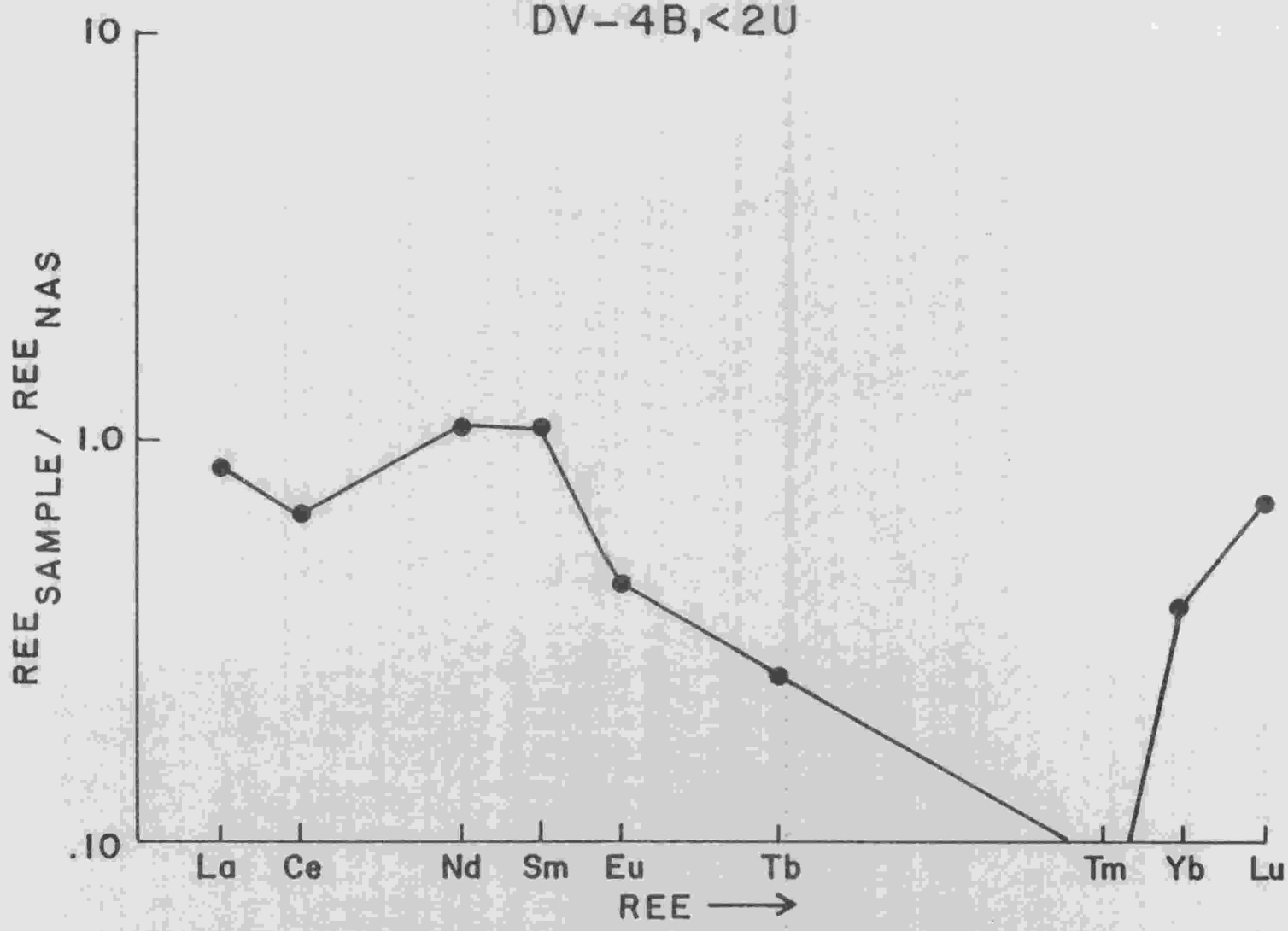

Figure A17. NAS normalized REE plot of clay mineral sample from the Salado Formation.

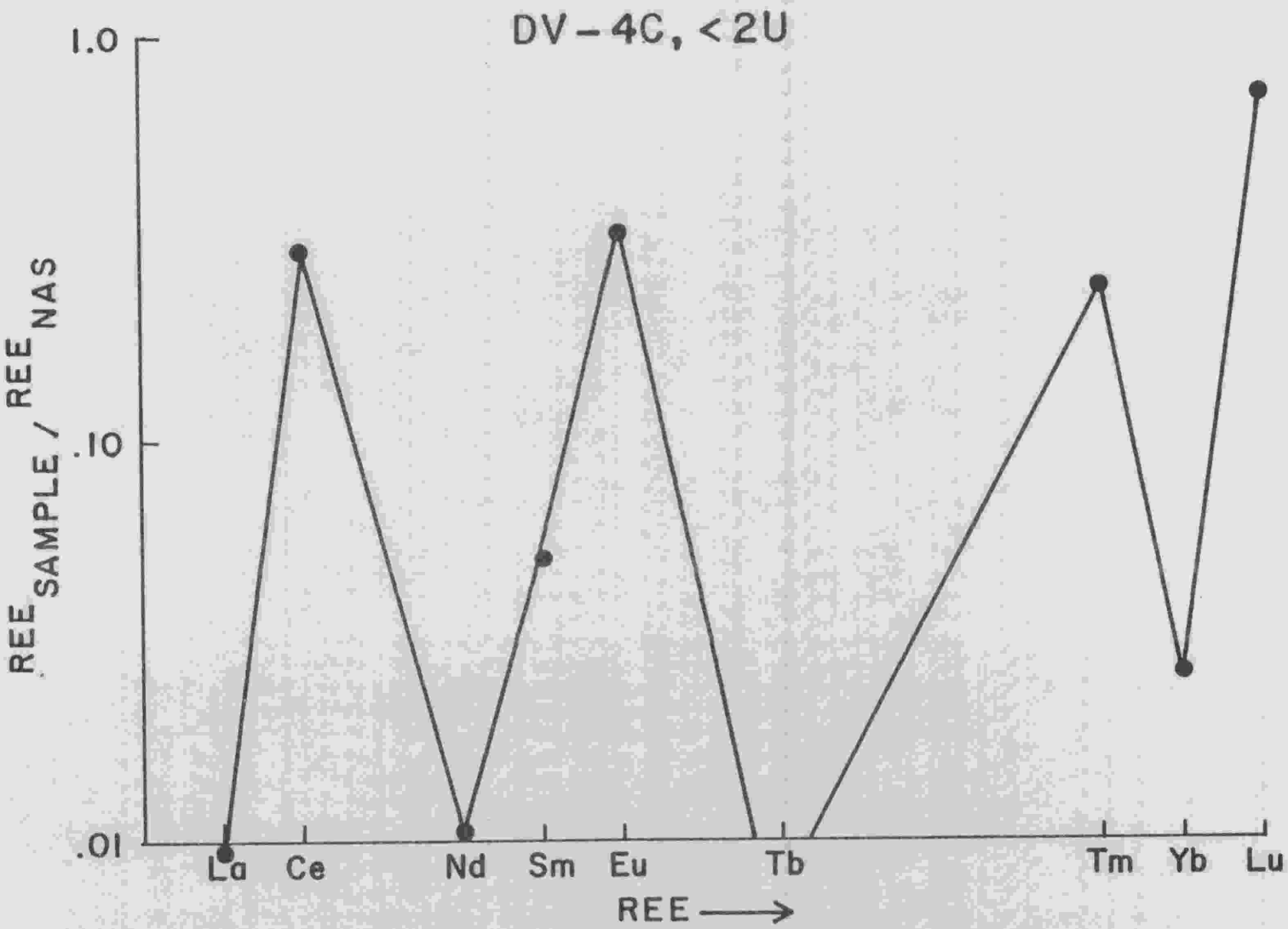

Figure A18. NAS normalized REE plot of clay mineral sample from the Salado Formation.

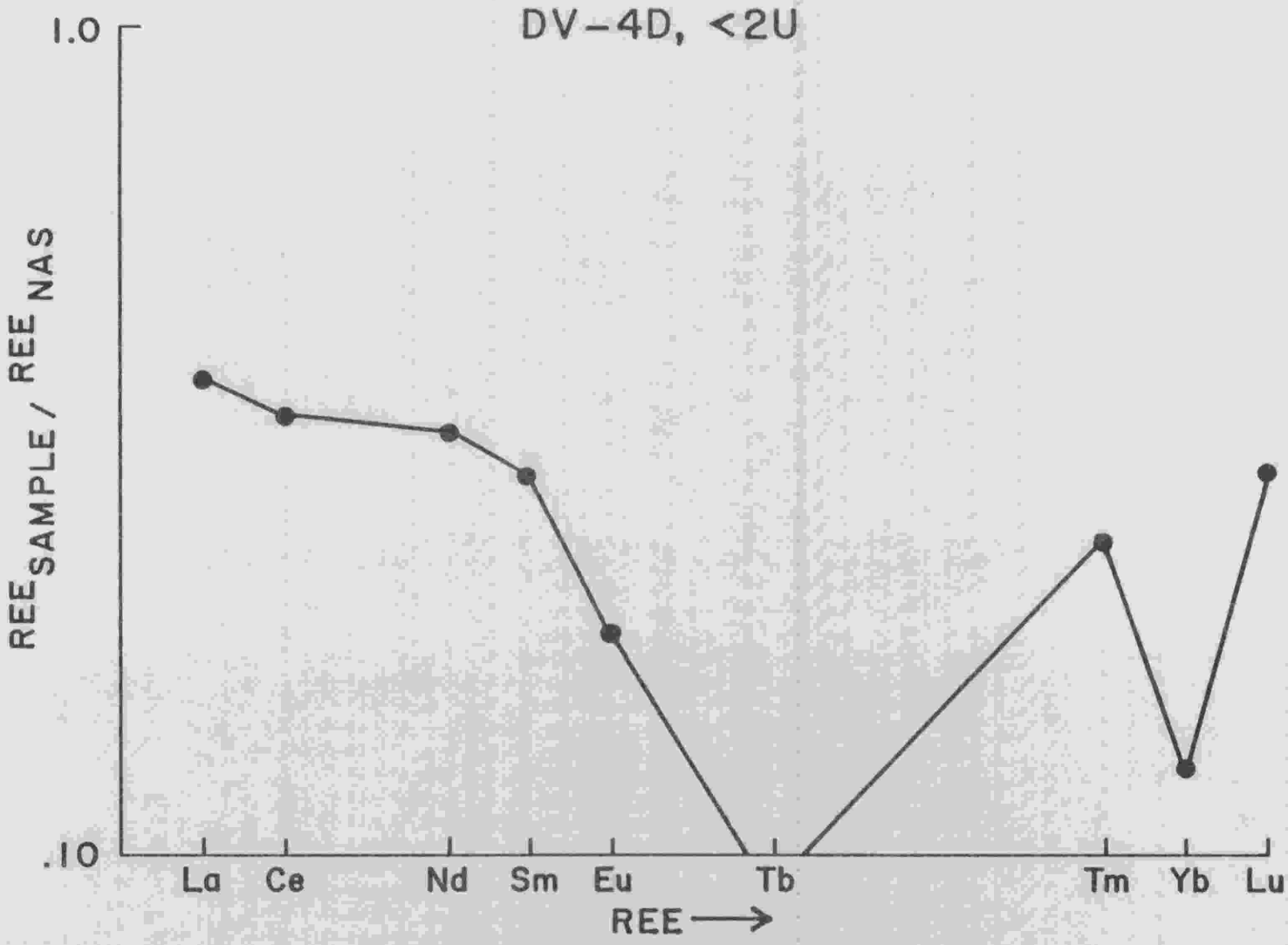

Figure A19. NAS normalized REE plot of clay mineral sample from the Salado Formation.

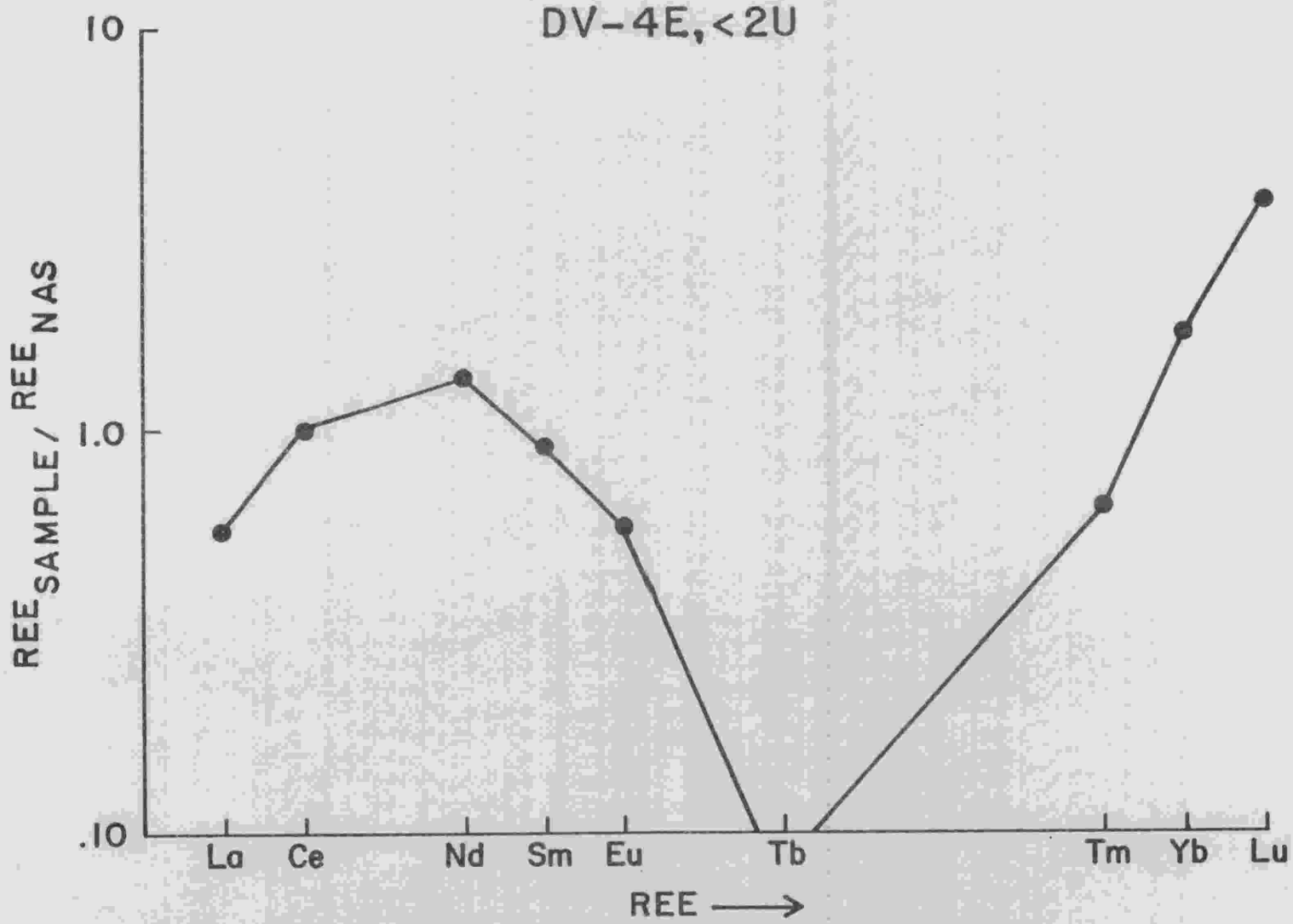

Figure A20. NAS normalized REE plot of clay mineral sample from the Salado Formation.

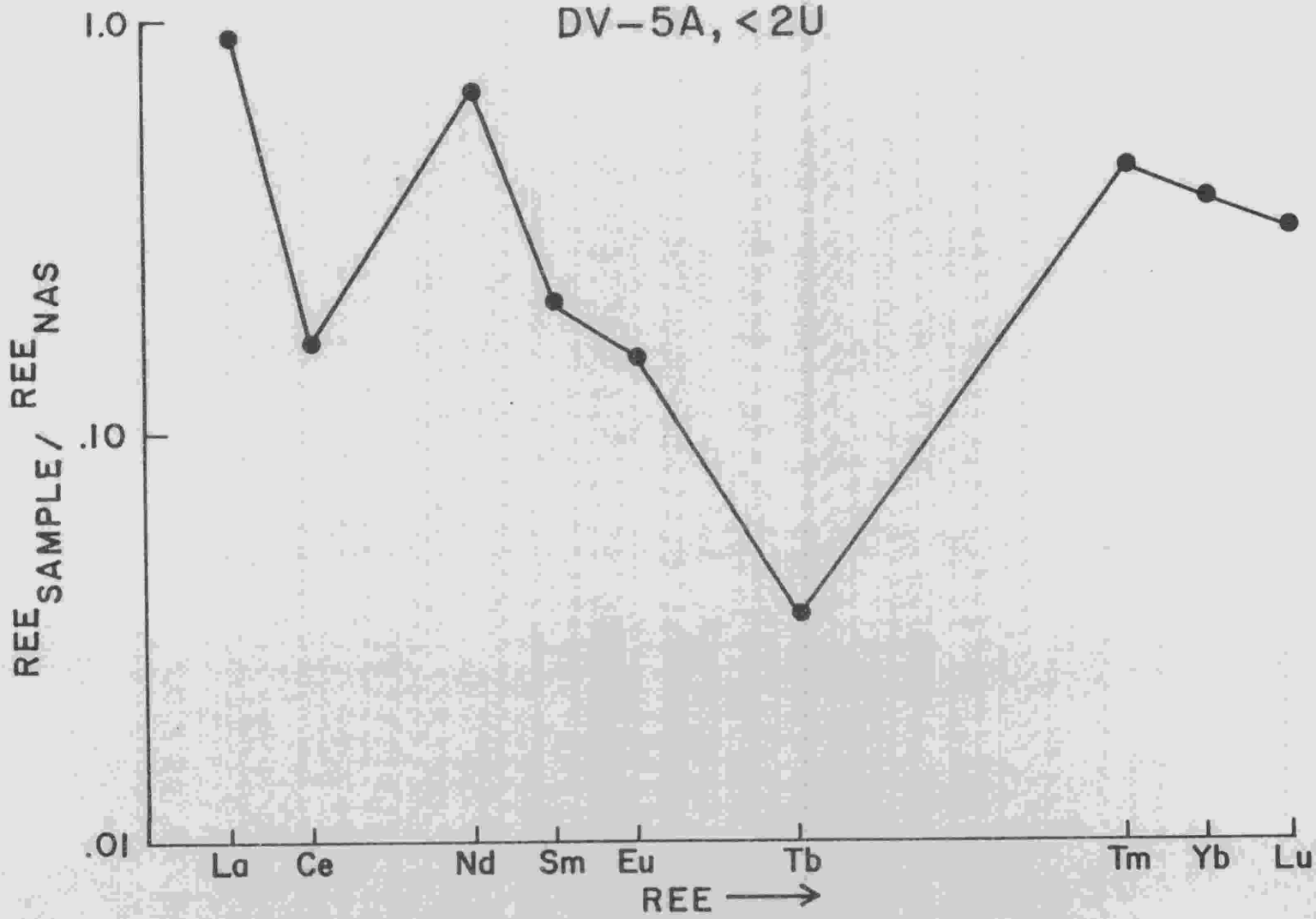

Figure A21. NAS normalized REE plot of clay mineral sample from the Salado Formation.

REFERENCES CITED

Adams, J. A. S., Osmond, J. K., and Rodgers, J. J. W., 1959, The geochemistry of uranium and thorium: Physics and Chemistry of Earth, v. 3.

Adams, J. E., 1939, Standard Permian section of North America: Am. Assoc. Petroleum Geologists Bull., v. 23, p. 1673-1681.

Adams, J. E., 1944, Upper Permian Ochoa series of the Delaware Basin, west Texas and southeastern New Mexico: Am. Assoc. Petroleum Geologists Bull., v. 28, p. 1596-1625.

Adams, J. E., 1965, Stratigraphic-tectonic development of Delaware Basin: Am. Assoc. Petroleum Geologists Bull., v. 49, p. 2140-2148.

Adams, S. S., 1967, Bromine in the Salado formation, Carlsbad Potash District, New Mexico (Ph.D. thesis): Harvard University, 202 p.

Anderson, R. Y., 1978, Report to Sandia Laboratories on deep dissolution of salt, northern Delaware Basin, New Mexico: Sandia Laboratories, New Mexico.

Anderson, R. Y., Dean, W. E., Jr., Kirkland, D. W., and Snider, H. I., 1972, Permian Castile varved evaporite sequence, west Texas and New Mexico: Geol. Soc. Am. Bull., v. 83, p. 59-86.

Anderson, R. Y., and Kirkland, D. W., 1966, Intrabasin varve correlation: Geol. Soc. Am. Bull., v. 77, p. 241-256.

Bachman, G. O., 1974, Geologic processes and Cenozoic history related to salt dissolution in southeastern New Mexico: U. S. Geol. Surv., Open-file report 74-194.

Bachman, G. O., 1976, Cenozoic deposits of southeastern New Mexico and an outline of the history of evaporite dissolution: U. S. Geol. Surv., Jour. of Res., v. 4, p. 135-149.

Baker, C. L., 1929, Depositional history of the red beds and saline residues of the Texas Permian: Univ. of Texas Bull. 2901, p. 9-72.

Beede, J. W., 1924, Report on the oil and gas possibilities of University Block 46 in Culberson County: Univ. Texas Bull. 2346, p. 13-14.

Braitsch, O., 1962, Entslehung und Stoffbestand der Salzlagerstatten: Berlin, Springer-Verlag, 232 p.

Brass, G. W., 1973, The sources of marine strontium and the $^{87}Sr/^{86}Sr$ ratio in the sea throughout Phanerozoic time (Ph.D. thesis): Yale University, 220 p.

Brokow, A. L., Jones, C. L., Cooley, M. E., and Hays, W. H., 1972, Geology and hydrology of the Carlsbad potash area, Eddy and Lea Counties, New Mexico: U. S. Geol. Surv. Open-file report 4339-1.

Bybee, H. P., 1931, Some major structural features of west Texas: Univ. Texas Bull. 3101, p. 19-26.

Carroll, D., and Starkey, H. C., 1960, Effect of sea water on clay minerals, in Swineford, A., ed., Clays and clay minerals, 7th national conference: Oxford, Pergamon Press, p. 80-101.

Curtis, C. D., 1972a, Cobalt: element and geochemistry, in Fairbridge, R. W., ed., Encyclopedia of geochemistry and environmental sciences: New York, Van Nostrand Reinhold Company, p. 180-181.

Curtis, C. D., 1972b, Scandium: element and geochemistry, in Fairbridge, R. W., ed., Encyclopedia of geochemistry and environmental sciences: New York, Van Nostrand Reinhold Company, p. 1060-1061.

Dean, W. E., and Anderson, R. Y., 1973, Trace and minor element variations in the Permian Castile Formation, Delaware Basin, Texas and New Mexico, revealed by varve calibration, in Coogan, A. H., ed., Fourth Symposium on Salt: Northern Ohio Geol. Soc., p. 275-285.

Eardley, A. J., 1949, Paleotectonic and paleogeologic maps of central and western North America: Am. Assoc. Petroleum Geologists Bull., v. 33, p. 655-683.

Fairbairn, H. W., and Hurley, P. M., 1971, Evaluation of X-ray fluorescence and mass spectrometric analyses of Rb and Sr in some silicate standards: Geochim. Cosmochim. Acta, v. 35, p. 149-156.

Flanagan, F. J., 1973, 1972 values for international geochemical reference samples: Geochim. Cosmochim. Acta, v. 37, p. 1189-1200.

Fleischer, M., 1955, Hafnium content and hafnium-zirconium ratio in minerals and rocks: U. S. Geol. Surv. Bull. 1021-A.

Folk, R. L., 1968, Petrology of sedimentary rocks: Austin, Texas, Hemphill's, 170 p.

Gaines, R. V., 1972, Cesium: element and geochemistry, in Fairbridge, R. W., ed., Encyclopedia of geochemistry and environmental sciences: New York, Van Nostrand Reinhold Company, p. 147-148.

Gills, T. E., Marlow, W. F., and Thompson, B. A., 1970, Determination of trace elements in glass by activation analysis using hydrated antimony pentoxide for sodium removal: Anal. Chem., v. 42, p. 1831-1833.

Goldberg, E. D., 1961, Chemistry in the oceans, in Sears, M., ed., Oceanography, Am. Assoc. Advancement of Sci. publication 67, p. 588-597.

Goldberg, E. D., Koide, M., Schmitt, R., and Smith, R., 1963, Rare earth distributions in the marine environment: J. Geophys. Res., v. 68, p. 4209-4217.

Goldschmidt, V. M., 1954, Geochemistry: Oxford, Clarendon Press, 730 p.

Graham, S. A., Dickinson, W. R., and Ingersoll, R. V., 1975, Himalayan-Bengal model for flysch disposal in Appalachian - Ouachita system: Geol. Soc. Am. Bull., v. 86, p. 273-286.

Grim, R. E., 1968, Clay mineralogy: New York, McGraw-Hill, 384 p.

Hayes, P. T., 1964, Geology of the Guadalupe Mountains, New Mexico: U. S. Geol. Surv. Prof. Paper 446.

Heier, K. S., and Adams, J. A. S., 1964, The geochemistry of the alkali metals, in Ahrens, L., and others, eds., Physics and chemistry of the earth, v. 5: New York, Macmillan, p. 253.

Hills, J. M., 1972, Late Paleozoic sedimentation in west Texas Permian Basin: Am. Assoc. Petroleum Geologists Bull., v. 56, p. 2303-2322.

Hogdahl, O. T., 1968, Neutron activation analysis of lanthanide elements in sea water: Adv. Chem., v. 73, p. 308-325.

Holser, W. T., 1966, Bromide geochemistry of salt rocks, in Coogan, A. H., ed., Second symposium on salt: Northern Ohio Geol. Soc., p. 248-275.

Hurley, P. M., Heezen, B. C., Pinson, W. H., and Fairbairn, H. W., 1962, K-Ar age values in pelagic sediments of North Atlantic: Geochim. Cosmochim. Acta, v. 27, p. 393-399.

Jones, C. L., 1973, Salt deposits of Los Medanos area, Eddy and Lea Counties, New Mexico: U. S. Geol. Surv. Open-file report, 4339-7.

King, P. B., 1942, Permian of west Texas and southeastern New Mexico: Am. Assoc. Petroleum Geologists Bull., v. 26, p. 535-763.

King, P. B., 1948, Geology of the southern Guadalupe Mountains, Texas, U. S. Geol. Surv. Prof. Paper 215, 183 p.

King, R. H., 1947, Sedimentation in Permian Castile sea: Am. Assoc. Petroleum Geologists Bull., v. 31, p. 470-477.

Kroenlein, G. A., 1939, Salt, potash and anhydrite in the Castile formation of southeast New Mexico: Am. Assoc. Petroleum Geologists Bull., v. 23, p. 1682-1693.

Lang, W. T. B., 1935, Upper Permian formation of the Delaware Basin of Texas and New Mexico: Am. Assoc. Petroleum Geologists Bull., v. 19, p. 262-270.

Lang, W. T. B., 1939, Salado formation of the Permian Basin: Am. Assoc. Petroleum Geologists Bull., v. 23, p. 1569-1572.

Lang, W. T. B., 1942, Basal beds of the Salado formation in Fletcher potash core near Carlsbad, New Mexico: Am. Assoc. Petroleum Geologists Bull., v. 26, p. 63-69.

Lee, M. J., 1976, Geochemistry of the sedimentary uranium deposits of the Grants mineral belt, southern San Juan Basin, New Mexico (Ph.D. thesis): University of New Mexico, 241 p.

Mason, B., 1966, Principles of geochemistry: New York, John Wiley and Sons, p. 195.

McKee, E. D., 1967, Paleotectonic investigations of the Permian System in the United States: U. S. Geol. Surv. Prof. Paper 515, 271 p.

New Mexico Geological Society, 1954, A brief geologic sketch of the Delaware Basin, in New Mexico Geological Society Guidebook, Southeastern New Mexico, p. 131.

Peterman, Z. E., Hedge, C. E., and Tourtelot, H. A., 1970, Isotopic composition of strontium in sea water throughout Phanerozoic time: Geochim. Cosmochim. Acta, v. 34, p. 105-120.

Pilkey, O., 1972, Barium: element and geochemistry, in Fairbridge, R. W., ed., Encyclopedia of geochemistry and environmental sciences: New York, Van Nostrand Reinhold Company, p. 62-63.

Polevaya, N. I., Sprintsson, V. C., Izokh, E. P., LeDinh Huu, and Nguyen Van Chien, 1964, First absolute age data of magmatic rocks from North Vietnam: Inter. Geol. Congr. 22nd Session.

Rankama, K., and Sahama, Th. G., 1950, Geochemistry: Chicago, University of Chicago Press, 912 p.

Reynolds, R. C., 1972, Rubidium: element and geochemistry, in Fairbridge, R. W., ed., Encyclopedia of geochemistry and environmental sciences: New York, Van Nostrand Reinhold Company, p. 1050-1051.

Russell, K. L., 1970, Geochemistry and halmyrolysis of clay minerals, Rio Ameca, Mexico: Geochim. Cosmochim. Acta, v. 34, p. 893-907.

Samuelson, O., 1963, Ion exchange separations in analytical chemistry: New York, Wiley, 474 p.

Schaller, W. T., and Henderson, E. P., 1932, Mineralogy of drill cores from the potash field of New Mexico and Texas: U. S. Geol. Surv. Bull. 833, 124 p.

Smith, D. B., 1964, The Permian Period in The Phanerzoic Time Scale: Quart. J. Geol. Soc., London, p. 211-220.

Tremba, E. L., 1973, Isotope geochemistry of strontium in carbonate and evaporite rocks of marine origin (Ph.D. thesis): The Ohio State University, 124 p.

Udden, J. A., 1924, Laminated anhydrite in Texas: Geol. Soc. America Bull., v. 35, p. 347-354.

Vertrees, C., Atchison, C. H., and Evans, G. L., 1959, Paleozoic geology of the Delaware and Val Verde Basins, in West Texas Geol. Soc. Guidebook, p. 64-73.

Walter, J. C., Jr., 1953, Paleontology of the Rustler Formation, Culberson County, Texas: J. of Paleontology, v. 27, p. 679-702.

Webb, A. W., and McDougall, I., 1967, Isotopic dating evidence on the age of the Upper Permian and Middle Triassic: Earth Planet. Sci. Letters, v. 2, p. 483-488.

Webster, R. K., 1960, Mass spectrometric isotope dilution analysis, in Smales, A. A., and Wager, L. R., eds.: Methods in geochemistry, New York, Interscience Pub. Inc., p. 202-246.

Wildeman, T. R., and Haskin, L. A., 1965, Rare earth elements in ocean sediments: J. Geophys. Res., v. 70, p. 2903-2910.

Yoder, H. S., and Eugster, H. D., 1955, Synthetic and natural muscovites: Geochim. Cosmochim. Acta, v. 8, p. 225-280.

York, D., 1969, Least-squares fitting of a straight line with correlated errors: Earth Plan. Sci. Letters, v. 5, p. 320-324.

Young, R. S., 1957, The geochemistry of cobalt: Geochim. Cosmochim. Acta, v. 13, p. 28-41.